Ph.D Thesis

Study on Technology and Properties of Silver Plating on Flexible Substrate

March 2019

Tokyo University of Agriculture and Technology
Graduate School of Bio-Applications and Systems Engineering
Bio-Applications and Systems Engineering

Changchun Liu
Supervisor: Kenji Ogino

Study of Technology and Properties of Silver Plating on Flexible Substrate

ABSTRACT

Flexible electrically-conductive fabrics have attracted more and more attention for their wide variety of applications in industries such as clothing, medical, sports, and military. Polyester fiber is widely used as a flexible substrate in various fields because of its low price, easy availability, excellent physical and mechanical properties and chemical stability. Plating silver on the surface of the substrate enables the fabrics to have both the original properties of the polyester fiber and the excellent electrical conductivity, antibacterial property, metallic luster and other excellent characteristics of the metallic silver. Electroless plating is a simple and cost-effective method to coat a nano-silver layer on fibers in order to obtain conductive textiles. However, the electroless silver-plated fibers do not have enough bonding strength between the surface silver layer and substrate generally. Therefore, this work aimed to improve bonding between silver and fibers. Besides, the filter paper was utilized to replace polyester fabrics as the substrate to deposit patterned copper by means of electroless plating through laser-induced deposited silver particles as the seeds. In details, this work of silver plating on flexible substrate could be divided into the following parts as:

1) Preparing the silver-coated polyester fibers by a continuous two-step method, which combined the operations of continuous electroless plating without an activation step and subsequent cyanide-free electroplating step. Furthermore, a specialized

equipment for the continuous plating of silver on the polyester fibers was designed. The influence of the power supply method, control voltage, and electroplating time on electroplating silver were studied. The optimal conditions for electroplating silver conductive polyester fibers should include the power supply method having a constant voltage power, the best control voltage range of 1.5–2.0 V, and an electroplating time of 4 min. Moreover, the mechanical properties and washability of the electroplating silver-plating fibers were compared with the electroless silver-plating fibers. The results demonstrated that after the continuous two-step silver plating, the surface coating of the fiber was obviously thickened, and the surface silver particles were denser and continuous, with better mechanical properties and washability. The electrical resistivity reached 2.3 × 10^{-4} $\Omega\cdot$cm, and the conductivity was obviously improved. The light bulb experiment also showed that the conductive fiber prepared by the continuous two-step silver plating method had good electrical conductivity.

2) Preparing the composite conductive fibers by the two-step deposition of polyaniline and silver layers on the surface of polyester fibers through oxidative polymerization and redox reaction, respectively. Batch experimental results showed that the concentration of reagents and the reaction time could affect the resistance of polyaniline-silver coated conductive fibers. The optimal reaction condition of preparing conductive polyester fibers should be: the concentration of aniline was 0.3 mol/L, ammonium persulfate 0.2 mol/L, nitric acid 1 mol/L and the treating time was 3 min. The morphology, thermostability, mechanical properties, washing resistance and corrosion resistance of resultant fibers obtained from different synthesis condition were

characterized. The results demonstrated that the PANI-Ag-coated polyester fibers by the two-step depositing have much better properties than Ag-coated fibers.

3) Uniform copper patterns with good conductivity properties were obtained on a soft substrate of filter paper/polyacrylonitrile (FP/PANI) film. The pattern of Ag nanoparticles was first produced on an Ag^+-doped FP/PANI composite film using a pulsed laser source, followed by selective electroless plating of copper using the metal silver nanoparticles as activated seeds. The *in-situ* reductions of silver particles and the formation of the silver agglomeration patterns were induced by laser irradiation technology on the FP/PANI/$AgNO_3$ composite film. The morphology of metal particles on the fabric surface and the conductivity of copper deposited patterns were characterized. The experimental results demonstrated that the scanning speed of the laser pulse greatly affected the redox reaction. The current-voltage (I–V) curve indicated that the copper patterns on the FP/PANI composite films had good conductivity. This method provides new insight into preparing a flexible circuit board.

KEYWORDS

Conductive fibric; Polyester fiber; Polyaniline; Silver; Electroplating; Electroless plating; Laser-induced irradiation; Filter paper; Polyacrylonitrile; Copper pattern

Contents

Chapter 1 Introduction

1.1 Conductive Fibers

Flexible substrate devices have achieved tremendous attention in the past few decades because of their unique potential for use in flexible and wearable electronic devices [1]. Among them, electrically-conductive fabrics are achieving more and more research interest owing to their great potential applications in industries such as clothing, medical, sports, and military. Synthetic fabrics and papers are known as two of the important flexible substrates in these applications.

Since its invention in the early 1880s [2], synthetic fibers have been widely used in various fields due to their excellent physical and mechanical properties and chemical stability. However, the general synthetic fiber has a resistivity as high as 10^{14} Ω·cm-10^{16} Ω·cm, which tends to cause charge accumulation [3,4].

Polyester fiber is the most commonly used synthetic fiber due to its excellent performance such as good elasticity, shape retention, wrinkle resistance, excellent wash-and-wear performance and durability, and so on. However, ordinary polyester fiber has a poor ability in moisture absorption [5,6], higher electrical resistance [7,8], and can easily accumulate large amounts of electric charges on the surface, especially in dry conditions [9–11], which results in fibers repelling each other, clothing absorbing dust [12], clinging onto the body and poor comfort[13, 14], and can even produce electrical shocks [15] or ignite flammable substances [16, 17]. Polyester fibers' easily generating static electricity limit their applications in apparel and home furnishings

[18–20].

Generally, there are two kinds of antistatic techniques for materials [21]. One is to reduce the friction between materials to reduce the generation of electric charge; the other is to improve the conductivity of the material to increase the conduction speed of the charge. However, friction between materials is inevitable during the production and use, so the preparation of conductive fibers and fabrics has become the focus of researches.

With the rapid development and popularization of electronic technology, the problems caused by electromagnetic radiation have become more and more serious. Electromagnetic radiation can cause direct or indirect damage to people. Excessive electromagnetic radiation also affects the operation of electronic equipment. Therefore, electromagnetic protection has also become a research focus [20]. Electromagnetic shielding fabrics have both fabric characteristics and excellent properties. Electromagnetic shielding performance has been widely used in human life and industrial production. Among them, the electromagnetic shielding material prepared by using conductive fibers and fabrics has become a widely used electromagnetic shielding material because of its excellent electrical conductivity and fabric characteristics.

Since the 1950s, researchers have begun studying on conductive fibers and their fabrics. The conductive fiber refers to a fiber having a resistivity of less than 107 Ω·cm under the air condition of 20 °C and 65% relative humidity. The electrical resistivity of the conductive fiber is much lower than that of the ordinary fiber (about 1015 Ω·cm), which can quickly dissipate static charges by electron conduction and corona discharge

[22, 23]. Today, various types of conductive fibers and fabrics have been developed.

Among the known metals, silver has the best conductivity and thermal conductivity and has strong corrosion resistance and acid and alkali resistance. And silver also has chemical stability at room temperature and good ductility [24–25], thus it is widely used in modern industry. Silver-containing composite materials can not only maintain material properties but also have good electrical and antistatic properties, thermal conductivity, thermal insulation properties, radiation and electromagnetic shielding properties, antibacterial deodorizing properties, and decorative properties, so researches on silver-containing composites become the focus of research in this field. For example, Shieldex X-Static, which was developed by Statex Noble Fiber and coated metal silver with nylon 66 as the substrate, has excellent electrical conductivity and permanent antibacterial properties [26]. Malden Mills of the United States developed anti-static and quick-drying fabrics by embedding X-Static silver-plated fibers into fabrics [27]. Trevira Gmbh of Germany also produced polyester fibers with long-lasting antibacterial properties and used in the manufacture of underwear and bed sheets [28]. Japan's research on silver-plated fibers is also very active. μ-func, one silver-plated fiber developed by Toyoshima & Co., Ltd, is coated with a layer of pure silver (0.1 μm) between two transparent polyester layers with each thickness of 9 μm [29]. Silver-plated polyester fiber AGposs developed by Mitsutuji Textile has a fiber diameter of 15-25 μm and a silver-plated layer thickness of about 0.1 μm [30].

Plating a layer of silver on the surface of a polyester fiber will preserve the excellent properties of the polyester. Meanwhile, it also has the excellent electrical conductivity

[31], ductility [32,33], catalytic activity [34,35], and antibacterial deodorization properties of metallic silver [36–39], and the material can also obtain a certain metallic luster and decorative effect [40–43]. In addition, silver particles have broad application prospects in the field of catalytic materials because of their unique catalytic properties and their relative cost compared with palladium. They are often used as activating species for surface electroless plating reactions to induce chemical reactions on the surface of materials [44].

In this study, the polyester fibers and the filter paper were used as the flexible substrate, silver-plated conductive fibers and copper-plated conductive fabrics were prepared by the different method.

1.2 Preparation Method of Conductive Fibers

Because of the different conductive materials, there are many types of conductive fibers, and the corresponding preparation methods are also different. The fiber and its fabric are coated with a dense metal layer, which can make the material have excellent electrical conductivity similar with the metal, and the surface of the material also has other metal characteristics such as heat conduction, metallic luster, etc., so the preparation method of this type has been extensive research and application.

1.2.1 Metal-based Conductive Fiber

In the 1960s, Bekaert of the United States introduced a commercial stainless-steel fiber called "Bekinox", making metal-based conductive fibers the first conductive fibers to be used [45,46]. The metal-based conductive fiber is processed by a specific method for the metal material, and the conductive property of the metal is fully utilized to prepare a conductive fiber having good performance.

There are two main methods for preparing such conductive fibers. One method is to use a direct drawing method or a cutting method to form a metal into a fiber-shaped filament, which is generally blended with other fibers [47-49] and is used for preparing such a fiber. The metals are generally copper, stainless steel, and aluminum. Another method is a metal spraying method in which metal particles are deposited on the surface of the fiber by vacuum spraying or electroless plating after the surface of the fiber is treated [39].

The metal-based conductive fiber is a fiber having a uniform conductive component, has almost the same conductivity as a pure metal, and has the best electrical conductivity among all conductive fibers, and is still an important variety in the conductive fiber until now. It is generally not used alone and is usually made into a conductive fabric by blending short fibers with ordinary fibers, and can be used for antistatic overalls, antistatic carpets, radiation protection suits, anti-electromagnetic shielding of large-sized textiles, and the like. However, due to its poor hand feeling, difficulty in cohesion, unevenness with fiber blending, the limited color of finished products, and difficulty in manufacturing and processing metal wire drawing methods, the cost of making high-fineness fibers is high, thus limiting its further application and popularization.

1.2.2 Carbon Black Conductive Fiber

These conductive fibers use carbon black with electrical conductivity to enable the fibers to obtain electrical conductivity. There are three main types of common manufacturing methods. The first method is the doping method, in which carbon black is used as a conductive component, and melt-spun with a fiber-forming polymer and the carbon black in the fiber is in a continuous phase structure to make the obtained fiber have electrical conductivity [50]. The fiber prepared by the method maintains the original physical and mechanical properties and has also electrical conductivity, and its conductivity is greatly affected by the amount of carbon black-doped. The second method is the coating method which uses an adhesive or a high-temperature softening fiber to closely bond the carbon black to the surface of the fiber [51]. However, the bonding strength between the fiber carbon black and the surface of the fiber is poor, and the carbon black is not easily distributed uniformly, resulting in poor conductivity of the fiber. The third method is the carbonizing method, in which some fibers, such as polyacrylonitrile fibers, cellulose fibers, etc., are carbonized so that the main chain of the fibers is carbonized into carbon atoms. And the fibers have a certain conductivity due to the presence of continuous carbon atoms [52,53].

1.2.3 Metal Compound Conductive Fiber

Metal compound conductive fibers are prepared using the excellent electrical conductivity of certain metal compounds. These metal compounds are mainly sulfides and iodides of silver, nickel, copper and cadmium, of which copper sulfides and iodides are the most used [54]. The conductive fibers produced by this method have many applications and a wide range of applications because of their good electrical conductivity. There are mainly three methods for preparing metal compound conductive fibers.

1.2.3.1 Mixed Spinning Method

The mixed spinning method is to mix metal materials with good conductivity with fiber-forming polymers, and then spin them into a sheath-core structure. This method is applicable to various synthetic fibers in the same manner as the carbon black doping method described above. Carbon black composite coated conductive fiber has limited application in civil textiles due to its black color, and Japanese Teijin Limited first successfully developed a white dyeable conductive fiber named "T-25" [55]. The white conductive fiber is made by blending CuI and other metal oxides with fiber-forming materials by the mixed spinning method.

1.2.3.2 Chemical Reaction Method

The chemical reaction method is mainly to chemically treat the fiber, that is, the fiber is immersed into the reaction solution to cause adsorption on the surface of the fiber, and then the surface of the fiber is covered with a metal oxide by another chemical reaction. For example, the Cu^9S^5 conductive acrylic fiber developed in Japan is prepared by this method. The acrylic fiber is first treated in a solution containing copper ions and then treated in a sulfur reducing agent. Cu^{2+} on the fiber is reduced to Cu^+, and then complexed with ^-CN on the polyacrylonitrile (PANI) fiber to form a conjugated copper salt, the obtained fiber’s volume specific resistance reaches 8.2×10^{-1} Ω·cm [56,57], and the electrical conductivity is good. At present, the method for preparing conductive fibers is widely used, but the reaction conditions are harsh and the treatment process is complicated.

1.2.3.3 Adsorption Method

There are two main adsorption methods: one is the conventional adsorption, and the other is the complex adsorption between metal ions and fibers. Similar with the carbon black conductive fiber coating method, the conventional adsorption is to bond a metal compound to the fiber surface by an adhesive, which is suitable for fibers of strong polarity and weak polarity, or dense structural fibers such as polyester fibers. While the complex adsorption is especially suitable for nitrogen-containing fibers. The specific treatment methods include the high-temperature cooking method and the high temperature and high-pressure co-cooking method. The high-temperature cooking method is to apply compounds which containing metal ions to the surface of the high-temperature steam treated fiber to obtain the conductive fiber. The high temperature and high-pressure co-cooking method is to co-cook the metal compound and the fiber under the condition of high temperature and high pressure, followed by adding the fiber dopants and the swelling agents. The conductive fibers having good electrical conductivity can be obtained as well.

1.2.3.4 Conductive Polymer Fiber

Conductive polymer fibers are made from some conductive polymer materials with electrical conductivity, such as polyaniline, polypyrrole, polythiophene, etc. There are two preparation methods [58]. One is the direct spinning method, that is, direct spinning using a conductive polymer material, generally using wet spinning, such as preparation of polyaniline conductive fibers [59]. The second type is the post-treatment method, which usually involves a conductive reaction on the surface of the fiber to adsorb the conductive polymer on the surface of the fiber, thereby imparting electrical conductivity to the fiber [60].

1.3 Electroless Plating and Electroless Silver Plating

1.3.1 Electroless Plating

Electroless plating, also known as chemical plating, refers to the use of catalytic activity on the surface of the substrate in the absence of an applied current to catalyze the redox reaction of the reducing agent with the metal ions in the catalytic solution, depositing a metal coating on the surface of the substrate [61]. At present, there are many types of electroless plated metals, such as electroless copper plating, electroless nickel plating, electroless silver plating, etc., which are used in different fields according to different metal characteristics [62].

The electroless plating bath has a strong dispersing force, and any part of the substrate that is in contact with the plating solution will produce a metal plating layer with the same thickness, and the obtained plating layer has the characteristics of continuous compactness and corrosion resistance. Compared with other methods, electroless plating has simple preparation process, wide range of coatable materials, high bonding strength between coatings and materials, simple equipment and less investment, uniform thickness and compactness of coatings, and good conductivity of matrix [63].

1.3.2 Electroless Plating Process

Electroless plating is generally divided into two parts: the pretreatment process of the material and the electroless plating of the material. The pretreatment is to treat the substrate to increase the surface roughness (coarsening) to increase the adhesion between the coating and the substrate, and at the same time impart a certain catalytic activity to the substrate to facilitate catalytic electroless plating on the surface of the substrate. The process flowchart is shown in Figure 1-1.

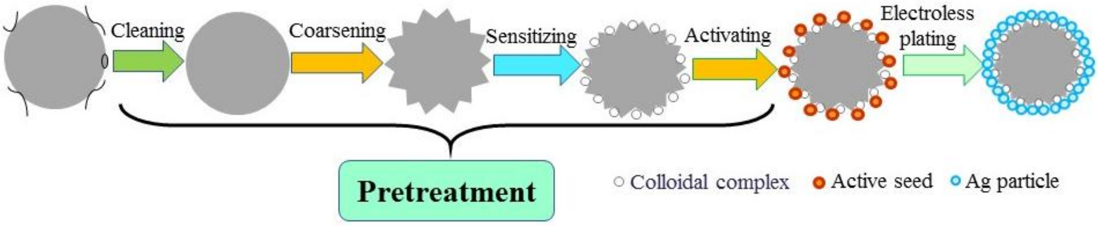

Figure 1-1. Electroless plating process flow chart

1.3.2.1 Cleaning

In the process of production and transportation, the fiber will inevitably be contaminated with oil stains and other impurities. In the process of chemical deposition, impurities will affect the bonding force between the silver-deposited layer and the fiber and uniformity. Therefore, it is necessary to remove oil stains and other impurities before coarsening to clean the surface of the fiber.

The fiber can be cleaned by acetone, ethanol and other organic solvents, or by adding surfactants into alkaline aqueous solution. Since the oil can be well dissolved in an organic solvent, the organic solvent is widely used for degreasing in the surface of a polymer material. Using alkaline solution containing surfactant to remove oil is based on saponification reaction of oil in alkaline condition and emulsification reaction of surfactant, and the treatment process is non-toxic and non-flammable, and has great advantages in safe production.

1.3.2.2 Coarsening

The coarsening of the fiber surface includes both the mechanical coarsening and the chemical coarsening. The mechanical coarsening generally uses sand blasting to roughen the surface of the material, but the process is complicated and costly, and the bonding strength between the silver deposit layer and the fiber is poor. The chemical coarsening refers to immersing fibers into chemical reagents and increasing the roughness of the surface of the material by chemical etching to form uniform micro-holes and grooves on the material surface. The coarsening can increase the contact area between the fibers and the deposited layer, forming the "locking effect" required for electroless plating [64], and at the same time enhance the hydrophilicity of the fibers, thereby improving the bonding strength between the coating and the substrate.

1.3.2.3 Sensitizing

Since the fiber surface is not catalytically active, it is necessary to sensitize the fiber to adhere a layer of sensitizer to the surface of the fibers, ensuring a reduction reaction upon activation [65]. The commonly used sensitizer is $SnCl_2$, but $SnCl_2$ is easily oxidized and hydrolyzed. Therefore, it needs to be dissolved in concentrated hydrochloric acid first, and some $SnCl_2$ changed into $SnCl_4^{2-}$ in hydrochloric acid. The reaction formula is:

$$SnCl_2 + 2HCl \rightarrow SnCl_4^{2-} + 2H^+ \qquad (1\text{-}1)$$

During the water washing process after the sensitizing, $SnCl_2$ and $SnCl_4^{2-}$ are hydrolyzed to form Sn(OH)Cl and $Sn(OH)_2$. The reaction formulas are as follows.

$$SnCl_2 + 2H_2O \rightarrow Sn(OH)_2 + 2HCl \tag{1-2}$$

$$SnCl_2 + H_2O \rightarrow Sn(OH)Cl + HCl \tag{1-3}$$

$$SnCl_4^{2-} + 2H_2O \rightarrow Sn(OH)_2 + 2H^+ + 4Cl^- \tag{1-4}$$

$$SnCl_4^{2-} + H_2O \rightarrow Sn(OH)Cl + H^+ + 3Cl^- \tag{1-5}$$

Sn(OH)Cl reacts with $Sn(OH)_2$ to form $Sn_2(OH)_3Cl$ [66]. The reaction formula is:

$$Sn(OH)Cl + Sn(OH)_2 \rightarrow Sn_2(OH)_3Cl \tag{1-6}$$

$Sn_2(OH)_3Cl$, a slightly soluble water-like gelatinous substance, is adsorbed on the surface of the fiber and served as the reductant for subsequent activation step, so the quality of fiber sensitization depends on water washing process.

If the washing time is too short, the hydrolysis of $SnCl_2$ will be insufficient, which will affect the sensitization result. while if the washing time is too long, $Sn_2(OH)_3Cl$ will fall off, resulting in a decrease in the binding force of metallic silver to the fibers during silver deposition.

1.3.2.4 Activating

The activation treatment is to immerse the sensitized fibers into the activation solution containing noble metal ions. The Sn^{2+} on the surface of the fiber loses electrons and is oxidized to Sn^{4+}, and the noble metal ions in the activation solution are reduced to metal particles deposited on the surface of the fiber. The surface is catalytically activated, and then the electroless silver plating can spontaneously continue to conduct on the surface of the catalyzed fiber. At present, the widely used activation solutions include silver nitrate activation solution and palladium chloride activation solution. However, since palladium chloride is expensive as well as the great potential of polluting the plating layer [67,68], this study uses silver nitrate as an activator. The specific reaction is as follows:

$$2Ag^{+} + Sn^{2+} \rightarrow 2Ag\downarrow + Sn^{4+} \qquad (1\text{-}7)$$

1.3.3 Electroless Silver Plating

Electroless silver plating is one of the earliest developed electroless plating methods. It has a long history and is derived from the silver mirror reaction. It was widely used in the manufacture of light industrial products, such as glass and thermos liners. With the development of electroless plating, metallic silver is widely used in various industries due to its excellent electrical conductivity and chemical stability.

1.3.4 Mechanism of Electroless Silver Plating

At present, the reduction mechanism of silver ions in the electroless plating process is still controversial. One explanation is that the reaction is a non-autocatalytic reaction in which silver particles are deposited in solution and formed by agglomeration of colloidal particles. Another explanation is that the reaction has a weak autocatalytic capability. Since silver can be deposited immediately onto the activated material and the stability of the plating solution is poor, it is easily decomposed by autocatalytic reaction.

In order to ensure stable electroless silver plating, silver ions usually form a stable coordination complex with the ligand. The silver cyanide coordination compound is the most stable, but the cyanide is usually highly toxic. Therefore, the stability of the ammonia ligand $[Ag(NH_3)_2^+]$ is used to ensure the stability of the electroless plating reaction. Electroless silver plating is actually a redox reaction. The oxidizing solution generally consists of silver nitrate and aqueous ammonia. Since the aqueous solution of silver nitrate is unstable, it is easily decomposed to form a brown Ag_2O precipitate (Reaction 1-8). Therefore, a small amount of aqueous ammonia is added dropwise to the silver nitrate solution to precipitate Ag_2O during the dosing, and if the aqueous ammonia is continuously added dropwise, Ag_2O will be dissolved and then form a silver ammonia complex $Ag(NH_3)_2OH$ (Reaction 1-9), which further forms complex $[Ag(NH_3)_2]NO_3$ with NH_4NO_3 (Reaction 1-10). The whole reaction equation is as follows [69].

$$2AgNO_3 + 2NH_4OH \Leftrightarrow Ag_2O + 2NH_4NO_3 + H_2O \tag{1-8}$$

$$Ag_2O + 4NH_4OH \Leftrightarrow 2[Ag(NH_3)_2]OH + 3H_2O \tag{1-9}$$

$$[Ag(NH_3)_2]OH + NH_4NO_3 \Leftrightarrow [Ag(NH_3)_2]NO_3 + NH_3 \uparrow + H_2O \tag{1-10}$$

Commonly used reducing agents are formaldehyde, glucose, sodium potassium tartrate, etc. But because of the cheap price of glucose and the good quality of the prepared coating [70], this research used glucose as a reducing agent for the electroless silver plating reaction. The reaction equation is as follows.

$$\begin{aligned} CH_2OH(CHOH)_4CHO + 2Ag(NH_3)_2OH \xrightarrow{\Delta} CH_2OH(CHOH)_4COONH_4 + 2Ag \downarrow \\ + H_2O + 3NH_3 \uparrow \end{aligned} \tag{1-11}$$

1.3.5 Non-metal Electroplating Introduction

Electroplating refers to the process in which metal cations in the plating solution reach the surface of the plated material that served as a cathode under the action of an applied electric field, and electrons are reduced to metal atoms, then deposited on the surface of the material [71,72]. Since electroplating is an electrochemical reaction that occurs under the action of an electric field, it is required that the material to be plated must also be electrically conductive, so that the electroplating technique is initially a technique of plating with a metal material as a cathode. However, metallic materials tend to be scarce as non-renewable resources. Non-metallic materials are popularized for their excellent properties. At present, non-metallic materials cannot replace metals in terms of electrical conductivity, appearance, and touch feel. Therefore, plating metals on the non-metallic surface have gradually become the focus of research.

1.3.6 Non-metal Electroplating Process

Electroplating uses electrical energy as the electrochemical reaction power and provides electrons that can reduce metal ions to the cathode. Therefore, the plated materials are required to conduct electricity, but the non-metallic materials generally do not have conductivity and cannot be directly electroplated [73].

In order to enable non-metallic materials to be plated, it is necessary to impart a certain conductivity to the non-metal materials, and the surface of the non-metal materials is generally metalized by electroless plating to have a certain conductivity. Non-metal electroplating is divided into two processes, one is electroless plating of non-metallic materials for materials' obtaining conductivity, and the other is electroplating of non-metallic materials. The electroless plating of non-metallic materials is basically the same as the electroless plating process described in Section 1.3. The specific process flow is shown in Figure 1-2 as below.

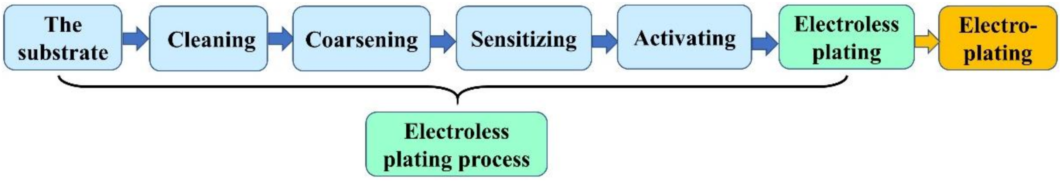

Figure 1-2. Non-metal Electroplating Process

1.3.7 Non-metal Cyanide-free Silver Plating

The cyanide silver plating is the first used and well-developed in the electroplating industry. The complex of CN^- and Ag^+ formed in the plating bath has higher stability and good dispersion of the plating solution. The bonding fastness between the cyanide silver plating layer and the matrix is high, and the solution is stable and easy to maintain [74]. However, cyanide is highly toxic and will cause great harm to people's production and life. With the continuous improvement of people's awareness of environmental protection, the cyanide electroplating silver process must be replaced.

Since 1913, an article systematically discussed the study of cyanide-free electroplating silver [75]. Until the 1950s, the research on cyanide-free silver plating mainly focused on the location of coordination agents. Most of the coordination agents used were potassium tartrate, thiourea, citric acid and so on, but the effect of these coordination agents was not satisfactory.

Thereafter, the cyanide-free silver-plating system with sodium pyrosulfate, sulfate, ammonia water, and ethylenediamine as coordinating agents appeared. The research of cyanide-free silver plating began to emerge in the 1960s [76]. Up to now, the more mature cyanide-free silver-plating systems mainly include succinimide system, thiosulfate system, sulfite system, ammonium imino sulfonate (NS) system, hydantoin system, and sulfosalicylic acid system, etc. [77]. Sulfosalicylic acid as a main complexing agent forms an anion with silver ions. The prepared silver-plating layer is bright and dense, and its performance is close to that of cyanide silver plating, and the plating solution is relatively stable in a certain pH range. Therefore, this research used the sulfosalicylic acid system for non-cyanide electroplating silver experiments.

In chapter 2 of this thesis, the sulfosalicylic acid system was utilized to conduct non-cyanide electroplating silver experiments.

1.4 Electroless Copper Plating

1.4.1 Thermodynamic Principle of Electroless Copper Plating

Electroless copper plating occurs at the interface between the catalytic active surface and the plating solution， which can be regarded as a redox battery reaction. The gains and losses of electrons are as follows:

Oxidation reaction:

$$\mathrm{R} \rightarrow \mathrm{R}^{2+} + 2e^- \tag{1-12}$$

Reduction reaction:

$$\mathrm{Cu}^{2+} + 2e^- \rightarrow \mathrm{Cu} \tag{1-13}$$

The reductant R is oxidized to R^{2+}, and provides all electrons needed for the reduction of Cu^{2+}. Studied by the thermodynamic principle, the potential of the reducing agent like formaldehyde or sodium hypophosphite is lower than that of the copper ion, so it is feasible to use them to reduce copper ions. However, the electrode potential of copper ions is relatively negative, and its oxidizing property is not very strong, and there are certain requirements for the external environment of the reaction.

If formaldehyde is used as the reducing agent, in the acidic solution, the electrode reaction and the corresponding electrode potential E are as follows:

$$\mathrm{HCHO} + \mathrm{H_2O} \rightarrow \mathrm{HCOOH} + 2\mathrm{H}^{+} + 2e^{-} \tag{1-14}$$

E= -0.056-0.06 pH

In alkaline solution, the electrode reaction and corresponding electrode potential E are as follows:

$$2\mathrm{HCHO} + 4\mathrm{OH}^{-} \rightarrow 2\mathrm{HCOO}^{-} + \mathrm{H_2} + 2\mathrm{H_2O} + 2e^{-} \tag{1-15}$$

E= -0.32-0.12 pH

The electrode potential E of reduction of Cu^{2+} to Cu is 0.334V. It can be known that only in alkaline medium with pH greater than 11, formaldehyde could be reduced. However, in alkaline solution, Cu^{2+} is easy to be changed into the precipitation of $Cu(OH)_2$, so the complexing agent must be added to the plating solution.

1.4.2 Kinetic Principle of Electroless Copper Plating

Theoretically, the study of the electroless plating rate can be expressed by the speed of decrease of the reactants and the speed of increase of the product, but in the actual electroless plating process, some additives are usually added to the solution, which complicates the problem. Therefore, most researchers only consider the effects of the basic components in the bath. The rate of electroless copper plating with formaldehyde as a reducing agent can be shown as follows:

$$r{=}K\left[\mathrm{Cu}^{2+}\right]^{a}\left[\mathrm{OH}^{-}\right]^{b}[\mathrm{HCHO}]^{c}\left[\mathrm{L}\right]^{d} \tag{1-16}$$

Where L represents complexing agent and a, b, c, d represent the reaction order of the four main components, respectively.

Donahue et al. [78,79] used EDTA as a complexing agent to conduct experiments on a great number of different plating solutions and obtained the conclusion below:

$$r=2.81\frac{\left[\mathrm{Cu}^{2+}\right]^{0.43}\left[\mathrm{HCHO}\right]^{0.16}}{\left[\mathrm{OH}^{-}\right]^{0.70}\left[\mathrm{EDTA}\right]^{0.04}}\exp\left[11.5\frac{(T\text{-}313)}{T}\right] \tag{1-17}$$

Shippey et al. [80] selected tartrate as complexing agent, and the reaction rate of electroless copper plating was as follows:

$$r=k\left[\mathrm{Cu}^{2+}\right]^{0.47}[\mathrm{HCHO}]^{1.7}\left[\mathrm{OH}^{-}\right]^{0.08}[\mathrm{L}]^{\mathrm{d}}\exp\left(-\frac{E_a}{T}\right) \tag{1-18}$$

Although the researchers only consider the influence of the basic components in the plating solution, the data obtained are still quite different, mainly for the following reasons.

(1) Different material of electroless copper plating substrate

Some use metal substrates, while others use catalytically treated non-metallic materials. For a catalytically active metal matrix, the number of catalytic active centers on its surface is more than that on the surface of non-metallic materials after activation.

(2) Different measuring time

The reaction rate of electroless plating is not constant, and it will change with time. Usually the initial plating rate will be higher than the steady plating rate thereafter.

In order to obtain more realistic kinetic data, the researchers used many advanced testing techniques, such as quartz microbalance technology, to measure nanogram weight changes and can be used for in-situ real-time testing, but the kinetics process remains to be further studied.

(3) The influence of mass transfer factors

The interfacial concentration of the reactant is different from that of the solution itself. The interfacial concentration is affected by many factors, such as the thickness of the diffusion layer, the stirring method and the diffusion coefficient of the reactant.

In order to obtain more real kinetic data, researchers have adopted many advanced testing techniques, such as quartz microbalance technology, which can measure nanogram weight changes and can be used for in-situ real-time measurement, but the kinetics process still needs further study.

1.4.3 Reaction Mechanism of Copper Reduction by Formaldehyde

In an alkaline environment with PH greater than 11, there are two basic chemical reactions in the process of electroless copper plating using formaldehyde as reducing agent.

Reduction reaction:

$$\mathrm{Cu}^{2+} + 2e^{-} \rightarrow \mathrm{Cu}^{0} \tag{1-19}$$

Oxidation reaction:

$$2\mathrm{HCHO} + 4\mathrm{OH}^{-} \rightarrow 2\mathrm{HCOO}^{-} + \mathrm{H}_2 + 2\mathrm{H}_2\mathrm{O} + 2e^{-} \tag{1-20}$$

The chemical reaction takes place on the surface with catalytic activity. The electrons required for the reduction of copper ions are all provided by the reductant and there are no external electrons. The total reaction formula of electroless copper plating is as follows:

$$\mathrm{Cu}^{2+} + 2\mathrm{HCHO} + 4\mathrm{OH}^{-} \rightarrow \mathrm{Cu}^{0} + 2\mathrm{HCOO}^{-} + \mathrm{H}_2 + 2\mathrm{H}_2\mathrm{O} \tag{1-21}$$

The anodic reaction of electroless copper plating is much more complicated than the Reaction (1-20), and the process may be as follows:

$$\mathrm{HCHO} + \mathrm{H}_2\mathrm{O} \rightarrow \mathrm{H}_2\mathrm{C(OH)}_2 \tag{1-22}$$

$$\mathrm{H_2C(OH)_2} + \mathrm{OH}^{-}_{\mathrm{ad}} \rightarrow \mathrm{H_2C(OH)O}^{-}_{\mathrm{ad}} + \mathrm{H_2O} \tag{1-23}$$

$$\mathrm{H_2C(OH)O}^{-}_{\mathrm{ad}} \rightarrow \mathrm{HCOOH} + \frac{1}{2}\mathrm{H}_2 + e^{-} \tag{1-24}$$

$$\mathrm{HCOOH} + \mathrm{OH}^{-} \rightarrow \mathrm{HCOO}^{-} + \mathrm{H_2O} \tag{1-25}$$

The Reaction (1-22) indicates that formaldehyde is mainly present in the form of the hydrate $H_2C(OH)_2$ in an aqueous alkaline solution with pH value greater than 11. The Reaction (1-23) indicates that electrochemically active $H_2C(OH)_2$ and OH^- adsorbed on the reaction interface react to produce electrochemically active methylene dihydroxy anion, namely $H_2C(OH)O^-$. The Reaction (1-24) is an electronic transition process, and formaldehyde is oxidized to formic acid, which is a controlling step of plating rate.

1.5 Conductive Mechanism of Conductive Particle Filling Materials

There are many reports on the conductive mechanism of conductive particle filling materials, but most of them are different. This chapter mainly introduces the formation process of the conductive network and the migration process of carriers during the filling process of conductive particles. The former is the macroscopic performance of the matrix fibers in the process of increasing the conductive particles in the early stage. The description of the latter mainly describes the microscopic phenomenon in the conductive fibers accompanying the increase of conductive particles after the formation of the late conductive network. The mechanism of the formation of conductive networks in conductive filled conductive materials is also widely discussed. The most convincing and representative ones mainly are the percolation theory, the interface thermodynamics theory, and the effective medium theory.

1.5.1 Percolation Theory

The percolation theory mainly explains the influence of the change of the conductive particle content on the electrical conductivity of the fiber. Generally, the formation of the conductive channels requires the conductive fillers to contact each other or the particle gap is less than 1 nm. When the content of the conductive particles in the matrix fibers is low, the spacing between the conductive particles is too large to form an effective conductive network. The electrical conductivity depends on the electrical conductivity of the matrix fibers themselves.

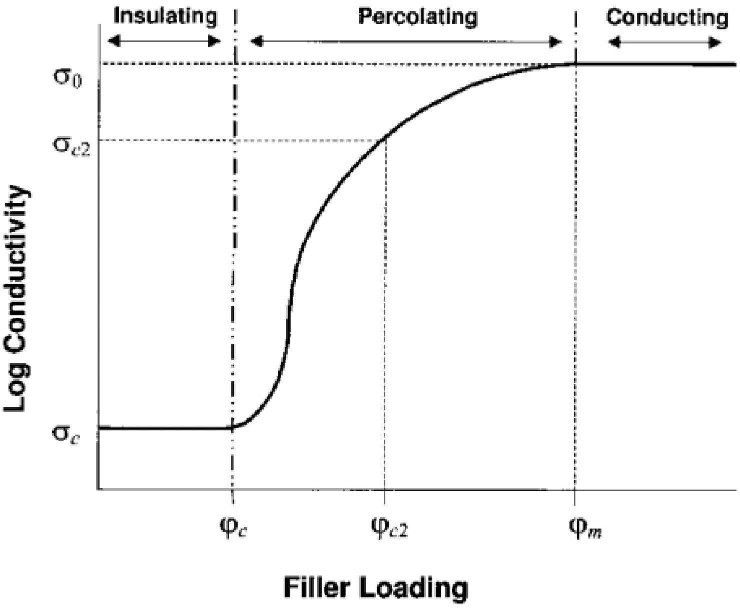

Figure 1-3. Theoretical shape of an electrical percolation curve of a composite [81]

As the conductive filler increases, the electrical conductivity of the composite initially increases slightly, which is called the insulating region. When the amount of conductive filler reaches a certain critical value, the conductivity suddenly increases, increasing by several orders of magnitude. This phase is called the percolating region. This phenomenon is the percolation effect [81], and the critical value φ_c is called percolation. When the content of the conductive filler exceeds the value of the percolation threshold, the conductive network is basically perfect, and the change in conductivity tends to be stable, which is a conducting region, as shown in Figure 1-3 [81]. This is because the conductive filler is randomly distributed in the polymer matrix and is distributed in isolation at low contents. With the increase of conductive fillers, the conductive grid gradually evolves from a partial construction to an infinite continuous conductive network, providing a channel for electron transmission, which is also an increase in the conductivity performance. The percolation theory uses a statistical method to calculate the degree of contact of conductive particles in a simulated polymer conductive composite, and then to estimate the relationship between the amount of filler and the conductivity.

Kirkpatrick [82,83] first successfully applied the classical statistical percolation model to a binary conductive hybrid system. Subsequently, Aharoni [84] improved it, and Janzen [85] used Aharoni's concept and combined with Kirkpartrick's percolation calculation results to derive the percolation equation:

$$\varphi_c = 1/\left(1+0.67z\rho\varepsilon\right) \tag{1-26}$$

In the above formula (1-26), φ_c is the percolation threshold, z is the coordination number, ρ is the packing density, and ε is the specific pore volume of the filler particles.

Near the percolation threshold, the relationship between the electrical conductivity of the composite and the volume fraction of the conductive filler in the matrix is as follows [86]:

$$\sigma_m = \sigma_h(\varphi - \varphi_c)^t \tag{1-27}$$

Where σ_m is the conductivity of the conductive composite, σ_h is the conductivity of the filler, φ is the volume fraction of the filler, φ_c is the percolation critical volume fraction of the filler, t is the fitting index, depends on the lattice dimension [81, 87]. This model does not accurately calculate the conductivity of the material but plays a fundamental role in subsequent theoretical model studies.

1.5.2 Interface Thermodynamics Theory

The percolation theory is mainly analyzed from the aspects of the influence of the change of conductive particle content on the electrical conductivity of the fiber. The interface thermodynamics theory mainly expounds the influence of the properties of the matrix polymer and the free energy of the interface on the conductivity of the material. The study by Sumitau [88] suggested that the formation of the conductive network in the matrix is related to the total interface free energy of the system. When the total interface free energy can reach a universal constant Δg which is independent of the matrix, the conductive network begins to form. The critical volume fraction (Φ_c) can be obtained by the formula below:

$$\Phi_c = \left\{1 + 3K/\Delta gR\left[1-\left(1-P_{(0)}/P_{(\omega)}\right)\exp\left(-t/\tau_0\right)\right]\right\}^{-1} \tag{1-28}$$

In the above formula, $P_{(0)}$ is the fraction of the contact particles in the initial state, $P_{(\omega)}$ is the fraction of the contact particles in the equilibrium state, t is the mixing time and the post-processing time, and τ_0 is the delay time of the matrix. The interface thermodynamics theory can explain the arrangement of conductive particles by analyzing the influence of matrix properties and interface free energy on conductivity, but this is often limited to ceramic materials [89].

1.5.3 Effective Medium Theory

The effective medium theory mainly analyzes the influence of the shape and distribution of conductive particles on the properties of conductive particle filling materials [89]. According to the effective medium theory, Mclachlan proposed the effective media universal equation (GEM), whose expression is [90,91]:

$$(1-\varphi)\left(\sigma_1^{1/t}-\sigma_m^{1/t}\right)\Big/\left(\sigma_1^{1/t}+A\sigma_m^{1/t}\right)+\varphi\left(\sigma_h^{1/t}-\sigma_m^{1/t}\right)\Big/\left(\sigma_h^{1/t}+A\sigma_m^{1/t}\right)=0 \qquad \text{(1-29)}$$

In the above formula (1-29), $A=\left(1-\varphi_c\right)\varphi_c$, φ is the volume fraction of the conductive filler, φ_c is the critical volume fraction, and σ_1, σ_h, σ_m are the low conductivity components, the high conductivity components and the composite conductivity, respectively. t is the parameter [89].

The single percolation theory can only fit the percolation threshold and dimensional parameters through the experimental results, and the above equation can not only accurately fit the percolation curve of binary composite system through the effective medium theory, but also analyze and discuss the influence of temperature, mechanical stress, magnetic field and other external fields on the composite material. The effective medium theory considers that the conductivity of materials is related to both the conductive filler and the matrix.

The GEM equation, which combines the effective medium theory with the percolation theory, can predict the conductivity of two-phase composite systems with different particle morphologies and distributions, which provides a strong basis for the design of conductive composites. However, this theory does not reveal how the matrix and interface participate in conduction [89].

1.6 Laser Plating Technology

1.6.1 Laser Induced Metal Deposition

Laser plating technology, also commonly known as laser-induced metal deposition, is to use the thermal and optical effects of laser light to plate metal particles on the surface of the material. Compared with the traditional electroless plating method, laser-induced deposition of precious metal particles has become a hot topic in current research because of its advantages of simple operation, material saving, pollution-free and efficient reduction of metal ions [92]. There are two main types of such photochemical reactions of metal particles [93]. One is that under the action of a laser, metal ions directly acquire electrons from the surrounding environment to form metal atoms, which are agglomerated to form metal nanoparticles. The other is that the photosensitive compound absorbs light to produce a reductive intermediate, which is then reduced by metal ions into metal atoms, which agglomerate to form nanoparticles. Figure 1-4 shows the reaction schematic diagram [94-96].

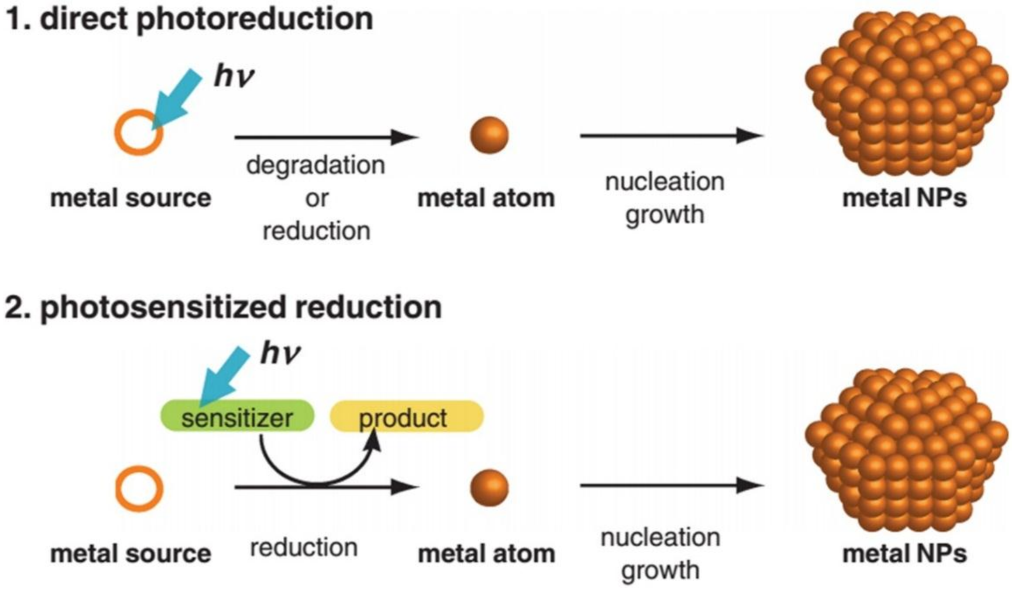

Figure 1-4. schematic scheme of photoreduction of metal ions [94]

In the chapter 4 of this thesis, silver nitrate is used as metal ion source. In the experiment, silver ions absorb the surrounding electrons directly under the action of laser and are reduced to metal atoms. The reaction formula is formula (1-30).

$$Ag^+ + e^- \rightarrow Ag^0 \downarrow \tag{1-30}$$

1.6.2 Laser Induced Metal Deposition Category

Since the 1980s, many attempts have been made on laser-induced metal deposition, mainly including laser-induced chemical vapor deposition (LCVD), laser-induced chemical liquid deposition (LCLD), laser-induced solid film decomposition and deposition, and laser induced electroless plating.

1.6.2.1 Laser-Induced Chemical Vapor Deposition (LCVD)

Laser-induced chemical vapor deposition (LCVD) is a method in which a gaseous substance is decomposed by photothermal or photolysis to form a metal particle deposited on the surface of the substrate under the action of a laser [96]. It is classified into two types: optical LCVD and thermal LCVD [97]. Schematic layout of the LCVD processing system is shown in Figure 1-5 [99]. It includes a gas delivery system, a reaction zone controlled by laser and computer, and a camera for monitoring.

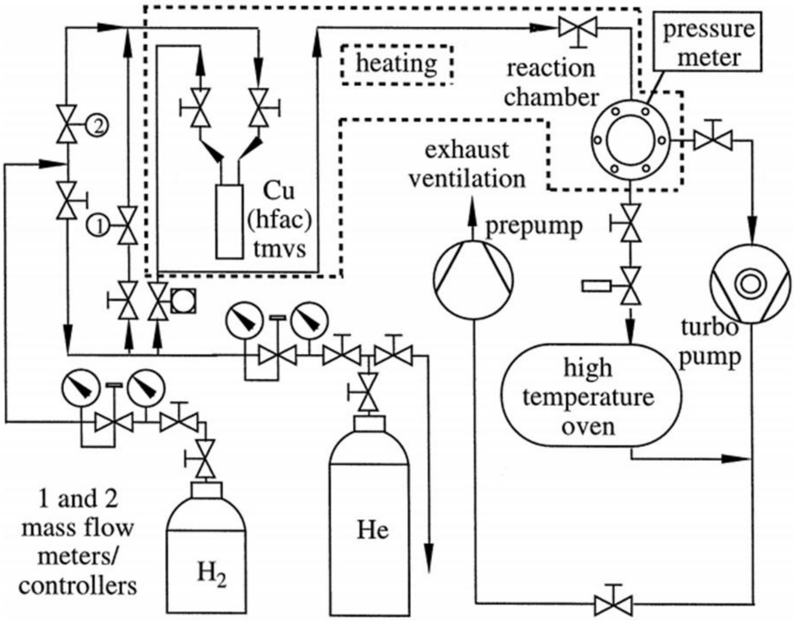

Figure 1-5. Schematic layout of the LCVD processing system [99]

Leppavaori [99] uses laser vapor deposition to treat copper metal compounds to produce pure copper without carbon and oxygen, which has low resistance and can be used to repair electromechanical circuit boards. The advantage of LCVD is the ability to deposit a variety of metals on a variety of substrates, but its shortcomings are also obvious, that is, not only expensive vacuum systems are required, but also some metal-organic vapors are very toxic, which is limited LCVD application in a certain extent.

1.6.2.2 Laser-Induced Chemical Liquid Deposition (LCLD)

Laser-induced chemical liquid deposition (LCLD) refers to the direct irradiation of a solution containing metal ions using a laser in which metal ions are reduced and deposited onto a substrate [100]. The schematic diagram of the experimental device is shown in Figure 1-6.

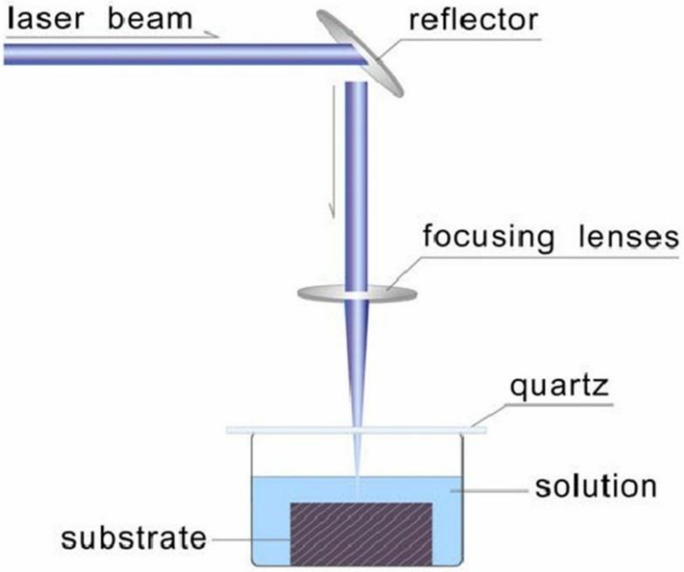

Figure 1-6. Scheme of the LCLD arrangement [99]

The early 1980s witnessed the earlier reports of this study. Yokoyama [101] deposited Mo and Cr from organic solvents of $Mo(C_6H_6)_2$ and $Cr(C_6H_6)_2$, respectively. Since then, people have studied the LCLD implementation methods of different systems [102-109]. Montgomery [101] dissolved an organometallic or inorganic salt in a polar organic solvent and added a photosensitive metal carbonyl compound such as $Mn_2(CO)_{10}$ to the solution. Under laser irradiation, the carbonyl compound undergoes a homogenization reaction which is shown below, and then the radicals produced by the reaction reduce the metal ions. They used this way to deposit silver, copper, and palladium on the glass and quartz.

$$Mn_2(CO)_{10} \xrightarrow{hv} 2Mn(CO)_5 \bullet \qquad (1\text{-}31)$$

Wehner [108] deposited gold and copper from Me_3PAuMe, PEt_3AuCl,and $(PH_3P)_2Cu\ BH_4$ solution with argon ion laser and double-conversion Nd:YAG laser on Polyimide (PI), and deposited gold on SiC with a scanning speed of 0.6 Mm/s. Zahavi [110] studied the process of laser-induced chemical deposition of gold on semiconductor wafers and gallium arsenide and polyimide materials using common gold, palladium, and nickel plating solutions. Liu [111] used CO_2 and laser-induced chemical liquid deposition to deposit metallic silver and studied its mechanism.

The operation of LCLD is also very simple, and there are many types of metal compounds suitable for LCLD. In addition to the organometallic solution, an inorganic salt solution (such as a sulfuric acid solution of nickel sulfate [104]) and an electroless plating solution can also be used for LCLD. Generally speaking, LCLD also has the disadvantage that the deposited metal is too thin. Therefore, CLD is also often used as a method for laser-induced electroless plating.

1.6.2.3 Laser-Induced Solid Metal Compound Film Decomposition and Deposition (LSFDD)

The laser-induced solid metal compound film decomposition and deposition (LSFDD) is to coat the solution containing metal compounds on the matrix material, and after the solvent is volatilized, a metal compound film is formed on the surface of the substrate, followed by a laser with a certain intensity and wavelength is used to act on the metal compound film. Eventually, the compound is deposited onto the surface of the substrate after decomposition by laser action. The schematic diagram is shown in Figure 1-7.

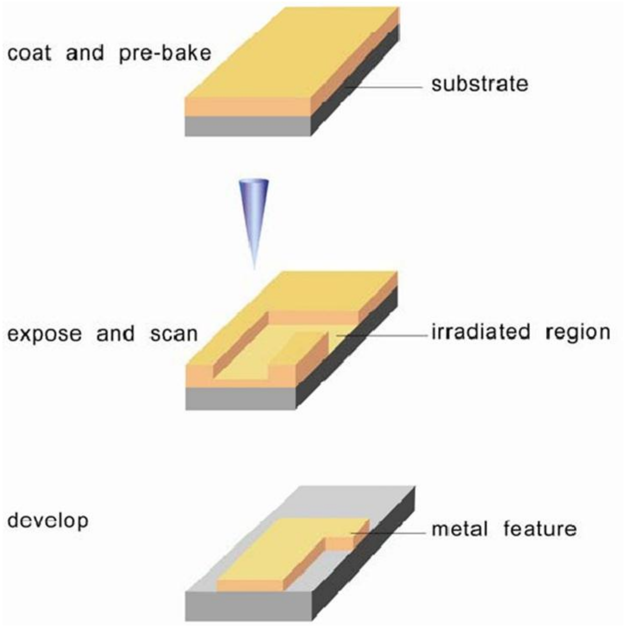

Figure 1-7. Scheme of the laser direct-write process on metal-organic films [115]

Gross [112] and Hilmar [113] respectively applied palladium acetate on quartz, silicon wafers, Al_2O_3, polyimide, and then successfully irradiated metal palladium with different wavelengths of laser irradiation. Gupta [114] produced high purity copper by irradiating the aqueous solution of copper formate coated on silicon wafer with 514 nm argon ion laser. The reaction process is complex and involves both physical and chemical reactions.

LSFDD is a very complex process. Different physical and chemical micro processes often occur at the same time, and it is difficult to distinguish and study them by means of existing research methods. The advantage of this method is that it is easy to operate, fast, and the scanning speed can be up to 1cm/s [115]. Its biggest drawback is that the deposited metal is too thin to meet the requirements of some specific applications. Therefore, this technique is generally used as a method of activating species in a laser-induced electroless plating method.

1.6.2.4 Laser Induced Electroless Plating

As described in section 1.3.1 of this chapter, electroless plating is widely used in various industries because of its ability in metallizing the surface of non-metallic materials, low cost, simple equipment, and good coating quality. However, for electroless plating of non-metallic materials, because electroless copper plating and nickel plating need to be carried out on the surface of materials with catalytic activity, complex pretreatment of the surface of non-metallic materials is needed to make the materials have catalytic activity, including four steps of cleaning, roughening, sensitizing, and activating. The usual method to give the material catalytic activity is to attach some noble metal particles such as gold, palladium and silver to the surface of the material during the pretreatment process.

Laser-induced electroless plating is a process in which noble metal particles are induced to deposit on the surface of materials by laser, and then the noble metal particles are used as activated seeds for direct electroless plating reaction.

The use of the laser-induced deposition of precious metals to activate seeds has many practices, starting with the induction of metal particles by laser-induced vapor deposition and laser-induced liquid deposition. For example, Cole [116] used argon ion laser to vapor-deposit palladium-containing metal compounds to prepare palladium particles and used this as an activated species for electroless copper plating. Zhang [117] used laser-induced vapor deposition and LSFDD method to laser-induced deposition of copper acetylacetonate to prepare copper particle activated seeds. Compared with the complex operation of LCVD, laser-induced solid film decomposition and deposition and LCLD are more widely used later because of their simple operation. Compared to the complex operation of LCVD, laser-induced solid film decomposition deposition and LCLD are applied more frequently after being simple to operate. Stoermer [118] prepared palladium metal particles by laser induction with LCLD method using palladium chloride as material, and selective electroless plating was carried out.

The fourth chapter of this thesis discusses laser-induced electroless plating technology, which is carried out by laser-induced plating on the surface of filter paper to form Nano-silver particles.

1.6.3 Laser Silver Plating Technology

Silver nanomaterials have broad application prospects due to their unique physical and chemical properties, such as electrical, non-linear optical effect, Raman enhancement, light energy conversion effect of biomarkers, catalytic effect and antimicrobial activity, etc. [119]. Therefore, the comprehensive use of various methods to prepare nano-silver particles has also become the focus of research. For example, Wang [120] reduced silver nitrate to silver nanoparticles by liquid phase chemical reduction with polyvinyl pyrrolidone (PVP) as protective agent and ammonium formate as reducing agent. Sun [121] successfully deposited metal Ag and Au on single crystal Si substrate by pulsed Nd:YAG laser. Chen [122] successfully prepared silver nanoparticles on polyimide film by laser-induced electroless plating using PVP/$AgNO_3$ as raw material. But on October 27, 2017, the World Health Organization's International Agency for Research on Cancer published a preliminary list of carcinogens in which Polyvinylpyrrolidone is listed in the list of Category 3 carcinogens.

1.7 Conductive Polymer Material – Polyaniline (PANI)

1.7.1 Overview of PANI

Conductive polymers or, more precisely, intrinsically conducting polymers (ICPs) are organic polymers that conduct electricity. After MacDiarmid Lab of the University of Pennsylvania [123] discovered iodine-doped polyacetylene had metal conductivity in 1976, people began to research and develop conductive polymers. Over time, many conjugated π-bonded polymers have been discovered. By doping these polymers, their electrical conductivity is comparable to that of semiconductors and metal conductors.

Among them, polyaniline is an intrinsic conductive polymer with conjugated electronic structure. It has various structures, special doping mechanism, excellent conductivity and physical properties, and good environmental stability. At the same time, its synthesis method is simple, and its preparation cost is low. Besides, polyaniline has good redox reversibility, electrochemical properties, electromagnetic microwave absorption properties, photoelectric properties, etc., and has become one of the most promising conductive polymers.

Because polyaniline has these advantages, synthesizing polyaniline on the fiber fabrics can make them have long-lasting electrical conductivity and good weather resistance. Therefore, polyaniline has broad application prospects in the textile field.

1.7.2 Structure of PANI

The characteristics of polyaniline mainly rely on its complex and diverse structure, and the changes in doping conditions and the different synthetic methods lead to large differences in the structure of polyaniline. In 1987, MacDiarmid proposed a head-to-tail linear polymer structure [123], which is a regular polyaniline structure. The polyaniline in intrinsic state generally consists of two parts, a reduction unit and an oxidation unit.

The reduced portion of polyaniline is phenylenediamine (Figure 1-8a) and the oxidized moiety is quinodiimide (Figure 1-8b). The molecular structure of the intrinsic polyaniline is shown in Figure 1-8c [124,125].

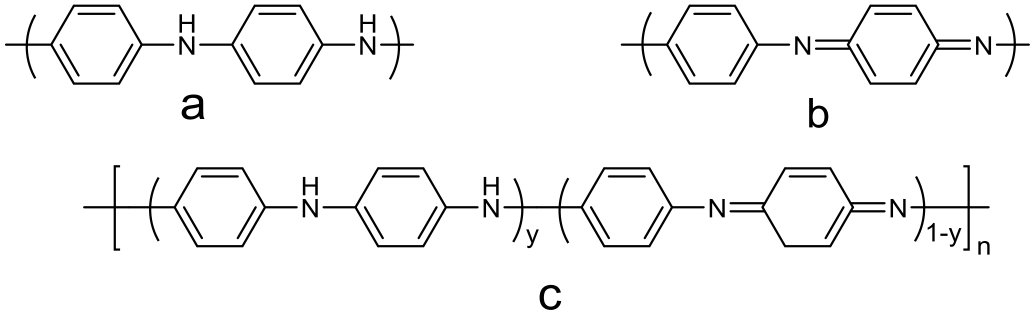

Figure 1-8. Molecular formula of intrinsic Polyaniline

Polyaniline is different from some intrinsic conductive polymers, such as poly-pyrrole and polythiophene, because the number of reducing units and oxidizing units can be relatively changed.

In the above structural model of polyaniline (Figure 1-8c), the degree of redox of polyaniline is represented by y value ($0 \leq y \leq 1$), n is the number of structural units, and polyaniline of different degrees of redox has different structures, components, colors, as well as their different electrical conductivity. There are three typical polyaniline structural forms [126, 127]. When y=1, polyaniline is the fully reduced state and full benzene structure, known as leucoemeraldine (LEB), at which time the polyaniline has no conductivity. When y=0, polyaniline is the fully oxidized state and "Benzo-quinone" alternating structure, known as pernigraniline (PE), at which time polyaniline is the highest oxidized state and has also no conductivity. When y=0.5, the number of oxidizing units is equal to that of the reducing units. At this time, polyaniline is a semi-oxidized and semi-reductive structure, known as emeraldine base (EB), with a Benzo-quinone ratio of 3:1. At this time, polyaniline is a stable intermediate oxidation, which can be abruptly changed from an insulating state to a conductive state by proton acid doping and has high electrical conductivity.

The color change is associated with polyaniline in different oxidation states. Polyaniline in LEB state often shows white or colorless, and that in PE shows blue or violet, while green for the emeraldine salt, blue for the emeraldine base [128-130].

The doping process of polyaniline is different from that of other conductive polymers. Usually, the doping of conductive polymers is always accompanied by the gain and loss of electrons in the main chain. While when polyaniline is doped with a protonic acid, the number of electrons does not change. During doping, H^+ first protonates the nitrogen atom on the imine, which causes holes in the valence band of the doped segment on the polyaniline chain, i.e. P-type doping, forming a stable delocalized form of emerald polyimide atom group.

The positive charge carried by the imine nitrogen atom is dispersed along the molecular chain to adjacent atoms by conjugation, thereby increasing the stability of the system. Under the action of the external electric field, the holes move over the entire segment by the resonance of the conjugated π electrons, showing conductivity.

1.7.3 Synthesis of PANI

The most common methods for the synthesis of polyaniline are the chemical synthesis and the electrochemical synthesis, which are obtained by chemical or electrochemical oxidation of aniline monomers, de-doped with a proton base, and then doped with a protonic acid. Besides, there are the plasma polymerization, vacuum evaporation, photopolymerization, and so on.

1.7.3.1 Chemical Synthesis

The chemical synthesis method for preparing polyaniline is to add an oxidizing agent to an acidic medium to initiate oxidative polymerization of the aniline monomer to obtain a doped polyaniline. The chemical reaction formula can be described as follows, where [O] is a generic oxidant [131].

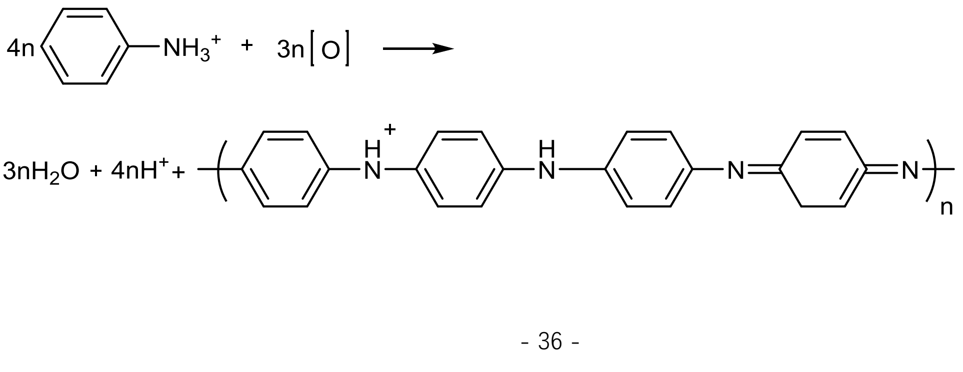

(1-32)

The properties of polyaniline prepared by chemical synthesis are mainly affected by the type and concentration of oxidant, the type of doped acid, the concentration of aniline monomer, the reaction temperature and time.

At present, the main oxidants used are $(NH_4)_2S_2O_8$, $K_2Cr_2O_7$, KIO_3, $FeCl_3$, $CuCl_2$, peroxidase, etc. The protonic acids used are mainly classified into inorganic protonic acids such as HCl, H_2SO_4, HNO_3, and organic camphoric acids such as formic acid, sulfosalicylic acid, camphorsulfonic acid and acetic acid, etc.

The synthesis of polyaniline by chemical synthesis is one of the most commonly used synthesis methods. The synthesis process is simple and low cost, and it is suitable for industrial production. However, other reagents easily remain as impurities in the polymer in the reaction, which affects its performance.

1.7.3.2 Electrochemical Synthesis

The electrochemical method is to carry out oxidative polymerization of the aniline monomers in the electrolyte solution on the anode by selecting appropriate electrochemical conditions and deposit a polyaniline film on the surface of the electrode [132].

The factors influencing the preparation of polyaniline by this method include monomer concentration, acidity of electrolyte solution, anion species in solution, reaction temperature and electrode materials.

The electrochemical synthesis of polyaniline is not only of good quality, but also of high polymerization speed. The reaction conditions of the electrochemical method are mild and easy to control. The product has high purity, no pollution caused by the oxidant, and the electrochemical polymerization and doping are completed in one step. However, the reaction equipment is complex, and the production cost is high, so it is suitable for the synthesis of small batch polyaniline.

1.8 Aim of This Thesis

The past decades have witnessed the emergence of numerous flexible conductive fabrics in pursuit of exploring high performance materials for a wide variety of applications, including biological products for health and sensors, wearable smart devices, static dissipation, electromagnetic shielding, microelectronics industry.

Polyester fibers are widely used in various fields, because of low price, their easy availability, excellent physical and mechanical properties, and chemical stability. Polyester fibers' easily generating static electricity and poor conductivity, limit their applications in clothing, medical, sports, and military [18–20]. Metallic silver is widely used in the surface treatment of materials due to its excellent electrical conductivity [31], ductility [32,33]and catalytic activity [34,35], antibacterial deodorization property [36–39]. The silver plating on the surface of the polyester can retain the original properties of the polyester fiber while imparting them the characteristics of the metallic silver, which enable the polyester fiber to obtain excellent electrical conductivity, antibacterial property, metallic luster and other excellent properties [40–43].

Polyaniline has excellent electrical conductivity, environmental stability and thermal stability and is widely used in various fields. The plating of polyaniline on the surface of the fiber enables the fiber to have excellent electrical conductivity, and has good electrical conductivity durability and weather resistance, which is an excellent property not possessed by the metal conductive fiber. However, polyaniline has poor comprehensive mechanical properties, is insoluble in common organic solvents, and is easily decomposed at high temperatures. It is difficult to process by conventional molding methods, and the electrical conductivity needs to be further improved compared with metallic silver, so the application of polyaniline is limited to some extent. Therefore, the conductive polymer polyaniline is combined with the metallic silver to jointly prepare the conductive fiber, which not only combines the original excellent properties of the two materials, but also enhances the bonding strength of the surface of the fibers by the synergistic effect between the two. It shows better conductive stability and environmental stability, broadens the application field of fiber materials, and provides reference value and theoretical guidance for future applications in military, industrial and civil applications.

There are many methods for preparing conductive fibers. Among them, electroless plating is used to deposit a conductive layer on the surface of the fibers, which does not require complicated machinery and equipment, and the preparation process is simple. Therefore, the electroless silver plating method is used to prepare silver-plated conductive polyester fiber with excellent conductivity in this research. However, in the process of preparing the electroless silver-plated conductive fiber, it was found that the bonding strength between the surface silver layer and the fiber matrix was not satisfactory, and the fiber weather resistance was poor, resulting in a great influence on the fiber properties. Therefore, this study aims to use two methods to improve the silver-plating effect.

One method is to perform cyanide-free electroplating of silver after electroless silver plating to enhance the thickness and bonding fastness of the fiber silver plating layer. Another method is to use electroless plating to coat a polyaniline flexible intermediate layer with good conductive durability and environmental stability between the fibers and silver, and then electroless silver plating to obtain polyaniline-silver double-layer conductive fibers.

In addition, because electroless plating requires complex pretreatment, we attempted to deposit Nano silver particles on polyester fabrics by a simple and efficient laser-induced deposition method as activate seeds, so that the polyester fabric can be directly subjected to patterned electroless copper plating without pretreatment. However, it was found that the laser-induced silver-plating effect of polyester fabrics is not satisfactory, so other flexible substrates are tried.

Paper is also a promising substrate material for flexible electronics fabrication [133–1352] because of its ubiquity, simple preparation, low cost, process-facilitating structure, and green attribute. Because of making from raw plant (such as rags, grasses or wood) cellulose fibers, paper is renewable and recyclable [136]. In addition, paper can be used as a substrate for humanized wearable electronic products due to its good mechanical deformability, biocompatibility, and the least adverse effect on human skin. Most importantly, the porous structure of the paper enhances its superiority over the counterpart in the application of electronic equipment. The porous structure is a masterpiece of interwoven cellulose fibers in paper, which facilitates the coating process that is a standard method of enhancing the electrical properties of paper by increasing the contact field, which further promotes the deposition of conductive additives in intrinsically electrically insulating cellulose fibers. Eventually, this study used flexible filter paper (FP) as the substrate to deposit copper by means of electroless plating through laser-induced deposited silver particles as the seeds.

1.9 Outline of This Thesis

The goal is to prepare flexible conductive fabrics made from polyester fibers or filter papers by means of electroless silver-plating, electroplating silver and laser-induced selective patterned electroless copper plating.

In Chapter 2, the silver-coated polyester fibers were prepared by a continuous two-step method under static condition, which combined the operations of continuous electroless plating and cyanide-free electroplating. Meanwhile, we designed specialized equipment for the continuous plating of silver on the polyester fibers without activating pretreatment. Influences of power supply method, plating voltage, plating time and other related parameters on the preparation of silver-plated fibers were discussed. The mechanical property, washability, electrical resistivity, and electrical conductivity of the resultant conductive polyester fibers obtained from different silver-plating conditions were also characterized.

In Chapter 3, the conductive fibers were prepared by the two-step deposition of PANI and Ag layers on the surface of polyester fibers through oxidative polymerization and redox reaction, respectively. The influence of the preparation process of PANI layer on the properties of PANI-Ag double-layer coated conductive fiber was discussed, and the optimal process parameters for preparing PANI layer were also determined. The surface morphology, surface microstructures, thermal stability, mechanical properties, washing resistance and corrosion resistance of different fibers such as polyaniline (PANI) coated fiber, silver-coated conductive fiber and PANI-Ag coated polyester fiber were characterized and compared, and the advantages of PANI-Ag coated conductive fibers in silver layer quality and conductive stability were further analyzed.

In Chapter 4, a uniform copper pattern with good conductivity properties was obtained on a soft substrate of filter paper/polyacrylonitrile (FP/PANI) film, where the filter paper was commercially available. The pattern of Ag nanoparticles was first produced on an Ag^+-doped FP/PANI composite film, followed by electroless plating of copper using the metal silver nanoparticles as activated seeds. The *in-situ* reduction of silver particles and the formation of the silver agglomeration pattern were induced by laser irradiation technology on the FP/PANI/$AgNO_3$ composite film. The morphology of metal particles on the fabric surface and the conductivity of copper deposited patterns were characterized.

References

1. Li, T.; Lee, J.; Akinwande, D. Nanofabrication down to 10 nm on a plastic substrate. *Journal of Vacuum Science & Technology B* **2011**, *29*, 06FG07, doi: 10.1116/1.3662081.
2. Horobin, W.; Thompson, P.; Clowes, M.; Stedman, L. *How It Works: Science and Technology*, 3rd ed.; Marshall Cavendish Corporation: Tarrytown, NY. USA, 2003; pp. 851, ISBN 9780761473145.
3. Zhou, W.; Reddy, N.; Yang, Y. *Textiles for Protection*; Scott, R.A.; Woodhead Publishing: Sawston, Cambridge, UK, 2005; pp. 3–30, ISBN 1855739216.

4. Šafářová, V.; Grégr, J. Electrical Conductivity Measurement Of Fibers And Yarns. In Proceedings of 7th International Conference-TEXSCI 2010, Liberec, Czech Republic, September 2010.
5. Liu, X.Y.; Xie, M.M.; Li, Y.C.; Zhou, L.; Shao, J.Z. Study on the reduction properties of thiourea dioxide and its application in discharge printing of polyester fabrics. *Fibers Polym.* **2018**, *19*, 1237, doi:10.1007/s12221-018-7765-3.
6. Chaudhary, H.; Gupta, D.; Gupta, C. Multifunctional dyeing and finishing of polyester with sericin and basic dyes. *J. Text. Inst.* **2017**, *108*, 314–324, doi:10.1080/00405000.2016.1165401.
7. Kogo, A.A.; Ismail, I.M.; Yakasai, M.Y. Effects on the electro-mechanical properties of aniline-doped polyester fibric. *Bayero J. Pure Appl. Sci.* **2017**, *10*, 159–162, doi:10.4314/bajopas.v10i1.22.
8. Rojas, J.P.; Conchouso, D.; Arevalo, A.; Singh, D.; Foulds, I.G.; Hussain, M.M. Paper-based origami flexible and foldable thermoelectric nanogenerator. *Nano Energy* **2017**, *31*, 296–301, doi: 10.1016/j.nanoen.2016.11.012.
9. Rastegar, L.; Montazer, M.; Gaminian, H. Multifunctional colored polyester fabric treated with dopamine hydrochloride at room temperature: Higher tensile, hydrophilicity and anti-bacterial properties along with aminolysis. *Fibers Polym.* **2017**, *18*, 1915–1923, doi:10.1007/s12221-017-7012-3.
10. Yin, J.; Nysten, B. Contact electrification and charge decay on polyester fibres: A KPFM study. *J. Electrostat.* **2018**, *96*, 16–22, doi: 10.1016/j.elstat.2018.09.002.
11. Kathirgamanathan, P.; Toohey, M.J.; Haase, J.; Holdstock, P.; Laperre, J.; Schmeer-Lioe, G. Measurements of incendivity of electrostatic discharges from textiles used in personal protective clothing. *J. Electrostat.* **2000**, *49*, 51-70, doi:10.1016/S0304-3886(00)00003-6.
12. Wang, T.; Xu, X.L.; Sui, X.Y.; Wang, L.N. The Antistatic Research of Polyester/Nylon Fabrics Finished by Triblock Copolymer Containing Organic Silicon. *Advanced Materials Research* **2012**, *535-537*, 1569-1572, doi: 10.4028/www.scientific.net/AMR.535-537.1569.
13. Feng, A.F. Properties of honeycomb polyester knitted fabrics. *IOP Conf. Series: Materials Science and Engineering* **2016**, *137*, 012023, doi:10.1088/1757-899X/137/1/012023.

14. Endo, T.; Takeuchi, M.; Hanada, T.; Nakagawa, K.; Komatsu, H.; Nakamura, I. Polyester filament having excellent antistatic properties and process for preparing the same. US: 4035441A, 1973-06-26.

15. Shyr, T.W.; Lien, C.H.; Lin, A.J. Coexisting Antistatic And Water-Repellent Properties Of Polyester Fabric. *Text. Res. J.* **2011**, *81*, 254–263, doi: 10.1177/0040517510380775.

16. Ma, C.Q.; Zhao, S.L.; Huang, G. Anti-static charge character of the plasma treated polyester filter fabric. *J. Electrostat.* **2010**, *68*, 111–115, doi: 10.1016/j.elstat.2009.11.005.

17. Karsunky, U.; Morrison, A.G.; Mach, H.R. Pigment printing process for flame-retardant, low-flammability or nonflammable fibers: polymer or copolymer of vinylidene chloride as pigment binder. US: 5102424A, 1989-06-30.

18. Wang, C.; Guo, R.H.; Lan, J.W.; Tan, L.; Jiang, S.X.; Xiang, C. Preparation of multi-functional fabric via silver/reduced graphene oxide coating with poly(diallyldimethylammonium chloride) modification. *J. Mater. Sci.: Mater. Electron.* **2018**, *29*, 8010–8019, doi:10.1007/s10854-018-8807-8.

19. Kumar, N.; Ginting, R.T.; Ovhal, M.; Kang, J.W. All-solid-state flexible supercapacitor based on spray-printed polyester/PEDOT:PSS electrodes. *Mol. Cryst. Liq. Cryst.* **2018**, *660*, 135–142, doi:10.1080/15421406.2018.1456125.

20. Smith, D.R.; Mock, J.J.; Starr, A.F.; Schurig, D. Gradient index metaterials. *Phys. Rev. E* **2005**, *71*, 211–230, doi:10.1103/PhysRevE.71.036609.

21. Liu, S.H.; Liu, Z.C.; Wei, G.H. *Electrostatic theory and protection.* Publishing Company of Weapon Industry: Beijing, China; 1999. ISBN:7801326180.

22. Kikunaga, K.; Terasaki, N. Characterization of electrical conductivity of carbon fiber reinforced plastic using surface potential distribution. *Jpn. J. Appl. Phys*. **2018**, *57*, 04FC02. doi:10.7567/jjap.57.04fc02.

23. Parveen, S.; Veena, C. Electrostatic charge dissipation and electromagnetic interference shielding response of polyaniline based conducting fabrics. *Indian J. Pure Ap. Phy.* **2013**, *51*, 112-117.

24. PANIgrahi, S.; Praharaj, S.; Basu, S.; Ghosh, S.K.; Jana, S.; Pande, S.; Vo-Dinh, T.; Jiang, H.J.; Pal, T. Self-aesembly of silver nanoparticles: synthesis, stabilization, optical properties,

and application in surface-enhanced Raman scattering. *J. Phys. Chem. B* **2006**, *110*, 13436–13444. doi: 10.1021/jp062119l.

25. Gulrajani, M.L.; Gupta, D.; Periyasamy, S.; Muthu, S.G. Preparation and application of silver nanoparticles on silk for imparting antimicrobial proper ties. *J. Appl. Polym. Sci.* **2008**, *108*, 614–623, doi: 10.1002/app.27584.
26. MacKeen, P.C.; Person, S.; Warner, S.C.; Snipes, W.; Stevens, S.E. Silver-coated nylon fiber as an antibacterial agent. Antimicro. Agents. Ch. 1987, 31, 93–99, doi: 10.1128/AAC.31.1.93.
27. Ulmer, R.R. Effective Crisis Management through Established Stakeholder Relationships. *Manage. Commun. Q.* **2001**, *14*, 590–615, doi:10.1177/0893318901144003.
28. Liu, M.C. Property and application of silver-based fiber. *Cotton Textile Technology* **2013**, *41*, 62–65.
29. Wakimoto, S.; Misumi, J.; Suzumori, K. New concept and fundamental experiments of a smart pneumatic artificial muscle with a conductive fiber. *Sensor. Actuat. A-Phys.* **2016**, *250*, 48–54, doi: 10.1016/j.sna.2016.08.004.
30. Ye, H.; Li, D.P. The progress in the R & D and application of silver-plated fiber. *China Textile Leader* **2006**, *6*, 54–56.
31. Sekhar, S.C.; Nagaraju, G.; Yu, J.S. Conductive silver nanowires-fenced carbon cloth fibers-supported layered double hydroxide nanosheets as a flexible and binder-free electrode for high-performance asymmetric supercapacitors. *Nano Energy* **2017**, *36*, 58–67, doi: 10.1016/j.nanoen.2017.04.019.
32. Zhang, Z.X.; Dou, J.X.; He, J.H.; Xiao, C.X.; Shen, L.Y.; Yang, J.H.; Wang, Y.; Zhou, Z.W. Electrically/infrared actuated shape memory composites based on a bio-based polyester blend and graphene nanoplatelets and their excellent self-driven ability. *J. Mater. Chem. C* **2017**, *5*, 4145–4158, doi:10.1039/C7TC00828G.
33. Lu, Y.; Jiang, J.W.; Yoon, S.; Kim, K.S.; Kim, J.H.; Park, S.; Kim, S.H.; Piao, L. High-performance stretchable conductive composite fibers from surface-modified silver nanowires and thermoplastic polyurethane by wet spinning. *ACS Appl. Mater. Interfaces* **2018**, *10*, 2093–2104. doi:10.1021/acsami.7b16022.

34. Liang, Y.Y.; Lin, C.X.; Guan, J.P.; Li, Y.J. Silver nanoparticle-immobilized porous POM/PLLA nanofibrous membranes: Efficient catalysts for reduction of 4-nitroaniline. *RSC Adv.* **2017**, *7*, 7460–7468, doi:10.1039/C6RA28167B.

35. Li, M.M.; Gong, Y.M.; Wang, W.H.; Xu, G.P.; Liu, Y.F.; Guo, J. In-situ reduced silver nanoparticles on populus fiber and the catalytic application. *Appl. Surf. Sci.* **2017**, *394*, 351–357, doi: 10.1016/j.apsusc.2016.10.094.

36. Mahmud, S.; Sultana, M.Z.; Pervez, M.N.; Habib, M.A.; Liu, H.H. Surface Functionalization of "Rajshahi Silk" Using Green Silver Nanoparticles. *Fibers* **2017**, *5*, 35, doi:10.3390/fib5030035.

37. Li, X.Q.; Shi, C.; Wang, J.D.; Wang, J.; Li, M.J.; Hua, Q.; Hong, S.; Ogino, K. Polyaniline-doped TiO_2/PLLA fibers with enhanced visible-light photocatalytic degradation performance. *Fibers Polym*. **2017**, *18*, 50–56, doi:10.1007/s12221-017-6895-3.

38. Islam, S.; Sun, G. Thermodynamics, kinetics, and multifunctional finishing of textile materials with colorants extracted from natural renewable sources. *ACS Sustain. Chem. Eng.* **2017**, *5*, 7451–7466, doi:10.1021/acssuschemeng.7b01486.

39. Gan, X.P.; Wu, Y.T.; Liu, L.; Shen, B.; Hu, W.B. Electroless copper plating on PET fabrics using hypophosphite asreducing agent. *Surf. Coat. Technol.* **2007**, *201*, 7018–7023, doi: 10.1016/j.surfcoat.2007.01.006.

40. Kim, M.S.; Kim, H.K.; Byun, S.W.; Jeong, S.H.; Hong, Y.K.; Joo, J.S.; Song. K.T.; Kim, K.; Lee, C.J.; Lee, J.Y. PET fabric/polypyrrole composite with high electrical conductivity for EMI shielding. *Synth. Met.* **2002**, *126*, 233–239, doi:10.1016/S0379-6779(01)00562-8.

41. Zhou, Q.H.; Chen, H.W.; Wang, Y. Region-selective electroless gold plating on polycarbonate sheets by UV-patterning in combination with silver activating. *Electrochim. Acta* **2010**, *55*, 2542–2549, doi: 10.1016/j.electacta.2009.12.024.

42. Li, X.Q.; Wang, J.D.; Li, M.J.; Yang, J.; Gu, Z.J.; Liu, C.C.; Ogino, K. Fe-doped TiO_2/SiO_2 nanofibrous membranes with surface molecular imprinted modification for selective removing 4-Nitrophenol. *Chin. Chem. Lett.* **2018**, *29*, 527–530, doi: 10.1016/j.cclet.2017.09.007.

43. Chen, D.X.; Kang, Z.X. ABS plastic metallization through UV covalent grafting and layer-by-layer deposition. *Surf. Coat. Technol.* **2017**, *328*, 63–69, doi: 10.1016/j.surfcoat.2017.08.020.

44. Qinghua Zhou, Hengwu Chen, Yi Wang. Region-selective electroless gold plating on polycarbonate sheets by UV-patterning in combination with silver activating. *Electrochimica Acta* **2010**, *55*, 2542–2549, doi.org/10.1016/j.electacta.2009.12.024
45. Jayaraman, S.; Park, S. Method and apparatus to create electrical junctions for information routing in textile structures. US: 10759691, 2004-01-15.
46. Ozen, M.S.; Usta, I.; Yuksek, M.; Sancak, E.; Soin, N. Investigation of the Electromagnetic Shielding Effectiveness of Needle Punched Nonwoven Fabrics Produced from Stainless Steel and Carbon Fibres. *Fibres Text. East. Eur.* **2018**, *127*, 94–100, doi: 10.5604/01.3001.0010.5636.
47. Wan, Z.P.; Tang, Y.; Liu, Y.J.; Liu, W.Y. High efficient production of slim long metal fibers using bifurcating chip cutting. *J. Mater. Process. Tech.* **2007**, *189*, 273–278, doi: 10.1016/j.jmatprotec.2007.01.036.
48. Lavenne, A.; Tatat, O.; Bonicel, J.P. Method for accessing optical fibers within a telecommunication cable. US: 7817891B2, 2007-04-11.
49. Dhaw,S.K.; Singh, N.; Venkatachalam, S. Shielding effectiveness of conducting polyaniline coated fabrics at 101GHz. *Synthetic met.* **2001**, *125*, 389–393, doi: 10.1016/S0379-6779(01)00478-7.
50. Geetha, S.; Kumar, K.K.S.; Rao, C.R.K.; Vijayan, M.; Trivedi, D.C. EMI shielding: Methods and materials—A review. *J. Appl. Polym. Sci.* **2009**, *112*, 2073–2086, doi: 10.1002/app.29812.
51. Alimohammadi, F.; Gashti, M.P.; Shamei, A. A novel method for coating of carbon nanotube on cellulose fiber using 1, 2, 3, 4-butanetetracarboxylic acid as a cross-linking agent. *Prog. Org. Coat.* **2012**, *74*, 470–478, doi: 10.1016/j.porgcoat.2012.01.012.
52. Zhang, H.; Guo, L.; Shao, H.; Hu, X. Nano-carbon black filled Lyocell fiber as a precursor for carbon fiber. *J. Appl. Polym. Sci.* **2006**, *99*, 65-74, doi: 10.1002/app.22184.
53. Chen, S.L.; Hou, H.Q.; Harnisch, F.; Patil, S.A.; Carmona-Martinez, A.A.; Agarwal, S.; Zhang, Y.Y.; Sinha-Ray, S.; Yarin, A.L.; Greiner, A.; Schröder, U. Electrospun and solution blown three-dimensional carbon fiber nonwovens for application as electrodes in microbial fuel cells. *Energy Environ. Sci.* **2011**, *4*, 1417–1421, doi: 10.1039/C0EE00446D.

54. Nakajima, T.; Kajiwara, K.; McIntyre, J.E. Advanced Fiber Spinning Technology; Woodhead publishing limited: Cambridge, England, 2000; pp. 25–63, ISBN 1855731827.
55. Li, J.X.; Jin, L.G. Development and Application of Conductive Fibers. *Knitting Industry*, **2004**, *4*, 72–73.
56. Chang, K.; Cheng, B.W.; Ren, Y.L. Development Status and Application Prospects of Conductive Fibers. *Textile Science Research*, **2016**, *3*, 32–39.
57. Tian, Q.W.; Jiang, F.R.; Zou, R.J.; Liu, Q.; Chen, Z.G.; Zhu, M.F.; Yang, S.P.; Wang, J.L.; Wang, J.H.; Hu, J.Q. Hydrophilic Cu_9S_5 Nanocrystals: A Photothermal Agent with a 25.7% Heat Conversion Efficiency for Photothermal Ablation of Cancer Cells in Vivo. *ACS Nano*, **2011**, *5*, 9761–9771, doi: 10.1021/nn203293t.
58. Li, Y.; Chen, T.T.; Yang, X.D. Conductive fibers for textiles and their applications. *Industrial Textiles*, **2010**, *4*, 32–34.
59. Tran, T.Q.; Fan, Z.; Liu, P.; Myint, S.M.; Duong, H.M. Super-strong and highly conductive carbon nanotube ribbons from post-treatment methods. *Carbon* **2016**, *99*, 407–415, doi: 10.1016/j.carbon.2015.12.048.
60. Jalili, R.; Razal, J.M.; Innis, P.C.; Wallace, G.G. One-step wet-spinning process of poly(3,4‐ethylenedioxythiophene): poly(styrenesulfonate) fibers and the origin of higher electrical conductivity. *Adv. Funct. Mater.* **2011**, *21*, 3363–3370, doi: 10.1002/adfm.201100785.
61. Li, N. *Practical Technology of Electroless Plating*; Chemical Industry Press: Beijing, China, 2004; pp. 1–20, ISBN 750254857.
62. China Asset Management Network. Introduction to electroless plating technology and related applications. *Surface Engineering Information*, 2008, 3, 42.
63. Liu, R.Z. *Non-metal plating and finishing*, Chemical Industry Press: Beijing, China, 2012; pp.248–250, ISBN 9787122138293.
64. Yoshio, K.; Verónica, S.M.; Luis, M. L.M. Deposition of silver nanoparticles on silica spheres by pretreatment steps in electroless plating. *Chem. Mater.* **2001**, *13*, 1630–1633, doi: 10.1021/cm001240g.

65. Liang, T.X.; Guo, W.L.; Yan, Y.H.; Tang, C.H. Electroless plating of silver on graphite powders and the study of its conductive adhesive. *Int. J. Adhes. Adhes.* **2008**, *28*, 55–58, doi: 10.1016/j.ijadhadh.2007.03.006.
66. Wang, Z.; Zhao, Y.X. Research on surface pretreatment of polyurethane fiber. *Synthesis Technology and Applications*, **2017**, *02*, 14–18.
67. Wataha, J.C.; Hanks, C.T. Biological effects of palladium and risk of using palladium in dental casting alloys. *J. Oral Rehabil.* **1996**, *23*, 309–320, doi:10.1111/j.1365–2842.1996.tb00858.x.
68. He, Z.; Zhan, L.; Wang, Q.; Song, S.; Chen, J.; Zhu, K.; Xu, X.H.; Liu, W.P. Increasing the activity and stability of chemi-deposited palladium catalysts on nickel foam substrate by electrochemical deposition of a middle coating of silver. *Sep. Purif. Technol.* **2011**, *80*, 526–532, doi: 10.1016/j.seppur.2011.06.007.
69. Ling, M.H.; Zhang, H. Effect of reducing agent on the electroless silver plating performance of polyester fabrics. *Electroplating & Environmental Protection* **2011**, *31*, 31–34.
70. Ye, H. Development and Application of Silver-plated Fibers. *Textile Review* **2006**, *6*, 54–56.
71. Li, H.W. *Experimental methods and techniques for electroplating process*; Publisher: Science Press, Beijing, China, 2016; pp. 135–161, ISBN 703017196.
72. Schlesinger, M.; Paunovic, M. *Modern electroplating*, 5th ed.; Publisher: John Wiley & Sons, Inc., Hoboken, New Jersey, Canada, 2011; pp. 1–3, ISBN: 978-1-118-06314-9.
73. Zhu. X.H.; Li, N.; Li, D.Y. Conducting treatment of nonmetallic substrate. *Electroplating & Finishing*, **2009**, *31*, 35–38.
74. Horner, J. Cyanide Copper Plating. *Plat. Surf. Finish*. **2004**, *91*, 13–15.
75. Dimitrijević, S.; Rajčić-Vujasinović, M.; Trujić, V. Non-Cyanide Electrolytes for Gold Plating – A Review. *Int. J. Electrochem. Sci.* **2013**, *8*, 6620–6646.
76. Fang, J.L. *Electroplating Complexes-Theory and Application*; Publisher: Chemical Industry Press, Beijing, China, 2010, ISBN:9787122011077.
77. Xiao, Y. Research on cyanide-free electrodeposited silver technology. *Guangdong Chemical Industry*, **2015**, 42, 98–99.
78. Donahue, F.M.; Wong, K. L. M.; Bhalla, R. Kinetics of electroless copper plating: IV. empirical rate law for formula baths. *J. Electrochem. Soc.* **1980**, *127*, 2340–2342, doi: 10.1149/1.2129409.

79. Donahue, F. M.; Sajkowski, D. J.; Bosio, A. C.; Schafer, L.L. Kinetics of electroless copper plating: VI. inhibition by adsorption of ligand, *J. Electrochem. Soc.* **1982**, *129*, 717–719, doi: 10.1149/1.2123957.
80. Shippey, F. L.; Donahue, F. M. Kinetics of Electroless Cu Plating. Pt. 1. Empirical Rate Law, *Plating*, **1973**, 60(1): 43–46.
81. Babince, S.J.; Mussell, R.D.; Lundgard, R.L.; Cieslinski, R. Electroactive Thermoplastics. *Adv. Mater.* **2000**, *12*, 23, 1823–1834, doi:10.1002/1521-4095(200012)12:23<1823:AID-ADMA1823>3.0.CO;2-6.
82. Kirkpatrick, S. Percolation and conduction. *Rev. Mod. Phys.* **1973**, *45*, 574, doi: 10.1103/RevModPhys.45.574.
83. Shante, V.K.S.; Kirkpatrick, S. An introduction to percolation theory. *Adv. Phys.* **1971**, *20*, 325–357, doi: 10.1080/00018737100101261.
84. Aharoni, S.M. Electrica I resistivity of a composite of conducting particles in an insulating matrix. *Appl. Phys.* **1972**, *43*, 2463–2465, doi: 10.1063/1.1661529.
85. Janzen, J. On the critical conductive filler loading in antistatic composites. *Appl. Phys.* **1975**, *146*, 966–969, doi: 10.1063/1.321629.
86. Stauffer D. Aharnoy A. *Introduction to percolation theory*, 2nd ed.; London: Taylor & Francis Ltd: London, UK, 1991; ISBN 0-203-26914-4.
87. Huang, J.C. Carbon black filled conducting polymers and polymer blends. *Adv. Polym. Tech.* **2002**, *21*, 299–313, doi.org/10.1002/adv.10025.
88. Sumita, M.; Takenaka, K.; Asai, S. Characterization of dispersion and percolation of filled polymers: Molding time and temperature dependence of percolation time in carbon black filled low density polyethylene. *Compos. Interface*, **1995**, *3*, 253–262, doi: 10.1163/156855495X00228.
89. Zhou, J.; Sun, H.B.; Zheng, W.; Liu, J.C. Electrical mechanism of particle-filled conductive composites. *Journal of Ceramics* **2009**, *30*, 281–285.
90. Clingerman, M.L.; King, J.A.; Schulz, K.H.; Meyers, J.D. Evaluation of electrical conductivity models for conductive polymer composites. *J. Appl. Polym. Sci.* **2002**, *83*, 1341–1356, doi: 10.1002/app.10014.

91. Mclachlan, D.S.; Blaszkiewicz, M.; Newnham, R.E. Electrical resistivity of composites. *Am. Ceram. Soc.* **1990**, *73*, 2187–2203, doi: 10.1111/j.1151-2916.1990.tb07576.x.

92. Wang, J.Q.; Zhang,X.Z.; Sun, L.P. Laser-induced silver nanoparticle film and microstructure. *China Laser*, **2011**, 38, 174–178.

93. Sakamoto, M.; Fujistuka, M.; Majima, T. Light as a construction tool of metal nanoparticles: Synthesis and mechanism. *J. Photoch. Photobio. C: Photochemistry Reviews* **2009**, *10*, 33–56, doi: 10.1016/j.jphotochemrev.2008.11.002.

94. Sakamoto, M.; Majima, T. Photochemistry for the synthesis of noble metal nanoparticles. *Bull. Chem. Soc. Jpn.* **2010**, *83*, 1133–1154, doi:10.1246/bcsj.20100097.

95. Tahir, M.; Tahir, B.; Amin, N.A.S. Synergistic effect in plasmonic Au/Ag alloy NPs co-coated TiO2 NWs toward visible-light enhanced CO2 photoreduction to fuels. *Appl. Catal. B-Environ.* **2017**, *204*, 548–560, doi: 10.1016/j.apcatb.2016.11.062.

96. Singh, S.C.; Zeng, H.B.; Guo, C.L.; Cai, W.P. *Nanomaterials: Processing and Characterization with Lasers*; Publishing: John Wiley & Sons: Toronto, Canada, 2012, 700; pp. ISBN: 9783527646845.

97. Baum, T.H.; Comita, P.B. Laser-induced chemical vapor deposition of metals for microelectronics technology. *Thin Solid Films* **2002**, *218*, 80–94, doi:10.1016/0040-6090(92)90907-S.

98. Bäuerle, D.; Irsigler,P.; Leyendecker, G.; Noll, H.; Wagner, D. Ar^+ laser induced chemical vapor deposition of Si from SiH_4. *Appl. Phys. Lett.* **1982**, *40*, 819, doi: 10.1063/1.93272.

99. Leppavuori, S.; Remes, J.; Moilanen, H. Utilisation of Cu(hfac)tmvs precursor gas in LCVD integrated circuit repair system. *Appl. Surf. Sci.* **1999**, *138–139*, 123–129, doi: 10.1016/S0169-4332(98)00418-8.

100. Müller, H.G. YAG laser direct writing of copper from copper formate films. *Appl. Phys. Lett.* **1990**, *56*, 904–906, doi: 10.1063/1.102624.

101. Yokoyama, H.; Kishida, S.; Washio, K. Laser induced metal deposition from organometallic solution. *Appl. Phys. Lett.* **1984**, *44*, 755–757, doi: 10.1063/1.94906.

102. Montgomery, R.K.; Mantei, T.D. UV laser deposition of metal films by photogenerated free radicals. *Appl. Phys. Lett.* **1996**, *48*,493–495, doi: 10.1063/1.96486.

103. Nánai, L.; Hevesi, I.F.; Bunkin, V. Laser-induced metal deposition on semiconductors from liquid electrolytes. *Appl. Phys. Lett.* **1999**, *54*, 736–738. doi: 10.1063/1.100877.

104. Lu, Y.F.; Takai,M.; Nakata, T. Laser-induced deposition of Ni lines on Ferrite in $NiSO_4$ aqueous solution. *Appl. Phys. A*, **2001**, *54*, 129–134, doi: 10.1007/BF00323729.

105. Geretovszky, Z.; SzÖrényi, T.; Bali, K. Dependence of deposition kinetics on precursor concentration and writing speed in pyrolytic laser depositionfrom solution. *Thin Solid Films,* **2004**, *241*, 67–70, doi: 10.1016/0040-6090(94)90398-0.

106. Minì, L.; Giaconia, C.; Arnone, C. Copper patterning on dielectrics by laser writing in liquid solution. *Appl. Phys. Lett.* **2004**, *64*, 3404–3406, doi: 10.1063/1.111292.

107. Geretovszky, Z.; Kelemen, L.; Bali, K. Kinetic model for scanning laser-induced deposition from the liquid phase. *Appl. Surf. Sci.* **2005**, *86*, 494–499, doi: 10.1016/0169-4332(94)00462-5.

108. Wehner, M.; Legewie, F.; Theisen, B. Direct writing of gold and copper lines from solution. *Appl. Surf. Sci.* **2006**, *106*, 406–411, doi:10.1016/S0169-4332(96)00388-1.

109. Geretovszky, Z.; SzÖrényi, T. Can laser deposition from the liquid phase be made competitive. *Appl. Surf. Sci.* **2007**, *109*, 467–472, doi:10.1016/S0169-4332(96)00786-6.

110. Zahavi, J; Tamir, S; Halliwell, M. Laser-induced deposition on semiconductor and polymeric substrates. *Plat. Surf. Finish.* **1986**, *73*, 57–64.

111. Liu, J.G.; Chen, C.H. Mechanism of CO_2 laser induced liquid deposition of silver. *Journal of Lasers* **2014**, *4*, 82–84.

112. Gross, M.E.; Appelbaum, A.; Gallagher, P.K. Laser direct-write metallization in thin palladium acetate films. *J. Appl. Phys*. **1997**, *61*, 1628–1631, doi: 10.1063/1.338049.

113. Hilmar, H.; Kogelschatz, U. Investigation of the mechanism of the UV-induced palladium deposition process from thin solid palladium acetate films. *Appl. Surf. Sci.* **2009**, *46*, 158–162, doi: 10.1016/0169-4332(90)90136-N.

114. Gupta, A; Jagannathan, R. Laser writing of copper lines from metalorganic films, *Appl. Phys. Lett.* **2017**, *51*, 2254–2256, doi: 10.1063/1.98928.

115. Rickerby, J.; Steinke, J.H.G. Current trends in patterning with copper, *Chem. Rev.* **2012**, *102*,1525–1549, doi: 10.1021/cr0104476.

116. Cole, H.S.; Liu, Y.S.; Rose, J.W.; Guida, R. Laser-induced selective copper deposition on polyimide. *Appl. Phys. Lett.* **1998**, *53*, 2111–2113, doi: 10.1063/1.100292.

117. Chen, D.S. Interaction between laser and polymer (III) Silver selective activation electroless plating on polyimide film to make fine lines [D]. Shanghai: Shanghai Jiaotong University, **2016**, 3–15.

118. Stoermer, R.L.; Sioss, J.A.; Keating, C.D. Stabilization of Silver Metal in Citrate Buffer: Barcoded Nanowires and Their Bioconjugates. *Chem. Mater.* **2015**, *17*, 4356–4361, doi: 10.1021/cm050910l.

119. Srivastava, R.; Tiwari, D.K.; Dutta, P.K. 4-(Ethoxycarbonyl) phenyl-1-amino-oxobutanoic acid–chitosan complex as a new matrix for silver nanocomposite film: Preparation, characterization and antibacterial activity. *Tnt. J. Biol. Macromol.* **2011**, 49, 863–870, doi: 10.1016/j.ijbiomac.2011.07.015.

120. Wang, C.X.; Li,Y.L.; Xu, L. Preparation and Characterization of Nano-silver Particles by PVP Protection by Liquid Phase Chemical Reduction. *Precious Metals*, **2014**, *35*, 30–33.

121. Sun, K.; Zhao, Y.; Zhang, C.Q. Pulsed Nd:YAG laser induced chemical deposition of Ag and Au. *Applied Laser* **2012**, *22*, 15–18.

122. Chen, D.S.; Lu, Q.H.; Zhao, Y. Laser-induced site-selective silver seeding on polyimide for electroless copper plating. *Appl. Surf. Sci.* **2016**, *253*, 1573–1580, doi: 10.1016/j.apsusc.2006.02.039.

123. Macdiarmid, A.G.; Epstein, A.J. Polyanilines: a novel class of conducting polymers. *Faraday Discuss. Chem. Soc.* **1989**, *88*, 317–332, doi: 10.1039/DC9898800317.

124. Chen, Y.; Kang, E.T.; Neoh, K.Q. Intrinsic redox states of polyaniline studied by high-resolution X-ray photoelectron spectroscopy. *Colloid Polym. Sci.* **2011**, *279*, 73–76, doi: 10.1007/s003960000418.

125. Huang, H.; Guo, Z.C. *Preparation and application of conductive polyaniline*. Science Press: Beijing, CN, 2010; pp. 23–25, ISBN 9787030292759.

126. Liu, W.J.; Yan, G.M. Preparation of Polyaniline and Polyaniline Conductive Fibers.*Synthetic Fiber Industry* **1996**, *4*, 47–51.

127. Uddin A.J.; Alagirusamy, R.; Das, A. *5-Coatings for technical textile yarns*; Woodhead Publishing Limited: Sawston, Cambridge, UK, 2010; pp.140–184, ISBN 978-1-84569-549-1.

128. Stejskal, J.; Kratochvíl, P.; Jenkins, A.D. Polyaniline: forms and formation. Collect. *Czech. Chem. Commun.* **1995**, *60*, 1747–1755, doi: 10.1135/cccc19951747.

129. Stejskal, J.; Kratochvíl, P.; Jenkins, A.D. The formation of polyaniline and the nature of its structures. *Polymer* **1996**, 37, 367–369, doi; 10.1016/0032-3861(96)81113-X.

130. Stejskal, J.; Sapurina, I.; Trchov, M. Polyaniline nano-structures and the role of aniline oligomers in their formation. *Progress in Polymer Science* **2010**, *35*, 1420–1481, doi: 10.1016/j.progpolymsci.2010.07.006.

131. Chiang, J.C.; MacDiarmid, A.G. 'Polyaniline': Protonic Acid Doping of the Emeraldine Form to the Metallic Regime". *Synthetic Met.* **1986**, *13*, 193–205, doi: 10.1016/0379-6779(86)90070-6.

132. Xu, W.L.; Xiong, J.; Xu, Q. Preparation and properties of electroless silver-plated polyester fabrics. *Journal of Textile Research*, **2011**, 32, 42–52.

133. Liao, X.Q.; Liao, Q.L.; Yan, X.Q.; Liang, Q. J.; Si, H.N.; Li, M.H.; Wu, H.L.; Cao, S.Y.; Zhang,Y. Flexible and Highly Sensitive Strain Sensors Fabricated by Pencil Drawn for Wearable Monitor. *Adv. Funct. Mater.* **2015**, *25*, 2395–2401, doi: 10.1002/adfm.201500094.

134. Lin, C.W.; Zhao, Z.B.; Kim, J.Y.; Huang, J.X. Pencil Drawn Strain Gauges and Chemiresistors on Paper. *Sci. Rep. 4* **2014**, 3812, doi: 10.1038/srep03812.

135. Lessing, J.; Glavan, A.C.; Walker, S.B.; Keplinger, C.; Lewis, J.A.; Whitesides, G.M. Inkjet Printing of Conductive Inks with High Lateral Resolution on Omniphobic “RF Paper” for Paper-Based Electronics and MEMS. *Adv. Mater.* **2014**, *26*, 4677–4682, doi: 10.1002/adma.201401053.

136. Liu, J.P.; Yang, C.; Wu, H.Y.; Lin, Z.Y.; Zhang, Z.X.; Wang, R.H.; Li, B.H.; Kang, F.Y.; Shi, L.; Wong,C.P. Future paper based printed circuit boards for green electronics: fabrication and life cycle assessment. *Energy Environ. Sci.* **2014**, *7*, 3674–3682, doi: 10.1039/C4EE01995D.

Chapter 2 Silver-Plating on Polyester Fibers by Continuous Two-Step Method Without Activation

2.1 Introduction

Polyester fibers are widely used in various fields, because of their excellent physical and mechanical properties and chemical stability. However, normal polyester fiber has a low moisture regain [1,2], higher electrical resistance [3,4], and can easily accumulate large amounts of electric charges on the surface [5,6], which results in fibers repelling each other, clothing absorbing dust and clinging onto the body, and can even produce electrical shocks or ignite flammable substances. Polyester fibers' easily generating static electricity and poor conductivity, limit their applications in apparel and home furnishings [7–9]. Therefore, it is necessary to improve the electrical conductivity of the fibers. Plating a layer of silver on the surface of a polyester fiber will preserve the excellent properties of the polyester. Meanwhile, it also has the excellent electrical conductivity [10], ductility [11,12], catalytic activity [13,14], and antibacterial deodorization properties of metallic silver [15–18], and the material can also obtain a certain metallic luster and decorative effect [19–22].

The electroless silver plating method is widely used in applications to the surface metallization of fibers, due to its simple operation process, uniform coating, and controllable thickness [23–26]. However, the surface of the fiber has no catalytic activity. Therefore, using electroless plating on the surface of the fiber to achieve metal deposition requires pretreatment to impart a certain catalytic activity to the surface of the fiber [27,28]. The conventional pretreatment process mainly includes the four steps of cleaning, coarsening, sensitization, and activation, and the activation is an important step to determine the catalytic activity of the substrate [29–31]. The activation of the fibers often uses palladium with high reactivity, such as the sensitization–activation two-step method [32–34], the colloidal palladium activation method [35,36], the liquid ion palladium activation method [37,38], and so on. Due to the highly toxic and expensive nature of palladium, as well as the great potential of polluting the plating layer [39,40], these types of methods are not conducive to the preparation and application of the electroless silver-plated fibers. It has been reported that in the process of pretreatment, silver nitrate has been used by replacing the palladium compound as an activation solution for electroless plating to form a silver catalytic center on the surface of the fiber [41], while nitrate is also considered as a potentially hazardous [42]. NaClO-HCl silver activation system also proved to be a good applicability in the silver-coating industry [43]. These activation steps all prolong the time of electroless silver-plating, which is not conducive to production.

To the best of our knowledge, the study of fiber electroless silver plating has mainly focused on chemical plating under static conditions where the technology tends to be more mature [44–49], but that the study of the dynamic continuous silver plating of fibers has been seldom reported. In addition, due to the shorter reaction time, the electroless silver-plated fibers have a thin silver coating on the surface with very poor durability. Therefore, further electroplating treatment is generally required [50,51]. The first and best developed process in the electroplating industry is cyanide electroplating silver plating. The plating solution forms a coordination complex with CN^- and Ag^+, which has high stability and good dispersion of the plating solution. The electrode reactions of cyanide silver electroplating are as follows.

(1) Cathode reaction

The main reaction of the cathode is $\left[Ag(CN)_2\right]^-$ reduction to metallic silver:

$$[\mathrm{Ag(CN)_2}]^- + e \rightarrow \mathrm{Ag}\downarrow + 2[\mathrm{CN}]^- \qquad (2\text{-}1)$$

In addition, there may be side effects of hydrogen evolution.

$$2\mathrm{H}^+ + 2e \rightarrow \mathrm{H_2}\uparrow \qquad (2\text{-}2)$$

(2) Anode reaction

Metallic silver is used as the soluble anode, so the main reaction of the anode is the electrochemical dissolution of silver:

$$\mathrm{Ag} - e \rightarrow \mathrm{Ag}^+ \qquad (2\text{-}3)$$

The Ag^+ ions dissolved from the anode form complex ions with free $[\mathrm{CN}]^-$:

$$\mathrm{Ag}^+ + [\mathrm{CN}]^- \rightarrow [\mathrm{Ag(CN)_2}]^- \qquad (2\text{-}4)$$

When the anode is passivated, the following oxygen evolution reaction occurs:

$$4[\mathrm{OH}]^- - 4e \rightarrow 2\mathrm{H_2O} + \mathrm{O_2}\uparrow \qquad (2\text{-}5)$$

The silver-plating layer using cyanide electroplating has high bonding fastness to the substrate [52,53], but cyanide is highly toxic, so cyanide electroplating silver must be replaced [54–56].

This chapter aimed to prepare silver coated polyester fibers by a dynamic continuous two-step method, which combined the operations of continuous electroless plating and electroplating. In the electroless silver-plating step, the activating pretreatment was eliminated, and the polyester fiber, after being pretreated by the sensitization washing, was directly immersed into the electroless plating solution for electroless plating silver. In the second step, the electroless silver-plated fiber was subjected to a cyanide-free electroplating silver treatment by using sulfosalicylic acid as the plating solution. The whole process was continuous, and specialized continuous industrial silver-plating equipment was also designed.

2.2 Experimental

2.2.1 Materials

Polyester fibers (210D/36F) were purchased from Vekstar Textile Co., Ltd. (Shanghai, China). Sodium hydroxide (NaOH, ≥96.0%), potassium hydroxide (KOH, ≥85.0%), lauryl sodium sulfate (LSS, >97.0%), stannous chloride dihydrate ($SnCl_2·2H_2O$, ≥98.0%), silver nitrate ($AgNO_3$, ≥99.8%), aqueous ammonia (NH_3H_2O, 25.0–28.0%), glucose ($C_6H_{12}O_6$, AR), sulfosalicylic acid dihydrate (≥99.0%), ammonium acetate (≥98.0%), and hydrochloric acid (36.0–38.0%, AR) were purchased from Sinopharm Chemical Reagent Co., Ltd (Shanghai, China) and used without further purification.

2.2.2 Deposition of Silver on Polyester Fibers by Electroless Plating Without Activation Under the Dynamic Condition

The general processes of preparing a conductive metal layer on polymeric fibers or plastics are mainly composed of two parts: (1) the pretreatment including cleaning, coarsening, sensitizing, and activating; and (2) the deposition of silver through the redox reaction. In this study, both the pretreatment and the silver deposition were continuously operated in a series of self-made reactive tanks, as shown in Scheme 2-1. The whole process had no activation step under a dynamic condition. The fiber winding collecting device at the end of the equipment provided the drafting force. The winding speed was controlled by the control panel, and the reaction time of the fibers in each plating tank could be controlled by different winding speeds. The fiber is first immersed in the plating bath in the plating tank, and after being wound for several cycles on the roller, it is drawn to the next step. The schematic diagram of the fiber inside the plating tank is shown in Scheme 2-2. The reaction time of the fibers in each bath can also be controlled by the number of winding cycles. The more the number of winding cycles, the longer the reaction time. The size of the groove in the equipment was 12.5 cm × 8.5

cm × 14.5 cm. The lining and the drum in the tank were made of polytetrafluoroethylene (PTFE) to prevent acid or alkali corrosion.

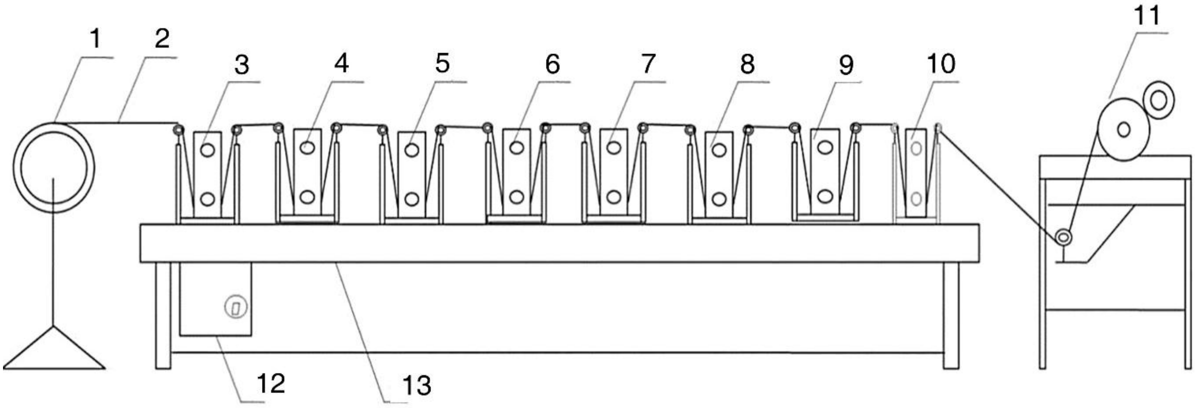

Scheme 2-1. The equipment for the continuous electroless plating of silver under a dynamic condition. (1) return wire rack; (2) polyester fiber (3) cleaning tank; (4) coarsening tank; (6) sensitizing tank; (8) electroless silver-plating tank; (10) drying tank; (11) fibers winding collecting device; (12) control panel; (13) heating device; (5), (7), and (9) washing tank.

Polyester fibers were cleaned using a mixture of 0.07 g/mL NaOH and 0.002 g/mL LSS at 60 ℃ for 3 min to remove the oil and other impurities, followed by coarsening in 100 g/L NaOH solution at 80 ℃ for 5 min. After washing by distilled water, the sensitizing of polymeric fibers was conducted by using Tin granule and sensitizing liquid consisting of 30 g/L $SnCl_2$ and 40 ml/L Hydrochloric acid at room temperature for 3 min to make a $Sn_2(OH)_3Cl$ gel-layer on the surface of the fibers.

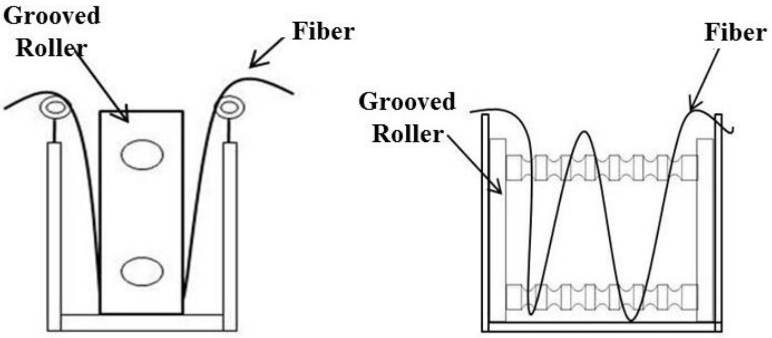

Scheme 2-2. Internal schematic diagram of plating bath

Then, the sensitizing fibers were washed by distilled water for 4 min and put into the solution of Tollens' reagent and glucose for the silver deposition (electroless silver-plating). As the main salt for silver deposition, silver-plating speed increases with the increase of silver ion concentration, but if the solution concentration is too high, it is easy to cause solution instability, so the concentration should not be too high. As a complexing agent, ammonia aqueous complexes with silver ions to form silver ammonia ions, which is beneficial to increase the stability of the plating solution. Sodium hydroxide, as a speed regulator, increases the deposition rate of silver particles with the concentration, but it should not be too high, otherwise, it will promote the self-decomposition of the plating solution. Glucose is a reducing agent whose concentration affects the reduction reaction speed. Ethanol can stabilize the bath and brighten the coating layer. Sodium thiosulfate is used as bath stabilizer to ensure solution stability. Specifically, the oxidation solution of the electroless silver plating bath is composed of 8 g/L silver nitrate, 3.2 g/L sodium hydroxide and ammonia aqueous. The reduction solution consists of 13 g/L glucose, 100 ml/L ethanol and 25 mg/L sodium thiosulfate. The electroless silver plating is carried out by ultrasonic treatment for 5 minutes at 30 ℃, followed by washing in deionized water and drying to obtain electroless silver-plated conductive fibers.

2.2.3 Deposition of Silver by Continuous Electroplating

The polyester fibers with silver deposition of electroless plating were connected to a negative wire for electroplating, as shown in Scheme 2-3. In detail, a pure silver plate with the dimension of 80 mm × 40 mm × 5 mm was used as an anode material and a direct current with a voltage ranging from 1 V to 10 V was used as an energy resource. The polyester fibers, after being coated with a thin layer of silver by electroless plating, were directly used for electroplating. The electroplating solution was a mixture with a pH of about 9, prepared by using 120 g/L of sulfosalicylic acid, 10 g/L of potassium hydroxide, 30 g/L of silver nitrate, 50 g/L of ammonium acetate, and 60 mL/L of aqueous ammonia.

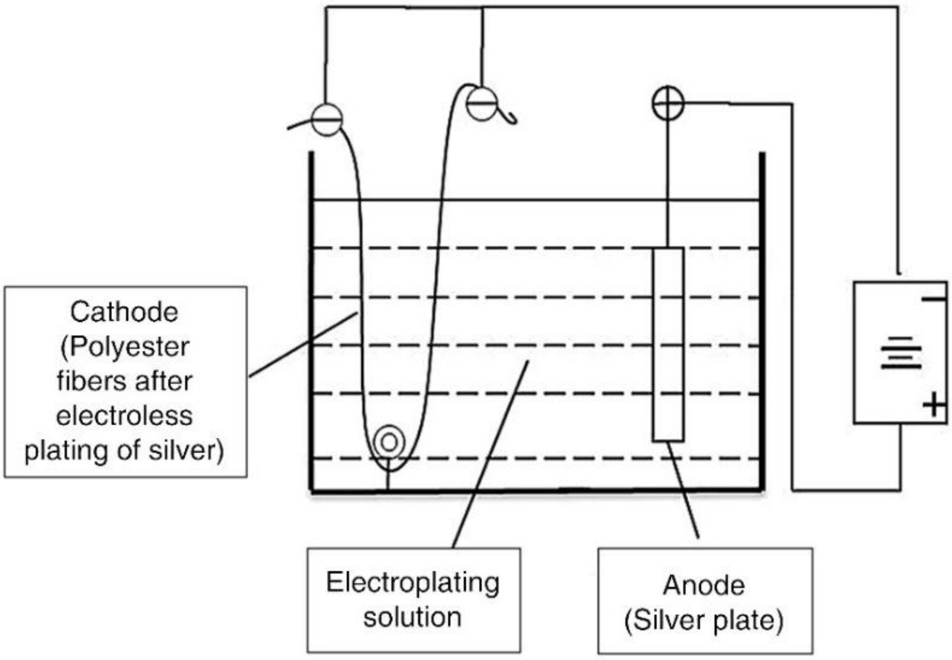

Scheme 2-3. The equipment for electroplating silver on polyester fibers.

Silver nitrate is the main salt of the electroplating silver process, and its content should not be too high, otherwise, the plating ability will decrease, and the crystal of the plating layer will become coarse. Sulfosalicylic acid, abbreviated with H_3SSA, is the main complexing agent and surfactant. In the plating solution, sulfosalicylic acid dissociates the acid ion and complexes with the silver ion in the plating solution to form a complex, which can maintain solution stability. When plating, sulfosalicylic acid in plating bath should be sufficient. Below 90g/L, the anode will passivate; but above

170g/L, the current density of the cathode will decrease. The content of sulfosalicylic acid in the plating solution is preferably maintained at 100 to 150 g/L. As an auxiliary complexing agent, ammonium acetate can form a stable complex with silver nitrate, improve the stability of the plating solution and the quality of the coating layer. At the same time, ammonium acetate also acts as a conductive salt in the plating solution to enhance the conductivity and dispersibility of the plating solution. Adding a certain amount of potassium hydroxide to the electroplating solution can improve the overall conductivity and cathodic polarization of the bath, which is conducive to improving the dispersion ability of the bath and the quality of the silver electroplating layer. Ammonia aqueous is mainly used to maintain the stability of the pH value of the electroplating solution. When the pH of the plating solution is about 9, a mixed complex can be formed in the solution to ensure the stability of the plating solution. The electrode reactions of silver electroplating in the sulfosalicylic acid system are as follows [57]:

(1) Cathode reaction

The main reaction of the cathode is $\left[\mathrm{Ag(SSA)(NH_4)}\right]^-$ reduction to metallic silver:

$$\left[\mathrm{Ag(SSA)(NH_4)}\right]^- + e \rightarrow \mathrm{Ag}\downarrow + [\mathrm{SSA}]^{3-} + [\mathrm{NH_4}]^+ \tag{2-6}$$

In addition, there may be side effects of hydrogen evolution.

$$2\mathrm{H}^+ + 2e \rightarrow \mathrm{H_2}\uparrow \tag{2-2}$$

(2) Anode reaction

Metallic silver is used as the soluble anode, so the main reaction of the anode is the electrochemical dissolution of silver:

$$\mathrm{Ag} - e \rightarrow \mathrm{Ag}^+ \tag{2-3}$$

The Ag^+ ions dissolved from the anode form complex ions with free $\left[\mathrm{SSA}\right]^{3-}$ and $\left[\mathrm{NH_4}\right]^+$:

$$Ag^+ + [SSA]^{3-} + [NH_4]^+ \rightarrow \left[Ag(SSA)(NH_4)\right]^- \tag{2-7}$$

When the anode is passivated, the following oxygen evolution reaction occurs:

$$4[OH]^- - 4e \rightarrow 2H_2O + O_2 \uparrow \tag{2-5}$$

2.2.4 Characterizations

Fourier-transform infrared (FTIR) spectra were obtained on a Spectrum Two IR Spectrometers (PerkinElmer, Billerica, MA, USA). The data were recorded from 600 cm^{-1} to 4000 cm^{-1} with the resolution of 1 cm^{-1}. The morphology of different fibers was examined with a JEOL JSM-5900 SEM (JEOL Ltd., Tokyo, Japan) at an accelerating voltage of 15 kV. The surface of fibrous samples was coated with thin layers of gold before the observation. The X-ray photoelectron spectrogram (XPS) of samples was performed by a Thermo ESCALAB 250XI XPS (Thermo Fisher Scientific, Waltham, MA, USA) at an accelerating voltage of 14 kV. X-ray diffraction (XRD) patterns of different fibers were measured with a D8 ADVANCE X-ray diffractometer (Bruker AXS, Karlsruhe, German) with a tube voltage of 40 kV, tube current of 1100 mA, a scanning ranges from 3° to 90°, and a scanning speed of 4°/min. The breaking strength and elongation at break of the fibers were characterized by a YG020B Electronic Single Yarn Strength Tester (Changzhou No.2 Textile Machine Co., Ltd, China) with a clamping length of 250 mm and a pre-tension of 10 CN.

A ZC-90G high insulation resistance tester and a DT-9205 digital multimeter is used to measure the surface resistance of the fibers. The clamping length of the fibers was 1 cm. Ten readings at different locations were taken randomly and the average was recorded. The resistivity of fibers was calculated by the following formula.

From the formula

$$R = \rho L / A \tag{2-8}$$

It is concluded that

$$\rho = RA / L \tag{2-9}$$

Where ρ, R, A, and L represent fiber resistivity (Ω·cm), the measured resistance of the fiber (Ω/cm), fiber cross-sectional area (cm^2), and test length (cm), respectively.

The resistivity of PANI-Ag coated polyester fibers was also measured after being washed for 25 times or treated with 5% NaCl solution.

For analyzing the corrosion resistance of fibers, samples were soaked in 5% NaCl solution for different time, then washed with clean water and dried. A DT-9205 digital multimeter and a ZC-90G high insulation resistance measuring instrument were used to measure the change of contact resistance on the coating surface, followed by calculating the resistivity of fibers and evaluating the corrosion resistance of fibers

The washability analysis refers to GB/T 8629-2001 "Standards for Home Washing and Drying Procedures for Textile Testing" and combines with the actual situation of fibers [58]. The sample was placed in a detergent (40 ℃) prepared by 2 g/L washing powder with the control bath ratio was 1:30, and stirred for 15 min, which was recorded as one wash. After washing, wash and dry with water. A DT-9205 digital multimeter and a ZC-90G high insulation resistance tester were used to measure the change of contact resistance on the coating surface, then calculate the resistivity of the fibers and evaluate the washing resistance of the fibers after plating.

The rate of weight gain is calculated by measuring the weight of the polyester fiber before and after silver-plating with the METTLER-TOLEDO precise balance. The dry weight of polyester fibers before silver plating is w_1, and that of polyester fibers after silver plating is w_2. The rate of weight gain of silver-plated polyester fibers is as follows [59]:

$$W = \frac{W_2 - W_1}{W_1} \times 100\% \tag{2-10}$$

2.3 Results and Discussions

2.2.1 Mechanism of Electroless Plating without Activation under the Dynamic Condition

2.2.1.1 Pretreatment without Activation on Polyester Fibers

The processes of pretreatment on polyester fibers for electroless plating have been thoroughly investigated in previous studies [44, 60–63]. To the best of our knowledge, only three steps are needed for the pretreatment including the cleaning, coarsening, and sensitizing.

The aim of cleaning is to remove the oil and/or other impurities that are located on the surface of the fibers in the processes of production and transportation. In this study, we used a mixture of 0.07 g/mL NaOH and 0.002 g/mL LSS to clean the surface of the polyester fibers. Both the NaOH and LSS could remove the oil from the surface of the polyester fibers, and the LSS also could serve as the surfactant to reduce the surface tension of the polyester fibers. The SEM image of the polyester fibers after cleaning is shown in Figure 2-1b.

The second step of pretreatment was coarsening. Coarsening is done to increase the roughness of the surface of the fibers by chemical etching and the chemical reaction between the plating solution and fibers to form uniform pores and grooves on the surface, thus forming the “locking effect” and enhancing the hydrophilicity of the substrate [28]. Therefore, the bonding strength between the coating and the substrate will be improved. In this work, the surface of the fibers was chemically etched by the NaOH solution, which should have an appropriate concentration. Too high a concentration will cause serious damage to the fiber surface and a high loss rate of the fiber mass, greatly reducing the mechanical properties of the fiber, while too low a concentration cannot meet the need of coarsening. In this study, the coarsening condition was that the fibers were coarsened in 100 g/L NaOH solution at 80 °C for 5 min. Figure 2-1c shows the SEM image of the coarsened polyester fibers where there were more pits and holes on the surface of the fiber, and the roughness obviously increased.

The next step of pretreatment was sensitizing. In this work, a mixed solution of 30 g/L of $SnCl_2$ and 40 mL/L of hydrochloric acid was used as the sensitizing solution. After the fibers were immersed in the sensitizing solution, $Sn_2(OH)_3Cl$ thin films with a slightly soluble gel were formed by the hydrolysis of stannous chloride during subsequent water washing [64]. This gel-like substance was adsorbed on the fiber surface to ensure the uniform adsorption of divalent tin ions onto the gel's surface, which facilitated the uniform deposition of silver particles during electroless silver plating. Therefore, sensitization mainly occurs in the water washing process, and the reaction process is shown in Reactions (2-11) and (2-12). $Sn(OH)Cl$ and $Sn(OH)_2$ combine to form a slightly soluble gelatinous substance, $Sn_2(OH)_3Cl$.

$$SnCl_2 + 2H_2O \rightarrow Sn(OH)_2 + 2HCl \tag{2-11}$$

$$SnCl_2 + H_2O \rightarrow Sn(OH)Cl + HCl \tag{2-12}$$

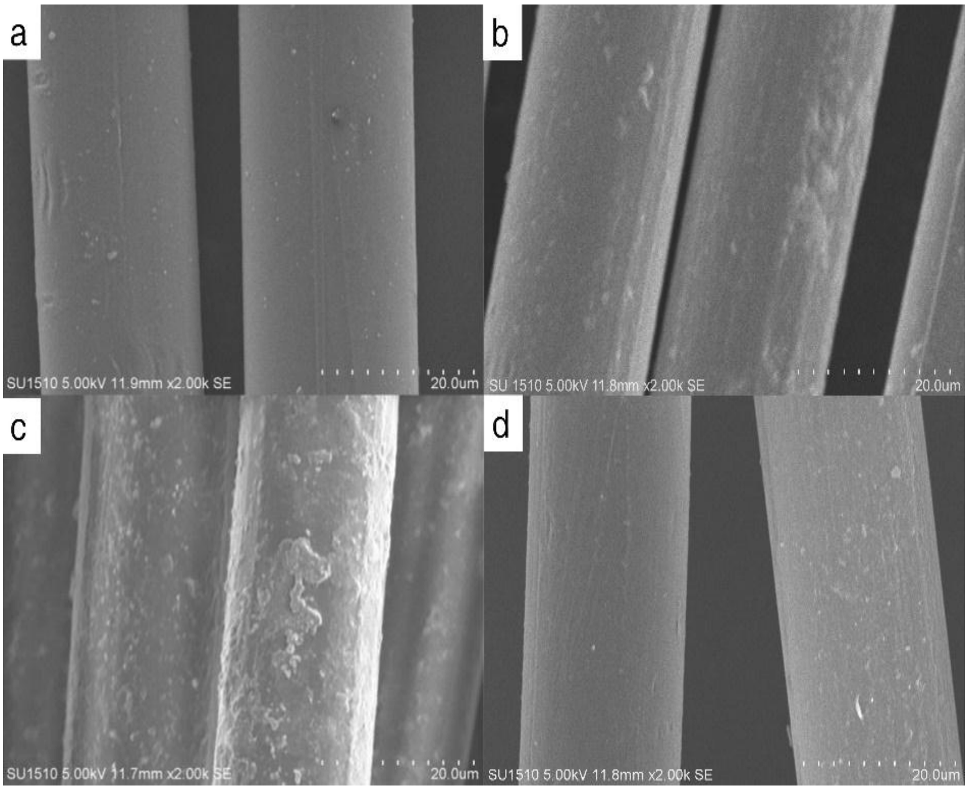

Figure 2-1. SEM images (×2000) of polyester fibers: (**a**) before any treatment; (**b**) after cleaning with NaOH and lauryl sodium sulfate (LSS); (**c**) after coarsening with NaOH; and (**d**) after sensitizing with $SnCl_2$.

Figure 2-1d shows the SEM image of the sensitized polyester fiber surface, showing that the polyester fiber surface was obviously covered with a more uniform and continuous gel-like film.

Eliminating conventional activation pretreatment is suitable for this continuous two-step plating silver on the polyester fibers.

2.2.1.2 Electroless Silver Plating on Polyester Fibers

In the electroless plating solution, $Ag(NH_3)_2^+$ is first reduced by Sn^{2+} adsorbed on the surface of the fiber to form metal Ag particles, the reaction formula of which is shown in Reaction (2-13). Thus, the Ag particles are deposited on the surface of the fiber where the stannous ion is dispersed. The Ag particles have strong catalytic activity and become the catalytic center of the electroless silver plating reaction. Similarly,

$[Ag(NH_3)_2]^+$ in the silver ammonia solution is reduced to metal Ag particles with glucose, and deposited on the surface of the fiber around the catalytic center to obtain a metallic silver layer, the reaction formula of which is shown in Reaction (2-14). Therefore, in this non-activated direct electroless silver plating process, the sensitized-washed fiber will first form Ag particles on the surface of the fiber as the catalytic center of the whole reaction, so that the surface of the fiber has catalytic activity.

$$2[Ag(NH_3)_2]^+ + Sn^{2+} \rightarrow Sn^{4+} + 2Ag\downarrow + 4NH_3 \qquad (2\text{-}13)$$

$$\begin{aligned} CH_2OH(CHOH)_4CHO + 2Ag(NH_3)_2OH \overset{\Delta}{\rightarrow} CH_2OH(CHOH)_4COONH_4 + 2Ag\downarrow \\ + H_2O + 3NH_3\uparrow \end{aligned} \qquad (2\text{-}14)$$

2.2.1.3 Stability of Electroless Plating Bath

Continuous electroless silver plating requires high stability of silver- plating bath, which can ensure continuous reduction reaction on fibers for a long time. The reason for the instability of the plating bath is that the standard electrode potential of silver is small (0.7995 V), and Ag^+ is easily precipitated from the bulk of the solution, causing the plating solution to be unstable. Besides, The Ag particles reduced have a self-catalytic reaction, which accelerates the reaction speed of redox and causes the instability of the plating bath as well.

Because the stability constant of silver ammonia ion is small, sodium thiosulfate is added in this experiment to increase the stability of the plating solution. The stability constants β_n of the two are as follows.

$$Ag^+ + NH_3H_2O \rightarrow [Ag(NH_3)]^+ + H_2O \qquad \lg\beta_n = 7.05 \qquad (2\text{-}15)$$

$$Ag^+ + 2S_2O_3^{2-} \rightarrow [Ag(S_2O_3)_2]^{3-} \qquad \lg\beta_n = 13.46 \qquad (2\text{-}16)$$

It can be known from the reaction formula (2-16) that the stability of silver thiosulfate is high. When sodium thiosulfate is added to the plating solution, $S_2O_3^{2-}$ in the solution binds to Ag^+, reduces the dissociation speed of Ag^+, resulting in decreasing the amount of Ag^+ participating in the reduction reaction in unit time, and improves the stability of the plating solution. However, if sodium thiosulfate is excessive, the amount of Ag^+ in reaction per unit time will be greatly reduced, resulting in a slow redox reaction, which is not conducive to continuous silver-plating. Therefore, after experiments, we found that 25 mg/L NaS_2O_3 is suitable.

2.2.1.4 Influence of the Transmission Condition on the Continuous Electroless Plating Silver

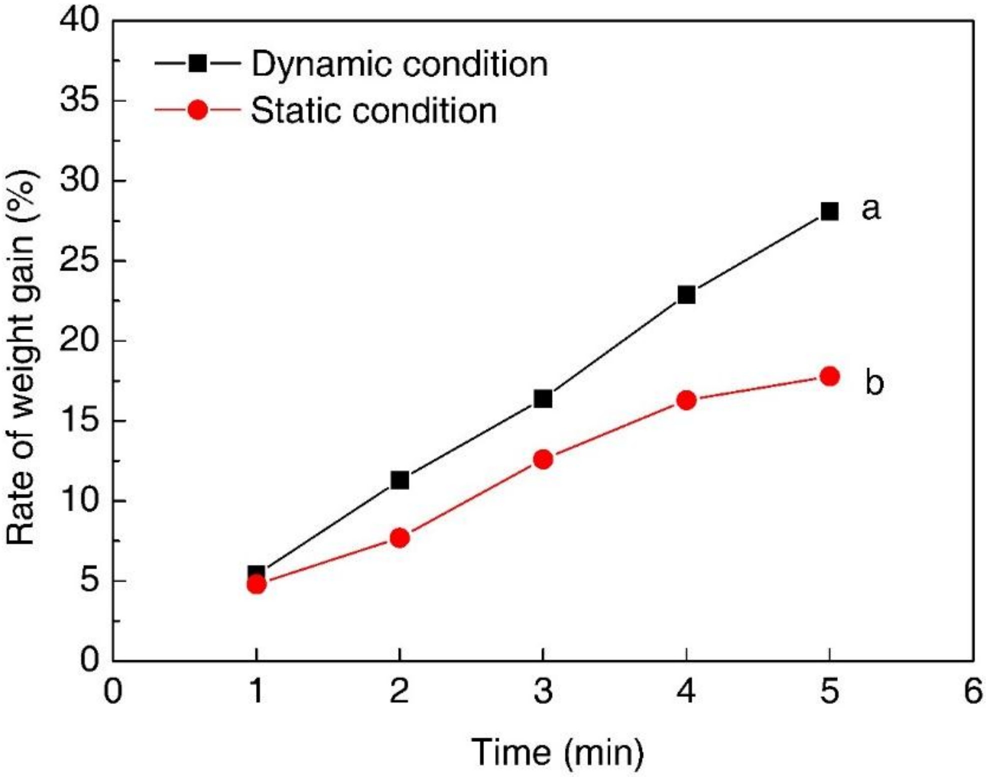

Figure 2-2. Deposition rate of silver particles under (**a**) dynamic, and (**b**) static conditions.

Continuous silver plating on fibers under a dynamic condition can facilitate deposition efficiency, which is significantly different from that under a static condition.

Under the same pretreatment conditions, we performed silver plating contrast experiments in a static beaker and a dynamic condition. The contrast chart of the deposition rate of silver particles under dynamic and static conditions at different plating times was obtained (Figure 2-2). It demonstrated that the weight gain of the fibers under the static condition was obviously lower than that under the dynamic condition, and the deposition rate under the static condition became lower and lower with the increase of plating time, while the deposition rate of silver particles under the dynamic condition was higher and had less influence on time.

When performing the electroless silver plating operation under a static condition, the fibers mainly reacted with the silver-ammonia ions around them, and the nearby silver ammonia ions are first reduced to silver particles and deposited on the surface of the fibers. However, with the reaction proceeding, the silver-ammonia ion concentration near the fibers will decrease, thus affecting the deposition rate of silver particles. At the same time, the ammonia gas released during the reaction process will stay on the surface of the fibers, thereby causing holes in the plating layer formed on the surface of the fibers, resulting in loose plating, affecting the conductivity of the silver-plated fiber and the firmness of the plating layer. When the fiber is dynamically driven in the plating tank under a dynamic condition, the diffusion speed of silver ammonia ions to the fiber surface can be increased, which can compensate for the decrease of local silver-ammonia ion concentration caused by electroless plating around the fibers, thus improving the deposition efficiency [65]. Therefore, the mass change rate of fibers under the dynamic condition is higher than that of the static condition. In a certain period of time with the increase of time, the increase of mass change rate is more obvious. Under the dynamic condition, due to the redox reaction, the fiber can stir and remove the ammonia gas accumulated on the surface of the fiber and obtained dense plating layer [66]. Generally speaking, when the coating weight is the same, the conductivity of the fibers is proportional to the weight gain rate of the fibers, so the conductivity of the fibers improves faster under dynamic conditions.

Similarly, when the self-made test equipment is used for pretreatment, the fibers can be fully contacted with each reaction fluid under the dynamic transmission, so that the pretreatment effect is faster and better than that under static conditions.

2.2.2 Influence of Electroplating Process Conditions on Deposition of Silver

2.2.2.1 Influence of Power Supply Method on Electroplating Silver

During the electroplating process, the silver layer was first deposited onto the fibers near the clamp and then extended along the radial direction of the fibers. In this process, the newly deposited silver was gradually coated onto the surface of the fibers and was closely combined with the metal silver coated by the previous electroless plating, which became the effective cathode area in the electroplating process. The new coating also reduced the fiber resistivity and increased the cathode area. In addition, due to the smaller diameter and longer length of the polyester fiber, the specific surface area of the fiber was larger, resulting in a more complex change in the cathode area of the fiber [67]. If the traditional constant current method was used to electroplate the fibers, the cathode area would change, and the cathode current density in the system would be unstable, which would cause the surface of the fibers to fluctuate greatly, which is not conducive to the formation of high-quality coatings. As such conditions are comparatively easier to control in the constant voltage method, in this study, we used a constant voltage power supply method to control the fiber electroplating experiment.

2.2.2.2 Influence of Control Voltage on Electroplating Silver

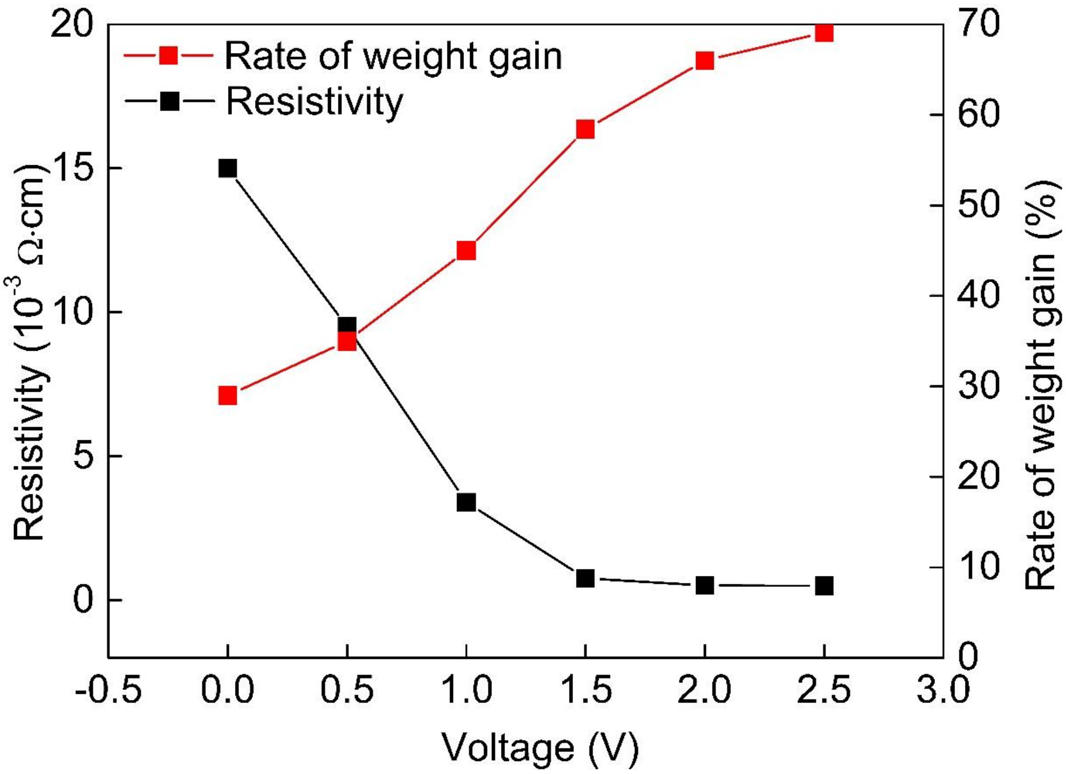

Figure 2-3. Influence of voltage on the resistivity and the rate of weight gain.

For the same electroplating time of 4 min, the influence of the plating voltage on fiber resistivity and the rate of weight gain is shown in Figure 2-3. With the increase in the electroplating voltage, the fiber rate of weight-gain always increased, while the resistivity of the fiber gradually decreased, and after the voltage rose to above 1.5 V, the resistivity did not substantially decrease. This is because with the increase in voltage, the deposition rate of silver particles on the fiber surface was accelerated, resulting in the increased rate of weight gain of the fiber, and the silver particles deposited on the fiber surface were closely combined with the existing silver layer, resulting in the decrease of the fiber resistivity [68]. When the voltage continues to increase, the deposition rate of silver particles will continue to increase; too fast a deposition rate will easily lead to the accumulation of particles on the silver layer, which makes the surface rough and uneven, resulting in a slow decline in resistivity. However, if the voltage is too high, it is easy to "scorch" the fibers. When the plating voltage reaches 2.6 V, the “scorch” phenomenon occurs in the fiber coating. When the voltage is lower, the deposition rate of silver particles is slow, and the silver-plating efficiency is also lower. Therefore, the best control voltage range is 1.5–2.0 V.

2.2.2.3 Influence of Electroplating Time on Electroplating Silver

Figure 2-4 presents the SEM images of the silver-plated layer on the surface of the fiber for different plating times. The silver particles were first uniformly deposited on the surface of the fiber to form a continuous dense silver coating (Figure 2-4b). With prolonged electroplating time, the deposition of silver particles increased and the coating on the surface of the fiber became thicker. However, with too long a time, the deposited silver particles tended to accumulate in certain parts of the coating and caused the coating to become rougher (Figure 2-4c).

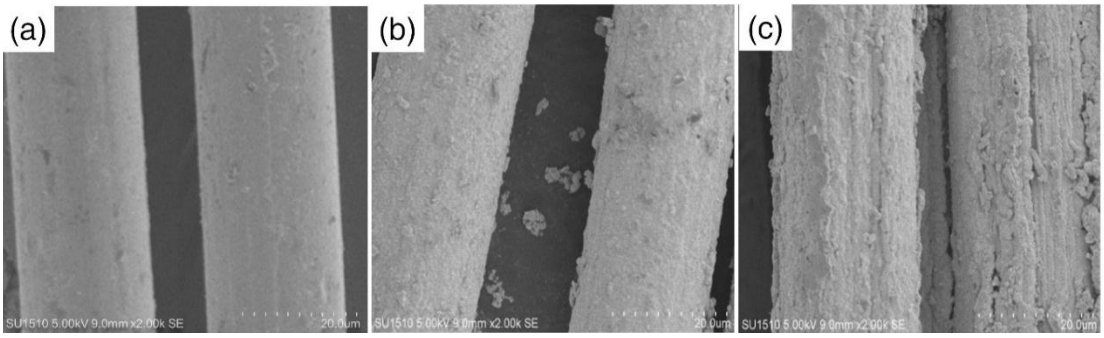

Figure 2-4. SEM images (×2000) of polyester fibers for different electroplating time: (**a**) 0 min; (**b**) 4 min; (**c**) 8 min.

The effects of different plating times on the resistivity and the rate of weight gain of the polyester fibers were investigated under the same plating voltage (1.6 V). The results are shown in Figure 2-5. With prolonged electroplating time, the rate of weight gain of the fiber increased constantly, and the resistivity decreased continuously, while the surface coating becomes rough which causing the resistivity to drop slowly until it no longer changes. Fig 2-5 shows the resistivity remained basically unchanged after 4 min of electroplating. That is maybe because within 4 minutes of electroplating time, the coating layer is discontinuous, and the time has a great influence on the decrease of resistivity. After four minutes, the coating layer is continuous, and the plating time is extended to increase the thickness of the plating layer, which has little effect on the resistivity [69]. Different plating times can produce different coating thicknesses, but if the coating is too thick, the flexibility of the fibers will deteriorate [70]. Therefore, in this work the electroplating time was controlled at 4 min.

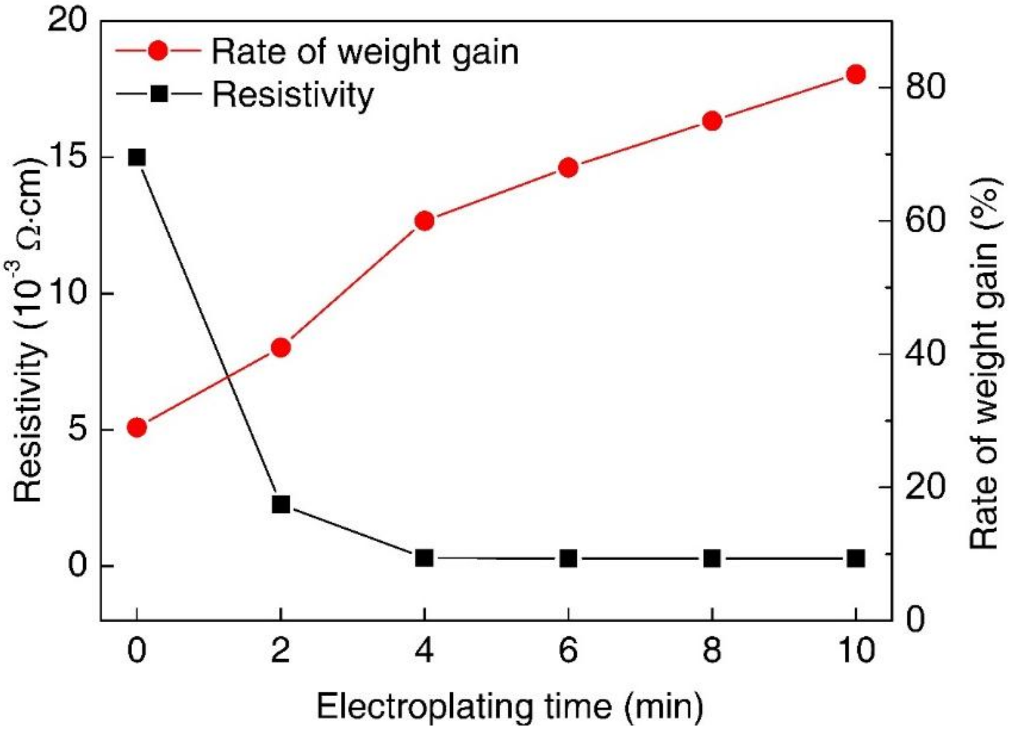

Figure 2-5. Influence of electroplating time on resistivity and the rate of weight gain.

2.2.2.4 Influence of Plating Temperature on Electroplating Silver

The plating temperature also has a great influence on the coating. Increasing the temperature can improve the conductivity of the solution, increase the cathodic current density and increase the cathodic polarization, which will accelerate the deposition rate of silver particles and improve the production efficiency.

However, the temperature should not be too high, otherwise the cathodic reaction speed and ion diffusion speed will be accelerated, but the cathodic polarization will be reduced, resulting in the coarsening of the coating crystallization. And if the temperature is too high, ammonia water and other substances in the bath would volatilize, resulting in the instability of the bath. Therefore, the plating temperature in this experiment was selected as room temperature

2.2.3 Silver Composition Analysis

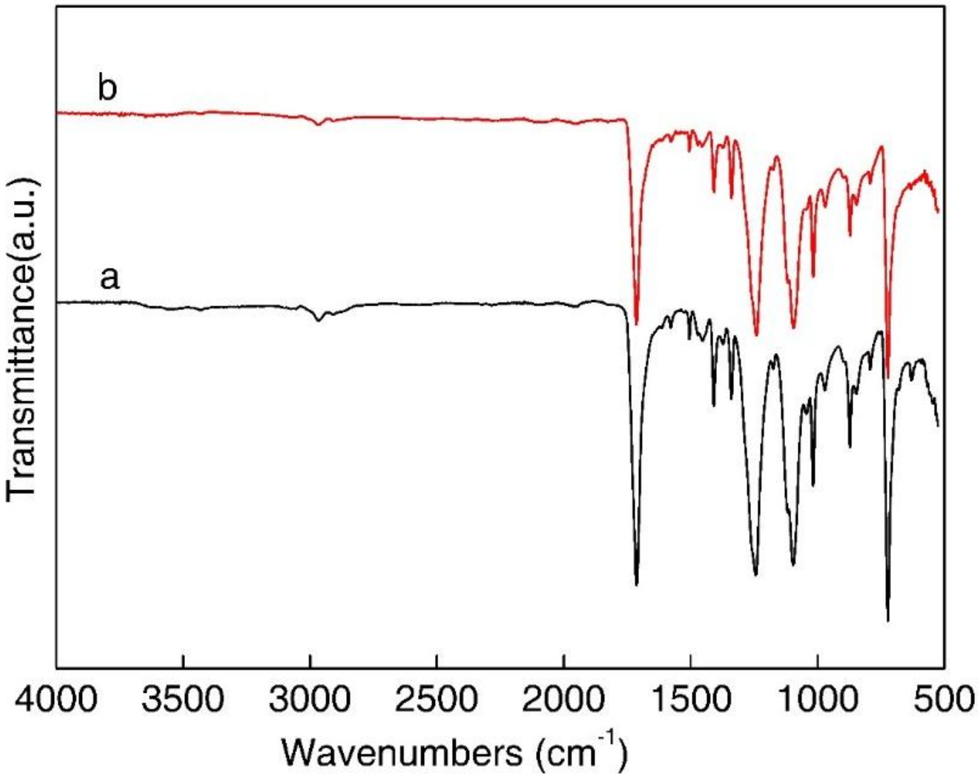

Figure 2-6. FTIR spectra of the polyester fibers (**a**) before and (**b**) after silver plating.

Figure 2-6 shows the infrared spectra of the polyester fibers before and after silver plating. It can be known that the positions of the absorption peaks of the polyester fibers did not change before or after silver plating, which indicates that the basic structure of the polyester fiber is not affected by silver plating. Meanwhile, the intensity of the infrared absorption peaks of the silver-plated fiber became weaker as the surface of the fiber was coated with a dense silver layer, which reflects part of the infrared light and weakens the infrared absorption intensity of the fiber. In addition, no other new absorption peaks were observed on the spectrogram, indicating that there was no other impurity on the surface of the fiber.

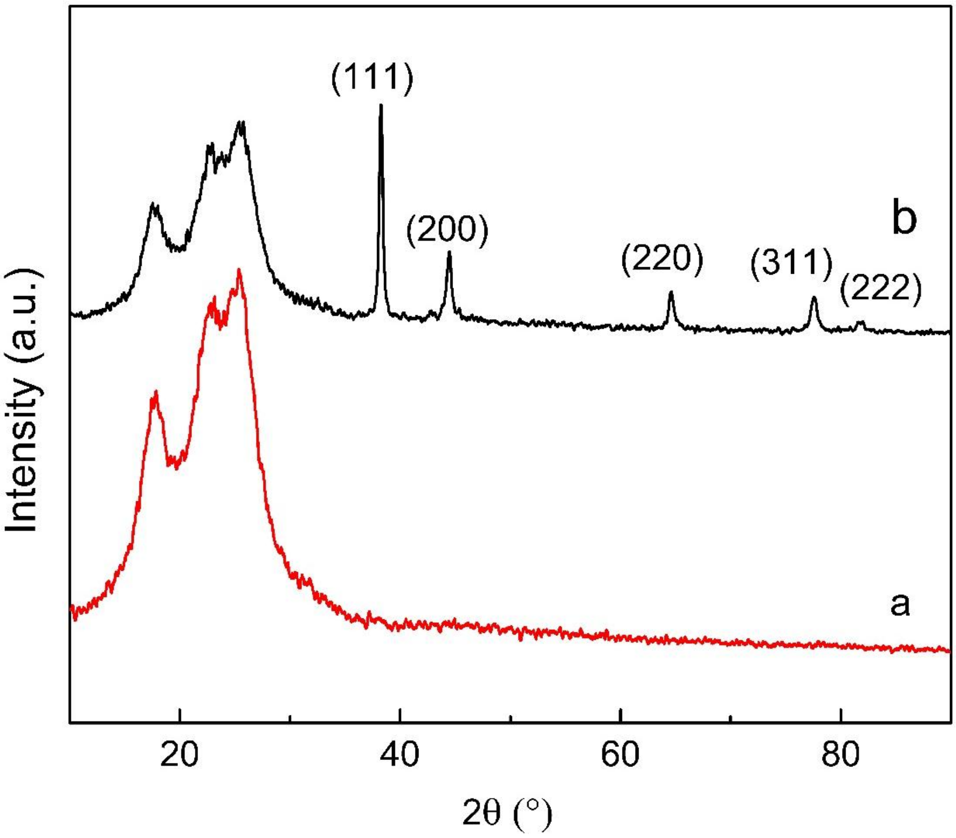

Figure 2-7. XRD patterns of the polyester fiber (**a**) before and (**b**) after silver plating.

The XRD patterns of the polyester fiber before and after silver plating are shown in Figure 2-7. Figure 2-7a demonstrates that the polyester fibers before silver plating had three diffraction peaks at 2θ values of 18°, 22°, and 26°, respectively, and had no other crystal diffraction peaks. Figure 2-7b shows that five clear diffraction peaks were observed in the 2θ range of 38°, 44°, 64°, 77°, and 82°, which corresponded to the (111), (200), (220), (311) and (222) crystalline planes of the face-centered cubic structures of silver, respectively, similar to the Joint Committee on Powder Diffraction Standards (JCPDS) File No: 04-0783 [71-77]. The diffraction peaks of the elemental silver were sharp and narrow, and there were no other diffraction peaks, indicating that the polyester fiber surface was coated with metallic silver with good crystallinity and high purity [78]. The characteristic diffraction peaks of the polyester fibers in Figure 7b were obviously weakened, which also indicated that the silver layer on the fiber surface was more uniform and denser.

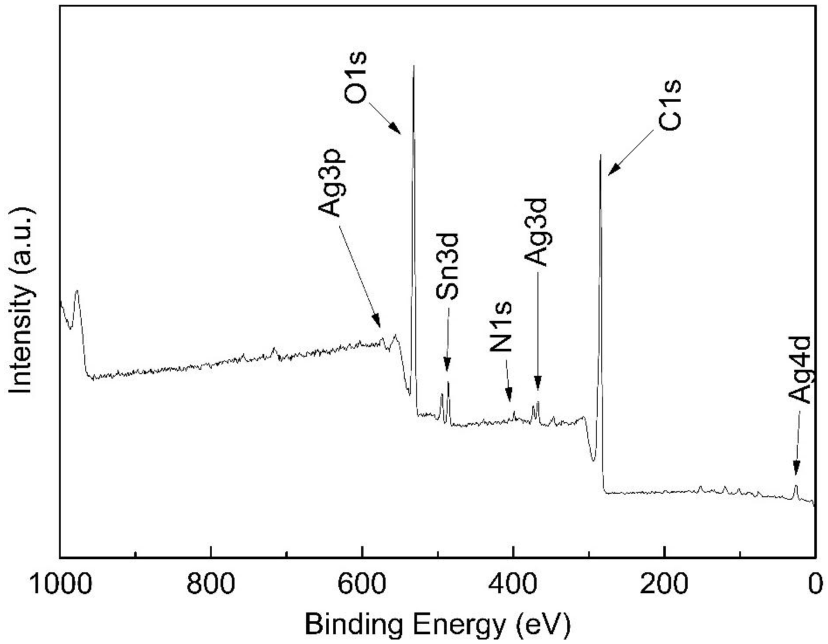

Figure 2-8. X-ray photoelectron (XPS) spectra of silver-plated fiber

The X-ray photoelectron spectrogram (XPS) of silver-plated polyester fibers is shown in Figure 2-8. The following energy peaks are observed at the given binding energies: O1s at 532.7 eV, Sn3d at 487.1 eV, N1s at 397.8 eV, Ag3d 367.9 eV and 373.2 eV, C1s at 285.3eV, and Ag4d at 25.7 eV. The peaks at 573.1 and 557.5 eV binding energies are Ag3p signals. These data are in excellent consistent with the literature [79,80], indicating that the surface of the silver-plated composite coated conductive fibers contains the silver element.

2.2.4 Mechanical Properties Analysis

The mechanical properties of the polyester fibers at different processing stages were tested by the Electronic Single Yarn Strength Tester (YG020B, Changzhou No. 2 Textile Machine Co., Ltd, Changzhou, China). Each group of samples was tested ten times and averaged. The results were shown in Table 2-1. Breaking strength represents the greatest stress especially in tension that a material is capable of withstanding without rupture. Elongation at break, also known as fracture strain, is the ratio between changed length and initial length after breakage of the test specimen, and elongation at break expresses the capability of natural plant fiber to resist changes of shape without crack formation [81].

Table 2-1. Comparison of the mechanical properties of different fibers.

Sample	Breaking Strength (cN)	Elongation at Break (%)
Original polyester fiber (210D/36F)	1041.81	22.57
Coarsening treated polyester fiber	911.23	16.35
Electroless silver-plated polyester fiber	934.25	18.81
Electroplated silver-coated polyester fiber	950.31	19.24

The results show that the fiber breaking strength and the elongation at break of the coarsened polyester fiber were reduced by 12.53% and 27.56%, respectively, when compared to those of the original polyester fiber. The breaking strength and elongation at break of the fibers after electroless silver plating were increased by 2.53% and 15.05%, higher than those before electroless plating, respectively. After electroplating, they further increased by 1.72% and 2.29%, respectively. This was because the fiber was hydrolyzed with a concentrated alkali at a high temperature during coarsening, and its surface was damaged by etching. After calculation, the mass loss rate after coarsening was about 9.8%, which led to a decrease in the mechanical property. After the electroless silver-plating, the surface of the fiber was covered with a dense silver layer. Furthermore, the metallic silver had good ductility. So, the silver layer can share part of the extra tensile force for the fiber when stretched, resulting in the increase of the breaking strength of the silver-plated fiber. The electroplated metallic silver layer completely covered the fibers and slightly enhanced the mechanical properties of the fibers. However, due to the thinner silver layer, there was less of an increase in the breaking strength of the silver-plated fiber [82].

2.2.5 Washability Analysis

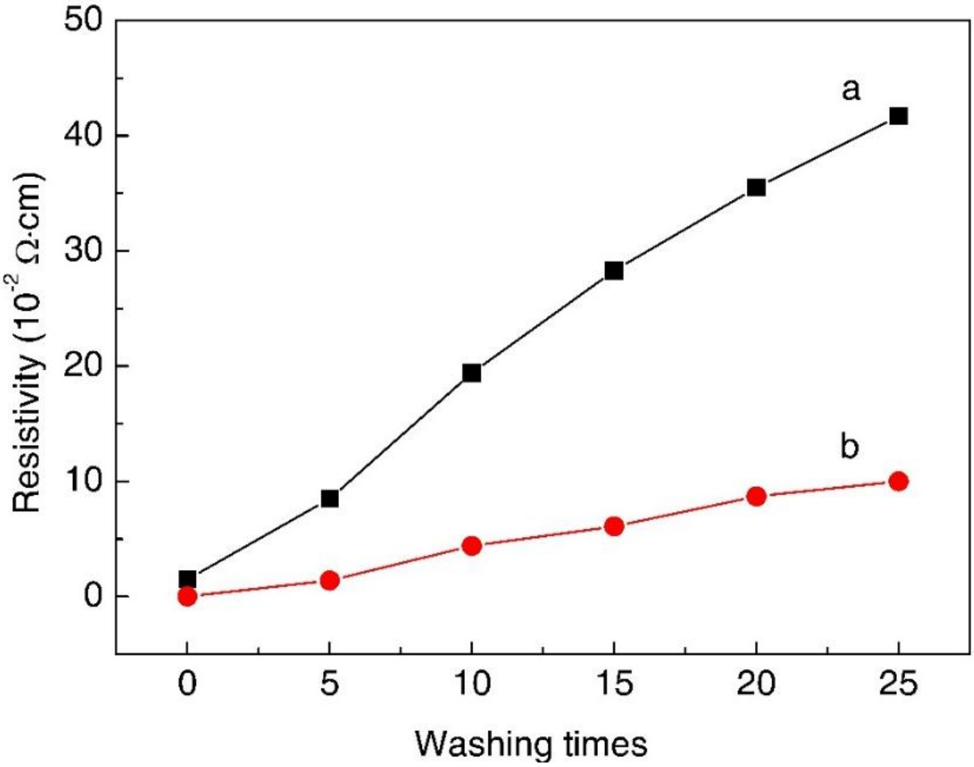

Figure 2-9. Influence of washing times on the resistivity of different fibers: (**a**) electroless silver-plated fiber; (**b**) electroplated silver-plated fiber.

The silver layers on the electroless or electroplated silver-coated polyester fibers have a great likelihood of being removed by the act of washing. Therefore, it is necessary to examine the washability. The resistivity changes and the SEM images of the electroless and electroplated silver-coated polyester fibers are shown in Figures 2-9 and 2-10, respectively.

In Figure 2-9, the resistivities of the electroless silver-plated fiber and electroplated silver-plated fiber increased with the increase of washing times, but the increase of resistivity of the electroplated silver-plated fiber was slower than that of the electroless silver-plated fiber, indicating that the electroplated silver-plated fiber had better surface fastness and washability. This was due to the rapid deposition of silver particles on the silver surface of the electroless silver-plated fiber during the electroplating process, resulting in a thicker and denser silver layer, which improved the washability of the electroplated silver-plated fiber [83].

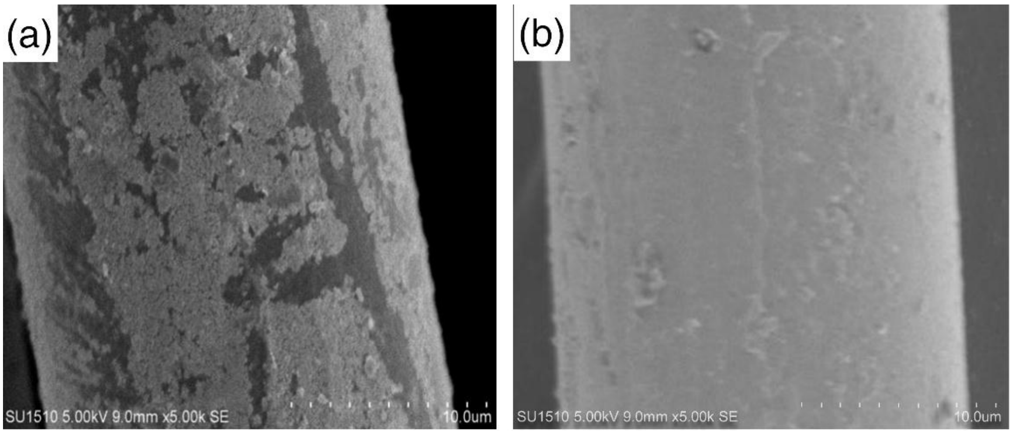

Figure 2-10. SEM images (×5000) of conductive polyester fibers after being washed for 30 times: (**a**) electroless silver-plated fibers; (**b**) electroplated silver-plated fibers.

Figure 2-10 shows the SEM images of the electroless silver-plated fibers and the electroplated silver-plated fibers after washing 30 times. After washing, the silver layer on the surface of the electroless silver-plated fiber severely peeled off, while only some loose silver particles peeled off from the surface of the electroplated silver-plated fiber, and the main body of the silver layer was in good condition. This may be because the shorter time of continuous electroless plating silver caused a thinner coating layer and a weaker binding force between the silver layer and the fiber, while the electroplating after continuous electroless plating significantly increased the thickness of the silver layer, and the binding force between the silver layer and the fiber was also obviously enhanced [84].

2.2.6 Conductive Properties Analysis

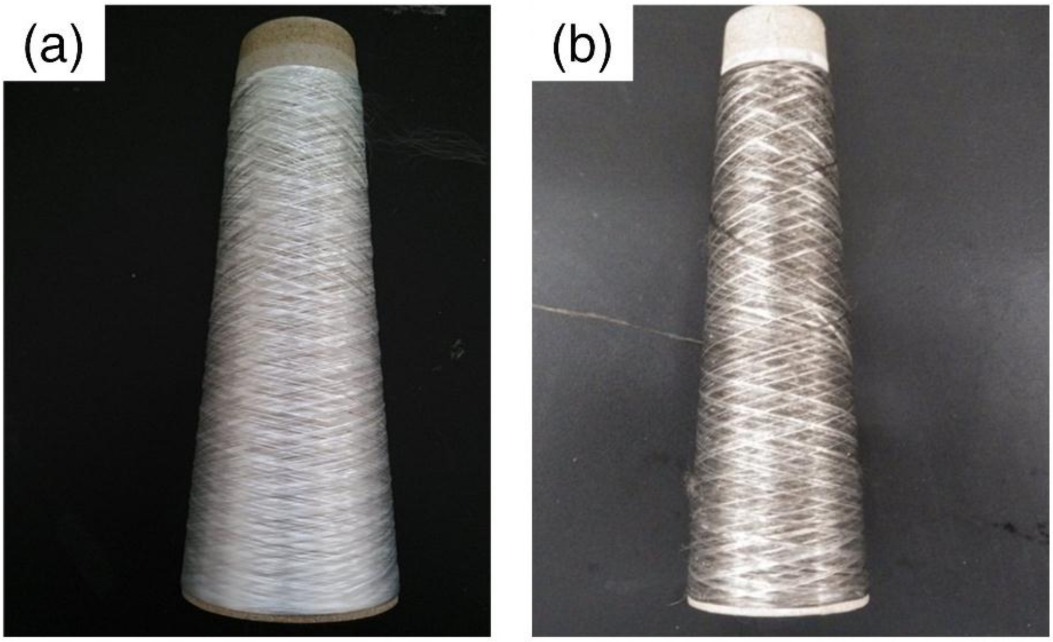

Figure 2-11. Photographs of winding bobbins of polyester fibers: (**a**) before silver plating; (**b**) after silver plating.

Figure 2-11b shows the polyester fiber prepared by using the self-made continuous silver-plating equipment. The winding bobbin made by the continuous silver-plating equipment was well-formed, and the silver-plated fiber had a silver-white metallic luster. We measured the resistivity of the polyester fibers before and after silver-plating. The resistivities of the original polyester fiber, electroless silver-plated fiber, and electroplated silver-plated fiber were 9.5×10^{10} Ω·cm, 1.5×10^{-2} Ω·cm, and 2.3×10^{-4} Ω·cm, respectively. The conductivity of the polyester fiber was significantly improved by silver-plating.

In this study, the light bulb experiment was also conducted. As shown in Figure 2-12, the two ends of the silver-plated fiber were connected to two wires and fixed on insulating paper with an insulating tape. After the wires connected the LED bulb to the power supply (3 V), the small bulb emitted an obvious bright light and the brightness was constant and stable for 10 min, which indicated that the prepared fiber surface was uniformly and continuously covered with the silver-plating layer, and the fiber could conduct electrons and had good electrical conductivity.

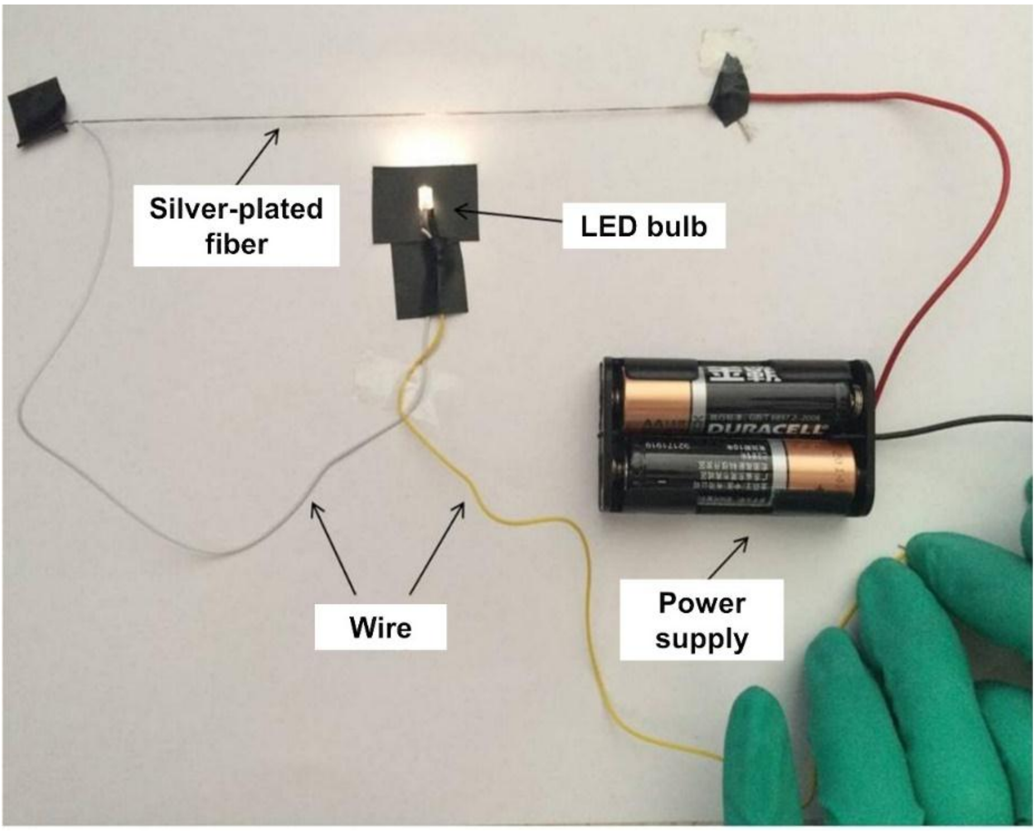

Figure 2-12. The light bulb experiment of a small bulb.

2.4 Conclusions

In this chapter, a continuous two-step silver plating method was developed with polyester fibers used as the substrate material, which combined the operations of continuous electroless plating step without activation under a dynamic condition and cyanide-free electroplating step. Furthermore, we designed specialized equipment for the continuous plating of silver on the polyester fibers. According to the machine conditions, the pretreatments, electroless silver-plating, and electroplating silver-plating process were improved accordingly, and the silver-plated conductive fibers were successfully prepared. The influence of the power supply method, control voltage, and electroplating time on electroplating silver was studied. The optimal conditions for electroplating silver conductive polyester fibers should include the power supply method having a constant voltage power, the best control voltage range of which is 1.5–2.0 V, and an electroplating time of 4 min. The silver-composition and morphology of Ag-coated polyester fibers were characterized by SEM, FTIR, XPS and XRD. Moreover, the mechanical properties and washability of the electroplating silver-plating fibers were compared with the electroless silver-plating fibers. The results demonstrated that after the continuous two-step silver plating, the surface coating of the fiber was obviously thickened, and the surface silver particles were denser and continuous, with better mechanical properties and washability. The electrical resistivity reached 2.3×10^{-4} Ω·cm, and the conductivity was obviously improved. The light bulb experiment also showed that the conductive fiber prepared by the continuous two-step silver plating method had good electrical conductivity.

References

1. Liu, X.Y.; Xie, M.M.; Li, Y.C.; Zhou, L.; Shao, J.Z. Study on the reduction properties of thiourea dioxide and its application in discharge printing of polyester fabrics. *Fibers Polym.* **2018**, *19*, 1237, doi:10.1007/s12221-018-7765-2.
2. Chaudhary, H.; Gupta, D.; Gupta, C. Multifunctional dyeing and finishing of polyester with sericin and basic dyes. *J. Text. Inst.* **2017**, *108*, 314–324, doi:10.1080/00405000.2016.1165401.

3. Kogo, A.A.; Ismail, I.M.; Yakasai, M.Y. Effects on the electro-mechanical properties of aniline-doped polyester fibric. *Bayero J. Pure Appl. Sci.* **2017**, *10*, 159–162, doi:10.4314/bajopas.v10i1.22.
4. Rojas, J.P.; Conchouso, D.; Arevalo, A.; Singh, D.; Foulds, I.G.; Hussain, M.M. Paper-based origami flexible and foldable thermoelectric nanogenerator. *Nano Energy* **2017**, *31*, 296–301, doi: 10.1016/j.nanoen.2016.11.012.
5. Rastegar, L.; Montazer, M.; Gaminian, H. Multifunctional colored polyester fabric treated with dopamine hydrochloride at room temperature: Higher tensile, hydrophilicity and anti-bacterial properties along with aminolysis. *Fibers Polym*. **2017**, *18*, 1915–1923, doi:10.1007/s12221-017-7012-2.
6. Yin, J.; Nysten, B. Contact electrification and charge decay on polyester fibres: A KPFM study. *J. Electrostat.* **2018**, *96*, 16–22, doi: 10.1016/j.elstat.2018.09.002.
7. Wang, C.; Guo, R.H.; Lan, J.W.; Tan, L.; Jiang, S.X.; Xiang, C. Preparation of multi-functional fabric via silver/reduced graphene oxide coating with poly(diallyldimethylammonium chloride) modification. *J. Mater. Sci.: Mater. Electron.* **2018**, *29*, 8010–8019, doi:10.1007/s10854-018-8807-8.
8. Kumar, N.; Ginting, R.T.; Ovhal, M.; Kang, J.W. All-solid-state flexible supercapacitor based on spray-printed polyester r/ PEDOT : PSS electrodes. *Mol. Cryst. Liq. Cryst.* **2018**, *660*, 135–142, doi:10.1080/15421406.2018.1456125.
9. Smith, D.R.; Mock, J.J.; Starr, A.F.; Schurig, D. Gradient index metaterials. *Phys. Rev. E* **2005**, *71*, 211–230, doi:10.1103/PhysRevE.71.036609.
10. Sekhar, S.C.; Nagaraju, G.; Yu, J.S. Conductive silver nanowires-fenced carbon cloth fibers-supported layered double hydroxide nanosheets as a flexible and binder-free electrode for high-performance asymmetric supercapacitors. *Nano Energy* **2017**, *36*, 58–67, doi: 10.1016/j.nanoen.2017.04.019.
11. Zhang, Z.X.; Dou, J.X.; He, J.H.; Xiao, C.X.; Shen, L.Y.; Yang, J.H.; Wang, Y.; Zhou, Z.W. Electrically/infrared actuated shape memory composites based on a bio-based polyester blend and graphene nanoplatelets and their excellent self-driven ability. *J. Mater. Chem. C* **2017**, *5*, 4145–4158, doi:10.1039/C7TC00828G.

12. Lu, Y.; Jiang, J.W.; Yoon, S.; Kim, K.S.; Kim, J.H.; Park, S.; Kim, S.H.; Piao, L. High-performance stretchable conductive composite fibers from surface-modified silver nanowires and thermoplastic polyurethane by wet spinning. *ACS Appl. Mater. Interfaces* **2018**, *10*, 2093–2104. doi:10.1021/acsami.7b16022.
13. Liang, Y.Y.; Lin, C.X.; Guan, J.P.; Li, Y.J. Silver nanoparticle-immobilized porous POM/PLLA nanofibrous membranes: Efficient catalysts for reduction of 4-nitroaniline. *RSC Adv.* **2017**, *7*, 7460–7468, doi:10.1039/C6RA28167B.
14. Li, M.M.; Gong, Y.M.; Wang, W.H.; Xu, G.P.; Liu, Y.F.; Guo, J. In-situ reduced silver nanoparticles on populus fiber and the catalytic application. *Appl. Surf. Sci.* **2017**, *394*, 351–357, doi: 10.1016/j.apsusc.2016.10.094.
15. Mahmud, S.; Sultana, M.Z.; Pervez, M.N.; Habib, M.A.; Liu, H.H. Surface Functionalization of "Rajshahi Silk" Using Green Silver Nanoparticles. *Fibers* **2017**, *5*, 35, doi:10.3390/fib5030035.
16. Li, X.Q.; Shi, C.; Wang, J.D.; Wang, J.; Li, M.J.; Hua, Q.; Hong, S.; Ogino, K. Polyaniline-doped TiO_2/PLLA fibers with enhanced visible-light photocatalytic degradation performance. *Fibers Polym*. **2017**, *18*, 50–56, doi:10.1007/s12221-017-6895-2.
17. Islam, S.; Sun, G. Thermodynamics, kinetics, and multifunctional finishing of textile materials with colorants extracted from natural renewable sources. *ACS Sustain. Chem. Eng.* **2017**, *5*, 7451–7466, doi:10.1021/acssuschemeng.7b01486.
18. Gan, X.P.; Wu, Y.T.; Liu, L.; Shen, B.; Hu, W.B. Electroless copper plating on PET fabrics using hypophosphite asreducing agent. *Surf. Coat. Technol.* **2007**, *201*, 7018–7023, doi: 10.1016/j.surfcoat.2007.01.006.
19. Kim, M.S.; Kim, H.K.; Byun, S.W.; Jeong, S.H.; Hong, Y.K.; Joo, J.S.; Song. K.T.; Kim, K.; Lee, C.J.; Lee, J.Y. PET fabric/polypyrrole composite with high electrical conductivity for EMI shielding. *Synth. Met.* **2002**, *126*, 233–239, doi:10.1016/S0379-6779(01)00562-8.
20. Zhou, Q.H.; Chen, H.W.; Wang, Y. Region-selective electroless gold plating on polycarbonate sheets by UV-patterning in combination with silver activating. *Electrochim. Acta* **2010**, *55*, 2542–2549, doi: 10.1016/j.electacta.2009.12.024.

21. Li, X.Q.; Wang, J.D.; Li, M.J.; Yang, J.; Gu, Z.J.; Liu, C.C.; Ogino, K. Fe-doped TiO_2/SiO_2 nanofibrous membranes with surface molecular imprinted modification for selective removing 4-Nitrophenol. *Chin. Chem. Lett.* **2018**, *29*, 527–530, doi: 10.1016/j.cclet.2017.09.007.
22. Chen, D.X.; Kang, Z.X. ABS plastic metallization through UV covalent grafting and layer-by-layer deposition. *Surf. Coat. Technol.* **2017**, *328*, 63–69, doi: 10.1016/j.surfcoat.2017.08.020.
23. Micheli, D.; Apollo, C.; Pastore, R.; Morles, R.B.; Laurenzi, S.; Marchetti, M. Nanostructured composite materials for electromagnetic interference shielding applications. *Acta Astronaut.* **2011**, *102*, 699, doi: 10.1016/j.actaastro.2011.06.004.
24. Qin, X.; Wang, H.C.; Shan, R.F. Morphology-controlled synthesis of Ag nanoparticle decorated glassy carbon electrode and its electrochemical performance. *Ionics* **2018**, *24*, 1765, doi:10.1007/s11581-017-2327-z.
25. Kim, S.M.; Kim, I.Y.; Kim, H.R. Production of electromagnetic shielding fabrics by optimization of electroless silver plating conditions for PET fabrics. *J. Text. Inst.* **2017**, *108*, 1065–1073, doi:10.1080/00405000.2016.1219449.
26. Li, X.Q.; Shi, C.; Qiu, H.; Sun, H.; Ogino, K. Fabrication of fluorescent poly(L-lactide-co-caprolactone) fibers with quantum-dot incorporation from emulsion electrospinning for chloramphenicol detection. *J. Appl. Polym. Sci.* **2016**, *133*, 44584, doi:10.1002/APP.44584.
27. Fukuhara, C.; Ohkura, H.; Kamata, Y.; Murakami, Y.; Igarashi, A. Catalytic properties of plate-type copper-based catalysts, for steam reforming of methanol, on an aluminum plate prepared by electroless plating. *Appl. Catal. A Gen.* **2004**, *273*, 125–132, doi: 10.1016/j.apcata.2004.06.034.
28. Kobayashi, Y.; Salgueiriño-Maceira, V.; Liz-Marzán, L.M. Deposition of silver nanoparticles on silica spheres by pretreatment steps in electroless plating. *Chem. Mater.* **2001**, *5*, 1630–1633, doi:10.1021/cm001240g.
29. Zhu, L.; Luo, L.M.; Luo, J.; Wu, Y.C.; Li, J. Effect of electroless plating Ni–Cu–P layer on brazability of cemented carbide to steel. *Surf. Coat. Technol.* **2012**, *8*, 2521–2524, doi: 10.1016/j.surfcoat.2011.11.004.

30. Li, N.J.; Li, N.W.; Li, M.M.; Yi, D. The preparation and application of special performance ornamental alloy coating on plastic substrate. *Appl. Mech. Mater.* **2013**, *423–426*, 837–841, doi: 10.4028/www.scientific.net/AMM.422-426.837.

31. Li, Q.L.; He, X.Y.; Zhang, Y.Q.; Yang, X.F. Preparation and Microwave Absorbing Properties of an Electroless Ni-Co Coating on Multiwall Carbon Nanotubes Using $[Ag(NH_3)_2]^+$ as Activator. *J. Nanomater.* **2015**, 404698, doi:10.1155/2015/404698.

32. Matijević, E.; Poskanzer, A.M.; Zuman, P. Characterization of the stannous chloride/Palladium chloride catalysts for electroless plating. *Plat. Surf. Finish.* **1975**, *61*, 958–965.

33. Wang, X.W.; Ma, S.J.; Wang, X.H.; Ma, C.; Yuan, Z.H. Facile conversion of Zn nanowires to Zn nanotubes by heating-induced volatilization in nanopores of anodic aluminum oxide template. *Vacuum* **2016**, *132*, 86–90, doi: 10.1016/j.vacuum.2016.07.029.

34. Wei, L.; Yu, J.; Hu, X.J.; Huang, Y. Facile surface modification of porous stainless-steel substrate with TiO_2 intermediate layer for fabrication of H2-permeable composite palladium membranes. *Sep. Sci. Technol.* **2016**, *51*, 998–1006, doi:10.1080/01496395.2015.1136330.

35. Wei, L.; Yu, J.; Hu, X.J.; Wang, R.X.; Huang, Y. Effects of Sn residue on the high temperature stability of the H2-permeable palladium membranes prepared by electroless plating on Al_2O_3 substrate after $SnCl_2$–$PdCl_2$ process: A case study. *Chin. J. Chem. Eng.* **2016**, *24*, 1154–1160, doi: 10.1016/j.cjche.2016.04.008.

36. Wang, P.C.; Chang, C.P.; Youh, M.J.; Liu, Y.M.; Chu, C.M.; Ger, M.D. The preparation of pH-sensitive Pd catalyst ink for selective electroless deposition of copper on a flexible PET substrate. *J. Taiwan Inst. Chem. E* **2016**, *60*, 555–563, doi: 10.1016/j.jtice.2015.10.024.

37. Ang, L.M.; Hor, T.S.A.; Xu, G.Q.; Tung, C.H.; Zhao, S.P.; Wang, J.L.S. Electroless Plating of Metals onto Carbon Nanotubes Activated by a Single-Step Activation Method. *Chem. Mater.* **1999**, *11*, 2115–2118, doi:10.1021/cm990078i.

38. Absalan, G.; Akhond, M.; Soleimani, M.; Ershadifar, H. Efficient electrocatalytic oxidation and determination of isoniazid on carbon ionic liquid electrode modified with electrodeposited palladium nanoparticles. *J. Electroanal. Chem.* **2016**, *761*, 1–7, doi: 10.1016/j.jelechem.2015.11.041.

39. Wataha, J.C.; Hanks, C.T. Biological effects of palladium and risk of using palladium in dental casting alloys. *J. Oral Rehabil.* **1996**, *23*, 309–320, doi:10.1111/j.1365–2842.1996.tb00858.x.
40. He, Z.; Zhan, L.; Wang, Q.; Song, S.; Chen, J.; Zhu, K.; Xu, X.H.; Liu, W.P. Increasing the activity and stability of chemi-deposited palladium catalysts on nickel foam substrate by electrochemical deposition of a middle coating of silver. *Sep. Purif. Technol.* **2011**, *80*, 526–532, doi: 10.1016/j.seppur.2011.06.007.
41. Shukla, S.; Seal, S.; Rahaman, Z.; Scammon, K. Electroless copper coating of cenospheres using silver nitrate activator. *Mater. Lett.* **2002**, *57*, 151–156, doi:10.1016/S0167-577X(02)00722-X.
42. Zoppas, F.M.; Marchesini, F.A.; Devard, A.; Bernardes, A.M.; Miró, E.E. Controlled deposition of Pd and In on carbon fibers by sequential electroless plating for the catalytic reduction of nitrate in water. *Catal. Commun*. **2016**, *78*, 59–63, doi: 10.1016/j.catcom.2016.02.012.
43. Shao, Q.S.; Bai, R.C.; Tang, Z.Y.; Pang, H.W.; Yan, W.; Sun, J.L.; Ren, M.S. Preparation of silver-deposited aromatic polysulfonamide fibers with excellent performance via electroless nanoplating using a chlorine-aided silver activation system. *Ind. Eng. Chem. Res.* **2015**, *54*, 11302–11311, doi: 10.1021/acs.iecr.5b02657.
44. Fatema, U.K.; Gotoh, Y. A new electroless Ni plating procedure of iodine-treated aramid fiber. *J. Coat. Technol. Res.* **2013**, *10*, 415–425, doi:10.1007/s11998-012-9441-7.
45. Shu, Z.; Wang, X. Environment-friendly Pd free surface activation technics for ABS surface. *Appl. Surf. Sci.* **2012**, *258*, 5328–5331, doi: 10.1016/j.apsusc.2012.01.141.
46. Cha, S.H.; Koo, H.C.; Kim, J.J. The inhibition of silver agglomeration by gold activation in silver electroless plating. *J. Electrochem. Soc.* **2005**, *152*, C388–C391, doi:10.1149/1.1905984.
47. Okinaka, Y.; Hoshino, M. Some recent topics in gold plating for electronics applications. *Gold Bull.* **1998**, *31*, 3, doi:10.1007/BF03215469.
48. Lien, W.; Huang, P.; Tseng, S.; Cheng, C.H.; Lai, S.M.; Liaw, W.C. Electroless silver plating on tetraethoxy silane–bridged fiber glass. *Appl. Surf. Sci.* **2012**, *258*, 2246–2254, doi: 10.1016/j.apsusc.2011.09.059.

49. Liu, C.C.; Cheng, J.; Li, X.Q.; Gu, Z.J.; Ogino, K. Laser-Induced Silver Seeding on Filter Paper for Selective Electroless Copper Plating. *Materials* **2018**, *8*, 1348, doi: 10.3390/ma11081348.

50. De-Almeida, M.R.H.; Carlos, I.A.; Barbosa, L.L.; Carlos, R.M.; Lima-Neto, B.S.; Pallone, E.M.J.A. Voltammetric and morphological characterization of copper electrodeposition from non-cyanide electrolyte. *J. Appl. Electrochem.* **2002**, *32*, 763, doi:10.1023/A:1020182120035.

51. Varentsova, V.I.; Varenstov, V.K.; Bataev, I.A.; Yusin, S.I. Effect of surface state of carbon fiber electrode on copper electroplating from sulfate solution. *Prot. Met. Phys. Chem. Surf.* **2011**, *47*, 43–47, doi:10.1134/S2070205111010217.

52. Xie, B.G.; Sun, J.J.; Lin, Z.B.; Chen, G.N. Electrodeposition of mirror-bright silver in cyanide-free bath containing uracil as complexing agent without a separate strike plating process. *J. Electrochem. Soc.* **2009**, *156*, D79–D83, doi:10.1149/1.3046157.

53. Wang, L.Y.; Chen, X.G.; Cao, D.R. A cyanide-selective colorimetric “naked-eye” and fluorescent chemosensor based on a diketopyrrolopyrrole–hydrazone conjugate and its use for the design of a molecular-scale logic device. *RSC Adv.* **2016**, *6*, 96676–96685, doi:10.1039/C6RA21669B.

54. Kato, M.; Okinaka, Y. Some recent developments in non-cyanide gold plating for electronics applications. *Gold Bull.* **2004**, *37*, 37–44, doi:10.1007/BF03215515.

55. Bomparola, R.; Caporali, S.; Lavacchi, A.; Bardi, U. Silver electrodeposition from air and water-stable ionic liquid: An environmentally friendly alternative to cyanide baths. *Surf. Coat. Technol.* **2007**, *201*, 9485–9490, doi: 10.1016/j.surfcoat.2007.04.008.

56. Wang, Y.; Bian, C.; Jing, X.L. Adhesion improvement of electroless copper plating on phenolic resin matrix composite through a tin-free sensitization process. Appl. *Surf. Sci.* **2013**, *271*, 303–310, doi: 10.1016/j.apsusc.2012.01.188.

57. Wang, Y.H. Electrodeposition preparation and properties of foamed silver. *Huazhong University of Science and Technology*, **2006**, 40-43.

58. Hu, Z.W.; Fu, Y.Q. Structure and properties of metallized polyester fibers. *Printing and dyeing* **2001**, *27*, 8–11, doi: 10.3321/j.issn:1000-4017.2001.01.002.

59. Cui, X.; Zhang, H.P.; Chen, J.Y.; Xie, Y.F. Preparation of conductive nylon by silver deposition. *Journal of Textiles* **2011**, *32*, 12–17.

60. Li, X.Q.; Wang, J.D.; Hu, Z.M.; Li, M.J.; Ogino, K. In situ polypyrrole polymerization enhances the photocatalytic activity of nanofibrous TiO_2/SiO_2 membranes. *Chin. Chem. Lett.* **2018**, *29*, 166–170, doi: 10.1016/j.cclet.2017.05.020.

61. Mao, Y.; Zhang, S.Q.; Wang, W.; Yu, D. Electroless silver plated flexible graphite felt prepared by dopamine functionalization and applied for electromagnetic interference shielding. *Colloid. Surf. A* **2018**, *558*, 538–547, doi: 10.1016/j.colsurfa.2018.09.028.

62. Chang, S.Y.; Wan, C.C.; Wang, Y.Y.; Shih, C.H.; Tsai, M.H.; Shue, S.L.; Yu, C.H.; Liang, M.S. Characterization of Pd-free electroless Co-based cap selectively deposited on Cu surface via borane-based reducing agent. *Thin Solid Films* **2006**, *515*, 1107–1111, doi: 10.1016/j.tsf.2006.07.044.

63. Guo, R.H.; Jiang, S.Q.; Yuen, C.W.M.; Ng, M.C.F. An alternative process for electroless copper plating on polyester fabric. *J. Mater. Sci.: Mater. Electron.* **2009**, *20*, 33, doi:10.1007/s10854-008-9594-4.

64. Li, X.F.; Li, Y.Q.; Cai, J.; Zhan, D.Y. Metallization of bacteria cells. *Sci. China Ser. E-Technol. Sci.* **2003**, *46*, 161, doi:10.1360/03ye9017.

65. Stremsdoerfer, G.; Ghanem, F.; Saikali, Y. Fares-Karam, A. Copper deposition by dynamic chemical plating. *Mater. Sci.* **2003**, *38*, 3285–3291, doi: 10.1023/A:1025190022069.

66. Qiu, T; Chu, P.K. Self-selective electroless plating: An approach for fabrication of functional 1D nanomaterials. *Mat. Sci. Eng. R.* **2008**, *61*, 59–77, doi: 10.1016/j.mser.2008.03.001.

67. Yang, C.C.; Wang, Y.Y.; Wan, C.C. Synthesis and characterization of PVP stabilized Ag/Pd nanop-articles and its potential as an activator for electroless copper depositi-on. *J. Electrochem. Soc.* **2005**, *152*, C96–C100, doi:10.1149/1.1850379.

68. Kashimura, Y.; Nakashima, H.; Furukawa, K.; Torimitsu, K. Fabrication of nano-gap electrodes using electroplating technique. *Thin Solid Films* **2003**, *438*, 317–321, doi: 10.1016/S0040-6090(03)00737-5.

69. Lin, C.T.; Lin, K.L. Effects of current density and deposition time on electrical resistivity of electroplated Cu layers. *J. Mater. Sci-Mater. El.* **2004**, *15*, 757–762, doi: 10.1023/B:JMSE.0000043425.91103.da.

70. Liu, P.S.; Li, T.F.; Fu, C. Relationship between electrical resistivity and porosity for porous metals. *Mater. Sci. Eng., A* **1999**, *268*, 208–215, doi: 10.1016/S0921-5093(99)00073-8.

71. Bykkam, S.; Ahmadipou, M.; Narisngam, S.; Kalagadda, V.R.; Chidurala, S.C. Extensive Studies on X-Ray Diffraction of Green Synthesized Silver Nanoparticles. *Advances in Nanoparticles* 2**015**, *4*, 1–10, doi:10.4236/anp.2015.41001.

72. Thosar,N.; Basak, S.; Bahadure, R.N.; Rajurkar, M. Antimicrobial efficacy of five essential oils against oral pathogens: An in vitro study. *Eur. J. Dent*. **2013**, *7*, S71–S77, doi: 10.4103/1305-7456.119078.

73. Thapa, R.; Bhagat, C.; Shrestha, P.; Awal, S.; Dudhagara, P. Enzyme-mediated formulation of stable elliptical silver nanoparticles tested against clinical pathogens and MDR bacteria and development of antimicrobial surgical thread. *Ann. Clin. Microbiol. Antimicrob.* **2017**, *16*, 39, doi: 10.1186/s12941-017-0216-y.

74. Yang, X.; Du, Y.; Li, D.; Lv, Z.Z.; Wang, E.K. One-Step Synthesized Silver Micro-Dendrites Used as Novel Separation Medium and Its Applications in Multi-DNA Analysis. *Chem. Commun.* **2011**, *47*, 10581–10583, doi: 10.1039/c1cc11374g.

75. Corro, G.; Vidal, E.; Cebada, S.; Pal, U.; Bañuelos, F.; Vargas, D.; Guilleminot, E. Electronic state of silver in Ag/SiO_2 and Ag/ZnO catalysts and its effect on diesel particulate matter oxidation: An XPS study. *Appl. Catal. B-Environ.* **2017**, *216*, 1–10, doi: 10.1016/j.apcatb.2017.05.059.

76. Siddiqui, M.N.; Redhwi, H.H.; Achilias, D.S.; Kosmidou, E.; Vakalopoulou, E.; DIoannidou, M. Green Synthesis of Silver Nanoparticles and Study of Their Antimicrobial Properties. *J. Polym. Environ.* **2018**, *26*, 423, doi: 10.1007/s10924-017-0962-0.

77. Basavegowda, N.; Idhayadhulla, A.; Lee, Y. R. Phyto-synthesis of gold nanoparticles using fruit extract of Hovenia dulcis and their biological activities. *Ind. Crops Products* **2014**, *52*, 745–751, doi: 10.1016/j.indcrop.2013.12.006.

78. Dimeska, R.; Murray, P.S.; Ralph, S.F.; Wallace, G.G. Electroless recovery of silver by inherently conducting polymer powders, membranes and composite materials. *Polymer* **2006**, *47*, 4520–4530, doi: 10.1016/j.polymer.2006.02.112.

79. Bätz, P.; Schmeißer, D.; Göpel, W. Electronic structure of polypyrrole films. *Phys. Rev. B.* **1991**, *43*, 9178–9189, doi: 10.1103/PhysRevB.43.9178.

80. Roza, D.; Paul, S.M.; Stephen, F.R.; Gordon, G.W. Electroless recovery of silver by inherently conducting polymer powders, membranes and composite materials. *Polymer*, **2016**, *47*, 4520–4530, doi: 10.1016/j.polymer.2006.03.112.

81. Fan, M.Z.; Fu, F. *Advanced High Strength Natural Fibre Composites in Construction*; Woodhead Publishing: Sawston Cambridge, UK, 2017; pp. 596, ISBN:978-0-08-100411-1, doi: 10.1016/C2014-0-03942-1.

82. Peeters, P; Hoorn, G.v.d.; Daenen, T.; Kurowski, A.; Staikov, G. Properties of electroless and electroplated Ni–P and its application in microgalvanics. *Electrochimica Acta* **2001**, *47*, 161–169, doi: 10.1016/S0013-4686(01)00546-1.

83. Hegemann, D.; Amberg, M.; Ritter, A.; Heuberger, M. Recent developments in Ag metallised textiles using plasma sputtering. *Mater. Technol.* **2013**, *24*, 41–45, doi:10.1179/175355509X417981.

84. Niitsu, K.; Ota, S.; Gamo, K.; Kondo, H.; Hori, M.; Nakazato, K. Development of Microelectrode Arrays Using Electroless Plating for CMOS-Based Direct Counting of Bacterial and HeLa Cells. IEEE. T. Ind. Electron. 2015, 9, 607–619, doi: 10.1109/TBCAS.2015.2479656.

Chapter 3 Electroless Plate of Polyaniline-Silver Composite Layer on Polyester Fibers

3.1 Introduction

In industrial production and daily life, common synthetic fibers often produce electrostatic phenomena because of friction, which brings a lot of inconvenience and harm to people health. Therefore, studies of the antistatic performance of synthetic fibers have been the focus of attention from the very beginning of the appearance of synthetic fibers. Furthermore, with the development of the society and the progress of science and technology, especially the development of electronic industry and information technology, more and more attention has being paid to the development of synthetic fiber antistatic technology. Electricity conductive fiber can eliminate static electricity by corona discharge mechanism in various environmental conditions and is widely applied to clothing, electronics, medicine, biological science and aerospace and other fields [1-4].

Electroless silver plating originated from the ancient silver mirror reaction, is one of the main methods for the preparation of conductive fiber; the method has a history of hundreds of years [5, 6]. Different from electroplating, the silver layer formed through electroless plating is not deposited by external electrons as a reductive agent but obtained by the redox reaction between the metal ion solution and a chemical reductive agent [7-10]. There are many advantages in preparing silver deposition by means of electroless or chemical plating, such as being without an external power supply and the uneven coating thickness caused by power distribution, simple process equipment, convenient operation and the uniform of conductive layer with excellent electric conductivity [11-16].

Conductive textile or fibers obtained from π-electron conjugated polymers are widely used as filters, electromagnetic interference shielding materials, antimicrobial and flame retardancy materials. Traditionally, a conductive composite can be produced by coating conductive polymers on the surface of scaffold, *in-situ* polymerization of various monomers in the scaffold matrix, or simply blending the conductive polymer with structural materials. Among various conductive polymers, polyaniline (PANI) is regarded as the most commercially promising conductive polymer, because of inexpensive monomer, the ease of which it is produced, its high yield and its thermal and chemical stability [17-19]. Many quite valuable studies have reported the possibility of producing an electrically conductive composite from incorporating PANI with polyester, chitosan, gelatin hydro-gel, and graphene [20].

PANI composite can be prepared from solution casting, spin coating, electrospinning and spraying [21-23]. In all these technologies, PANI should be dissolved into appropriate solvent followed by blending with other materials and then be produced. However, these aforementioned methods only fabricate a thin composite film but cannot be used to produce bulk or textile composite. Furthermore, PANI has to be prepared in a soluble-form, which demands much more complicated and time-costing processes. Hunting for a suitable chemical agent to dissolve PANI is another restriction in the preparation and final properties of the final composite. Unlike these techniques, the electroless plating of PANI on the object surfaces is much simpler and more effected method to obtain conductive textile or fibers.

In this chapter, conductive fibers were prepared by the two-step deposition of PANI and Ag layers on the surface of polyester fibers through oxidative polymerization and redox reaction, respectively. The morphology of polyester fibers before and after depositing of PANI-Ag layers was observed using scanning electron microscopy (SEM). The thermostability, mechanical properties, washing resistance and corrosion resistance of the resultant fibers obtained from different synthesis condition were also characterized.

3.2 Experimental

3.2.1 Materials

Polyester fibers (120D/72F) were commercially available. Aniline was purchased from J&K Scientific Ltd. (Beijing, China). Glucose and other chemical agents were purchased from Sinopharm Chemical Reagent Co., Ltd (Shanghai, China) and used without further purification.

3.2.2 PANI-Ag coating

The process of forming a PANI-Ag layer on the surface of polyester fibers is shown in Scheme 3-1. In details, polyester fibers were washed with acetone and distilled water several times to remove the oil and other impurities (or called cleaning), and then treated with 80g/L NaOH solution at 80 ℃ for 30min to obtain the coarsen surfaces. The fibers were immersed into the mixed solution of aniline, nitric acid and ammonium persulfate (APS) with ultrasonic concussion for 100–120 min at ice temperature to form the PANI layer on the surface of polyester fibers. Then, the fibers were sensitized by Tin granule and sensitizing liquid consisting of 30 g/L $SnCl_2$ and 40 ml/L Hydrochloric acid at room temperature for 3min. Thereafter, the fibers were dried and treated with 0.5 mol/L silver nitrate and 1 mol/L glucose solution for 1 h to obtain the Ag layer. The polyester fibers with PANI-Ag composite layer were washed with distilled water and dried in a vacuum at 60 ℃ for at least 1 h to remove the redundant water.

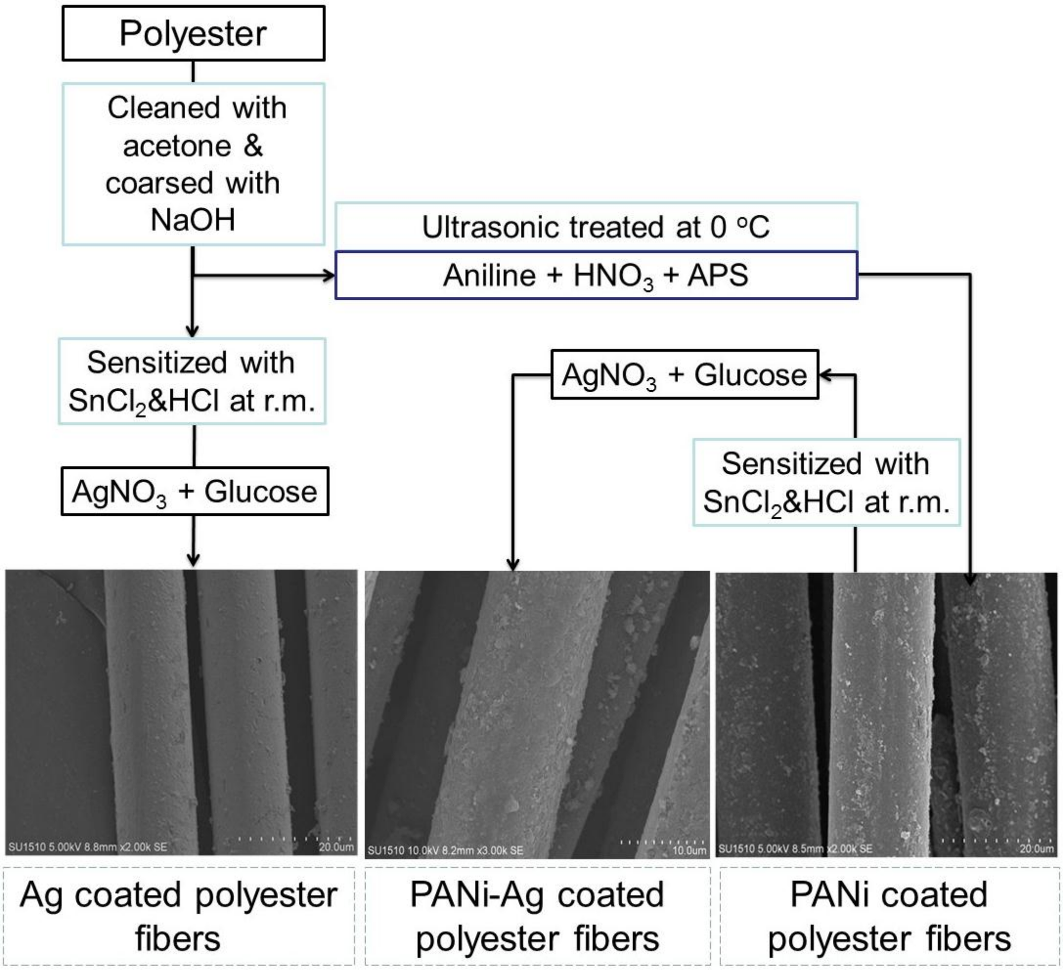

Scheme 3-1. Process of preparing polyaniline (PANI)-Ag layer on the surface of polyester fibers.

3.2.3 Characterizations

Fourier-transform infrared (FTIR) spectra were obtained on a Spectrum Two IR Spectrometers (PerkinElmer, Billerica, MA, USA). The data were recorded from 600

nm^{-1} to 2000 nm^{-1} with the resolution of 1 cm^{-1}. The morphology of different fibers was examined with a JEOL JSM-5900 SEM (JEOL Ltd., Tokyo, Japan) at an accelerating voltage of 15 kV. The surface of fibrous samples was coated with thin layers of gold before the observation. The surface morphology of samples was also characterized by an atomic force microscope (AFM; Dimension 3100, NanoScope IV, Digital Instrument, USA) in air under ambient condition, and the characterization was made in a non-contact mode. The X-ray photoelectron spectrogram (XPS) of samples was performed by a Thermo ESCALAB 250XI XPS (Thermo Fisher Scientific, Waltham, MA, USA) at an accelerating voltage of 14kV. X-ray diffraction (XRD) patterns of different fibers were measured with a D8 ADVANCE X-ray diffractometer (Bruker AXS, Karlsruhe, German) with a tube voltage of 40 kV, tube current of 1100 mA, a scanning ranges from 3° to 90°, and a scanning speed of 4°/min. The thermal gravity analysis (TGA) measurement was performed on a TGA/DSC1/1100SF instrument at a heating rate of 10ºC/min. The breaking strength and elongation at break of the fibers were characterized by a YG020B Electronic Single Yarn Strength Tester (Changzhou No.2 Textile Machine Co., Ltd, China) with a clamping length of 250 mm and a pre-tension of 10 CN.

A ZC-90G high insulation resistance tester and a DT-9205 digital multimeter are used to measure the surface resistance of the fibers. The clamping length of the fibers was 1 cm. Ten readings at different locations were taken randomly and the average was recorded. The resistivity of fibers was calculated by the following formula.

From the formula

$$R = \rho L / A, \tag{2-8}$$

It is concluded that

$$\rho = RA / L, \tag{2-9}$$

Where ρ, R, A, and L represent fiber resistivity (Ω·cm), the measured resistance of the fiber (Ω/cm), fiber cross-sectional area (cm^2), and test length (cm), respectively.

The resistivity of PANI-Ag coated polyester fibers was also measured after being washed for 25 times or treated with 5% NaCl solution.

For analyzing the corrosion resistance of fibers, samples were soaked in 5% NaCl solution for different time, then washed with clean water and dried. A DT-9205 digital multimeter and a ZC-90G high insulation resistance measuring instrument were used to measure the change of contact resistance on the coating surface, followed by calculating the resistivity of fibers and evaluating the corrosion resistance of fibers

The washability analysis refers to GB/T 8629-2001 "Standards for Home Washing and Drying Procedures for Textile Testing" and combines with the actual situation of fibers. The sample was placed in a detergent (40 ℃) prepared by 2 g/L washing powder with the control bath ratio was 1:30, and stirred for 15 min, which was recorded as one wash. After washing, wash and dry with water. ADT-9205 digital multimeter and a ZC-90G high insulation resistance tester were used to measure the change of contact resistance on the coating surface, then calculate the resistivity of the fibers and evaluate the washing resistance of the fibers after plating.

3.3 Results and Discussions

3.3.1 Influences of Preparing Parameters of PANI Layer on Conductivity

3.3.1.1 Aniline Concentration

The effect of different aniline concentrations for preparing PANI-Ag composite layers on the surface of polyester fibers was investigated. The details of preparing the PANI-Ag coated polyester fibers are described in Section 3.2.2. The polyester fibers were first immersed in aniline solution with concentrations ranging from 0.2 to 0.4 M for 30 min with 0.2 mol/L APS. The Ag was then deposited. The resistivity of the PANI-Ag coated polyester fibers with various aniline concentration is shown in Figure 3-1. Furthermore, the conductivity of the PANI-Ag coated polyester fibers was also measured after being washed and dried 25 times. The resistivity increase of fibers was calculated.

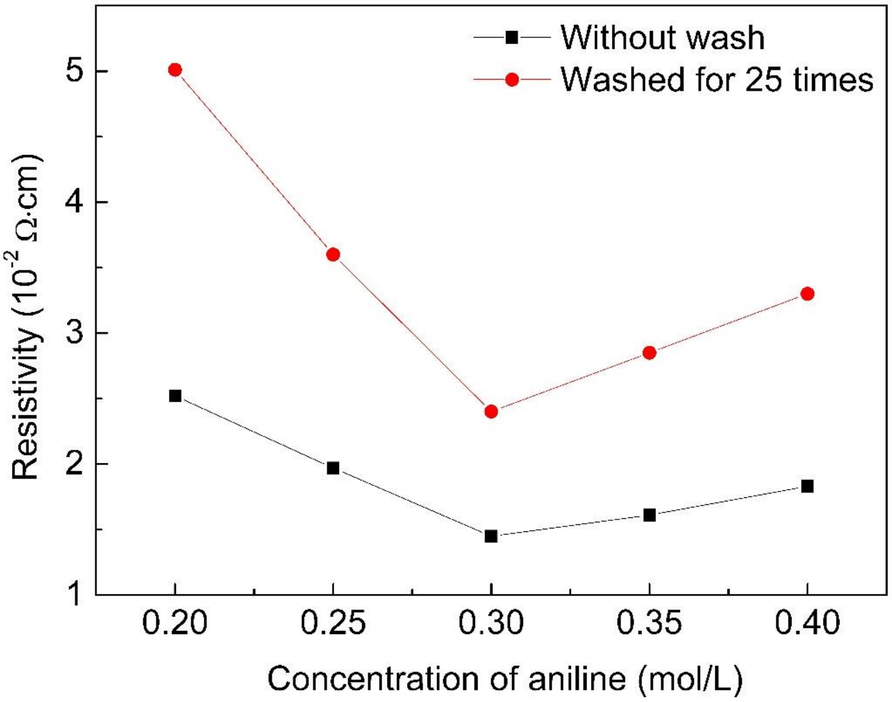

Figure 3-1. Effect of aniline concentration on the conductivity of PANI-Ag coated polyester fibers.

It can be seen from Figure 3-1 that the resistivity of the PANI-Ag coated fibers decreased from 0.05 Ω/cm to about 0.025 Ω/cm, as the concentration of aniline increased from 0.2 M to 0.3 M; then, the resistivity was increased to about 0.035 Ω/cm at an aniline concentration of 0.4 mol/L. And at an aniline concentration of 0.3mol/L, there is the lowest resistivity, indicating that the conductivity is best. When the concentration of aniline is too low, a continuous and dense polyaniline layer cannot be formed on the surface of the fiber, and the surface roughness of the fiber is insufficient, which affects the deposition of subsequent metallic silver on the surface of the fiber. As the aniline concentration increased, there was more PANI deposited on the fiber surface and the trend to form Ag on the surface of polyester fibers also increased; this led to a lower resistivity. However, the excessive aniline concentration led to the formation of uneven layers of PANI, which caused the discontinuous silver layer and affected the electrical conductivity of the resultant fibers [24,25]. Therefore, the optimal concentration of aniline should be 0.3 mol/L.

3.3.1.2 APS Concentration

Similar results were obtained as the concentration of APS ranged from 0.1 mol/L to 0.3 mol/L with an aniline concentration of 0.3 mol/L. The final resistivities of the PANI-Ag coated polyester fibers with various APS concentrations are shown in Figure 3-2, where the lowest resistivity was obtained at 0.20 mol/L.

In the process of preparing polyaniline prefabricated layer, When the concentration of ammonium persulfate (APS) is 0.1~0.2 mol/L, a continuous increase in the concentration of APS resulted in an adverse decrease on the resistivity of PANI layer and the color of the fiber changes from light green to dark green. With the continuous increase of the concentration, the resistivity increases and the color of the fiber changes from dark green to brown.

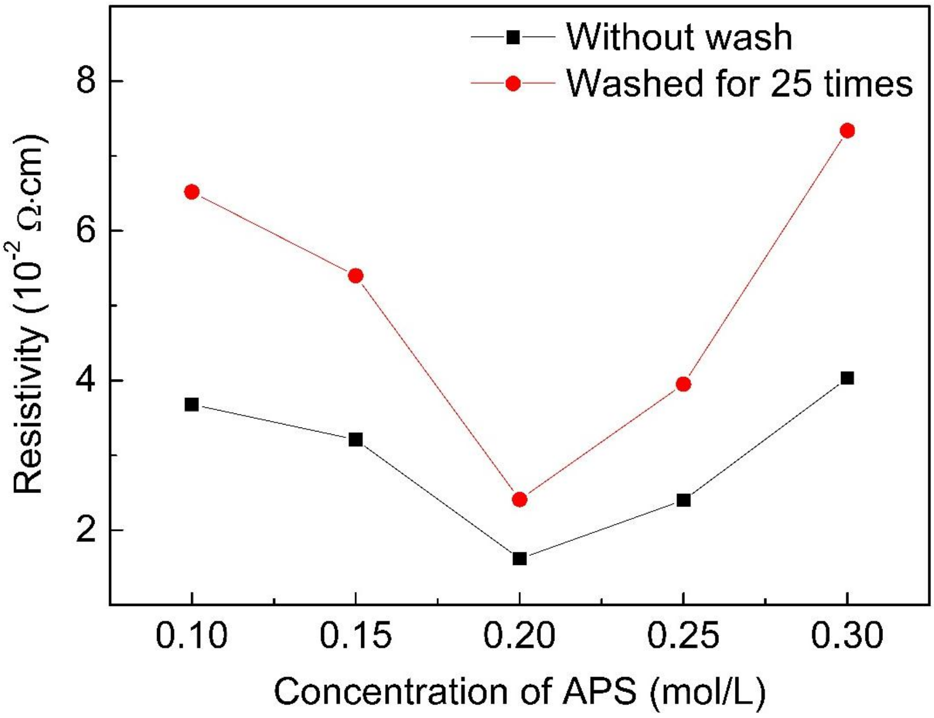

Figure 3-2. Influence of APS concentration on the conductivity of PANI-Ag coated polyester fibers.

This behavior dues to the effect of the degree of oxidation of polyaniline on the electrical conductivity of fibers. When the number of oxidation units and reduction units on the polyaniline macromolecule chain is approximately the same, the emerald green imine with high conductivity is formed, so the fibers present green color. On this basis, the fibers obtained by silver-plating have the lowest resistivity and the best conductivity. However, if the concentration of APS is too large, the degree of oxidation of polyaniline increases, the semi-reduced polyaniline becomes into the polyaniline of a fully oxidized structure, and the reducibility of the pre-formed polyaniline on the fiber surface becomes weakened. The silver layer obtained on this matrix by silver-plating deteriorates in quality and the resistivity of the fibers increases. It can be concluded that the electrical resistivity of the polyaniline pre-formed layer has a certain influence on the electrical resistivity of the PANI-Ag double-layer coated conductive fiber. Under different oxidation conditions, polyaniline with different structure can be produced on the surface of fibers, and polyaniline with special structure can promote the reduction deposition of silver in subsequent electroless silver-plating to some extent [26]. From Figure 3-2, we can see that when the concentration of APS is 0.2 mol/L, the prepared polyaniline prefabricated layer is most conducive to the deposition of silver particles on the surface of the fibers in the silver-plating process and to the preparation of silver layer with good properties. Therefore, the best concentration of APS is 0.2 mol/L.

3.3.1.3 Nitric Acid Concentration

As shown in Figure 3-3, with the increase of nitric acid concentration, the resistivity of PANI-Ag double layer coated conductive fiber firstly decreased continuously, while if the concentration of nitric acid continued to increase, the resistivity becomes to increase. When the concentration of nitric acid was 1mol/L, the resistivity was the lowest and the conductivity was the best. This is because the low concentration of nitric acid makes the polymerization reaction speed slower and prolongs the induction period of the formation of PANI chains, which reduces the content of polyaniline. However, too high a concentration of nitric acid results in the fast polymerization of PANI in the solution, but less deposition on the surface of the polyester fibers [27]. Therefore, too high or too low nitric acid concentration is not conducive to the effective deposition of polyaniline on the surface of the fiber, affecting the effect of electroless silver plating in the next step. Therefore, the optimal concentration of nitric acid was 1.0 mol/L.

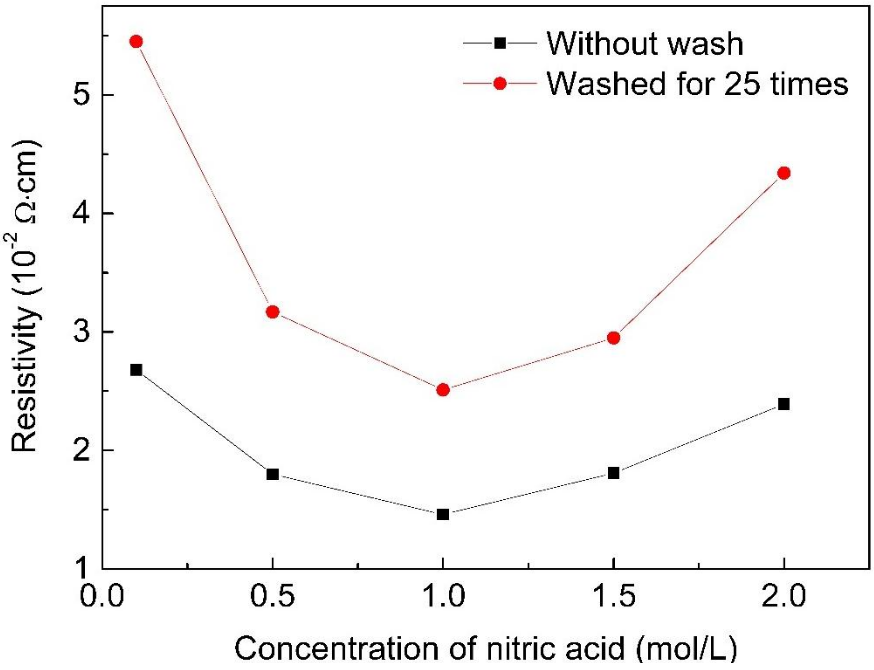

Figure 3-3. Influence of nitric acid concentration on the conductivity of PANI-Ag coated polyester fibers.

3.3.1.4 Dipping Time

The polyester fibers were immersed in the blended solution at ice temperature with a dipping time ranging from 5 min to 120 min. The blended solution was composed with APS 0.3 mol/L, aniline 0.2 mol/L and nitric acid 1.0 mol/L. The PANI-Ag composite coated fibers were washed with distilled water and dried. The effect of the dipping time of polyester fibers in the blended solution on conductivity is shown in Figure 3-4, which showed that as the reaction time increase, the resistivity decreased significantly first, and then increased. The minimum resistivity was obtained at 30 min and 60 min.

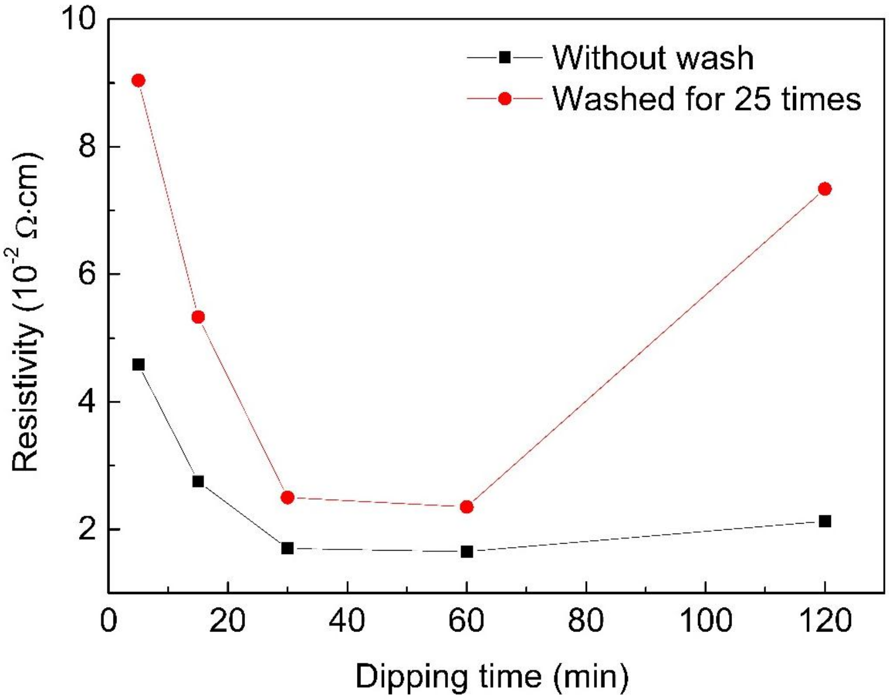

Figure 3-4. Influence of dipping time on the conductivity of PANI-Ag coated polyester fibers.

This is because when the reaction time is short, the oxidant cannot completely diffuse into the fiber interior and only the aniline outside the fiber is oxidized into macromolecules, resulting in an incomplete polymerization reaction, a small content of polyaniline on the fiber surface and uneven polyaniline layer [28]. The roughness is not enough, and the reduction is poor, which is not conducive to the subsequent silver-plating, therefore the PANI-Ag double-layered fiber has high resistivity. With the increase of reaction time, the oxidant can completely diffuse into the fiber, the monomer conversion rate increases, the content of polyaniline on the fiber increases, and the effect of silver-plating on the substrate becomes better. After the treatment time exceeds 30 min, the resistivity of the double-layer coated conductive fiber decreases slowly, but when the reaction time is 2 h, the resistivity increases again. This is due to the long ultrasonic treatment time and the excessive oxidation of Polyaniline, which leads to the decline of the conductivity of the fibers. In addition, the violent vibration causes the polyaniline which was partially polymerized on the surface of the fibers to fall off, resulting in unevenness of the pre-formed polyaniline and affecting the deposition of metallic silver.

As shown in Figure 3-4, the resistivity of the fiber after washing 25 times is basically the same as that of the unwashed fiber, and the performance of the double-layer coated conductive fiber prepared at the plating time of 30 min and 60 min is not much different, Although the fiber has the lowest electrical resistivity at 60 min, but taken into consideration the preparation efficiency and cost, 30 min was selected for the experiments.

3.3.2 Morphology

It can be seen in Figure 3-5 that the surface of de-oiled polyester fibers was very smooth, which is not beneficial for the deposition of Ag. However, after prefabrication of the PANI layer, the surface of polyester fibers became uneven and roughen obviously. Figure 3-5D shows that the silver layer of the PANI-Ag composite coated polyester fibers exhibits a continuous and dense surface. Compare to the Ag coated polyester fibers, the size distribution of silver particles on the PANI-Ag composite coated fibers is more even. These results demonstrated that the prefabricated PANI layer increases the surface roughness, which is of benefit in depositing the silver particles with uniform size.

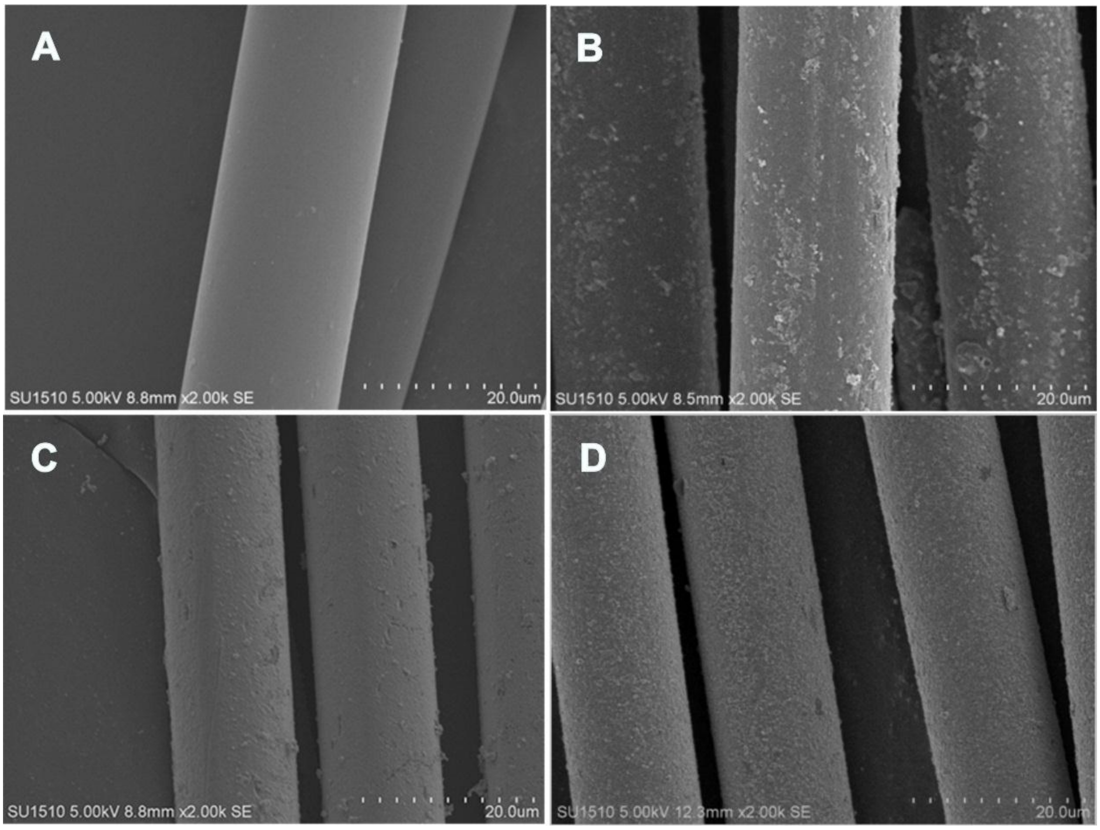

Figure 3-5. Scanning electron microscopy (SEM) images of different fibers: (**A**) polyester fibers; (**B**) polyaniline (PANI) coated polyester fibers; (**C**) Silver-coated polyester fibers; (**D**) PANI-Ag coated polyester fiber.

In order to acquire more details about the effect of silver coating, AFM was used to observe the surface of the polyester fibers with various conditions. The AFM images are shown in Figure 3-6.

As shown in Figure 3-6A, although the pretreatment enhanced the surface roughness of the polyester fibers, some parts of the fiber surface were severely eroded. The deposition of silver would be greatly affected. However, there were many uniform and convex PANI particles on the surface of the polyester fibers raised (Figure 3-6B). These PANI particles significantly increased the surface roughness of the polyester fibers which was beneficial for the formation of the dense and homogeneous silver layer (Figure 3-6D). The average size of the silver particles on the PANI-Ag coated fiber surface, which was calculated by the analysis software, was 70.32 nm (Figure 3-6D), which is much smaller than the average diameter of the silver particles on the surface of the silver-coated conductive fibers, which is 130.71 nm (Figure 3-6C). This demonstrates that the surface of the PANI-Ag coated fibers can deposit smaller and more uniform silver particles with more even distribution and a more compact surface coating structure, which is consistent with the observation of the SEM image in Figure 3-5.

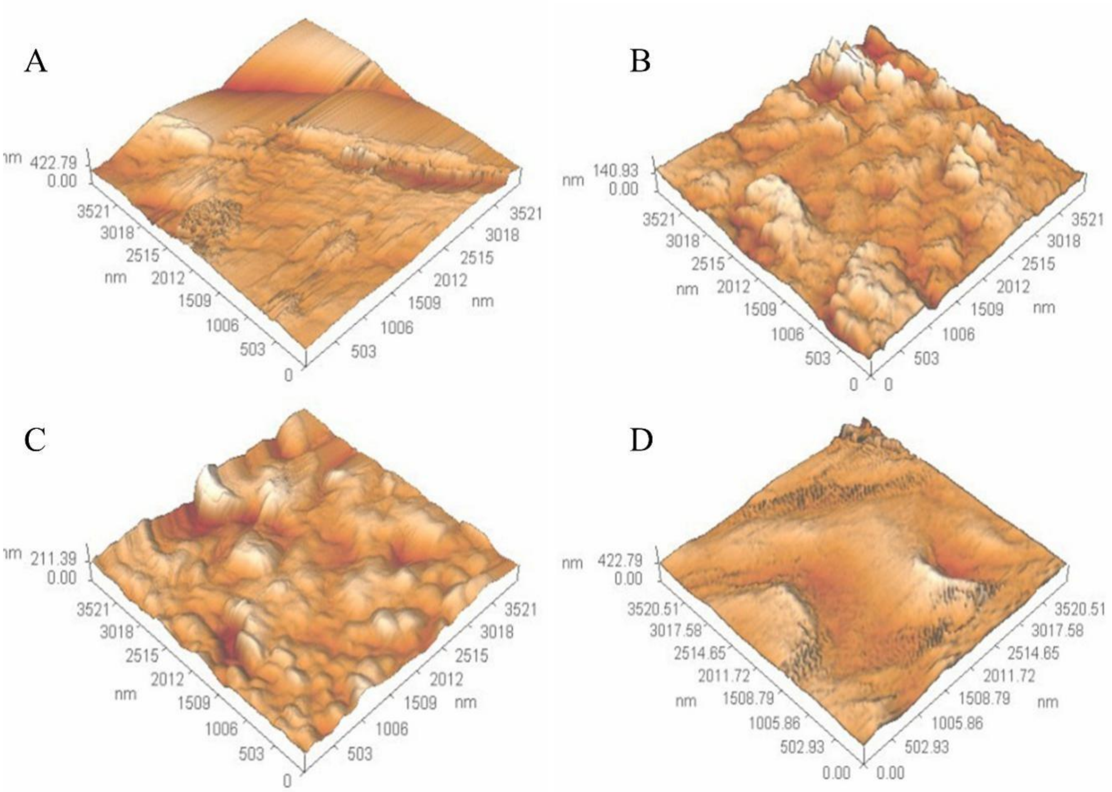

Figure 3-6. Atomic force microscope (AFM) images of (**A**) polyester fibers; (**B**) polyaniline (PANI) coated polyester fibers; (**C**) silver coated polyester fibers; (**D**) PANI-Ag coated polyester fibers.

3.3.3 Thermal Property

The thermal properties of samples were measured using a TGA instrument and the results are shown in Figure 3-7. In a nitrogen atmosphere, PANI coated and PANI-Ag coated polyester fibers had a similar thermogravimetric behavior and lost about 80% weight from 400°C to 480°C. By contrast, the pure polyester fibers lost about 89% weight as the temperature reached 480 °C. These results demonstrated that only a few silver particles were deposited on the PANI layer. It is also demonstrated that the deposition of PANI or PANI-Ag layer on the surface of the polyester fibers hardly affects the thermal properties.

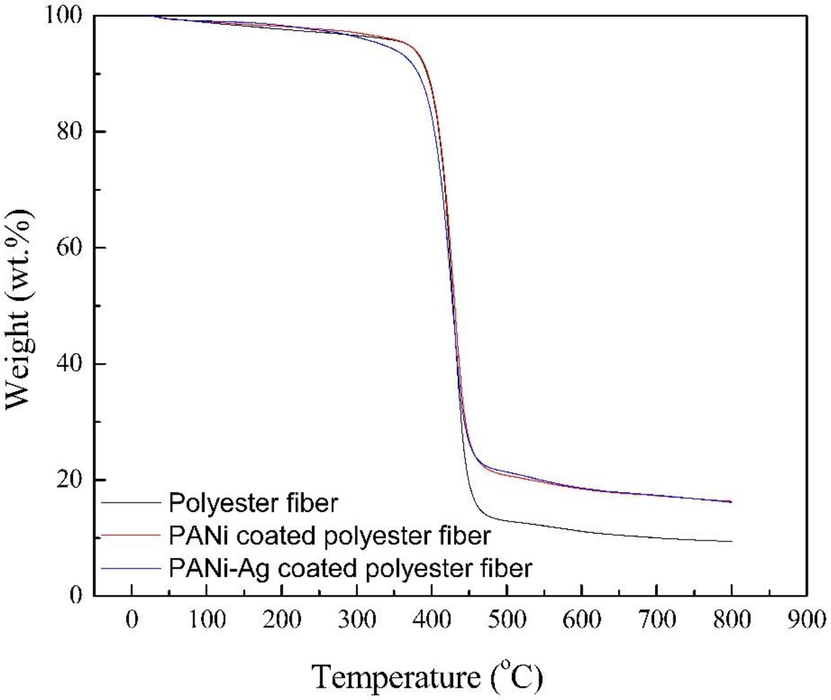

Figure 3-7. Thermal gravity analysis (TGA) curves of different fibers: (A) polyaniline (PANI) coated fiber; (B) Silver-coated conductive fiber; (C) PANI-Ag coated polyester fiber.

3.3.4 Mechanical Property

The mechanical properties of different coated polyester fibers were tested by an electronic single yarn strength tester. Each group of samples was tested 10 times and averaged. The results are shown in Table 3-1.

As shown in Table 3-1, the breaking strength and elongation at break of the fibers slightly increased after silver plating, while they both decreased after coating with PANI.

After silver plating, the surface of the fibers was covered with a layer of silver plating, which shared a part of the extra tensile force when stretched. Therefore, the breaking strength of the fiber after silver plating is increased. In the process of plating PANI on the surface of the fibers, the hydrochloric acid and APS used would cause some erosion of the fiber. By contrast, some PANI particles would also enter the amorphous region of the fibers, which caused a decrease of polyester crystallinity. Therefore, the internal structure of the fibers changed and resulted in loss of mechanical properties [29].

Table 3-1. Comparison of the mechanical properties of different fibers

Sample	Breaking strength（cN）	Elongation at break（%）
Original Polyester fiber (120D/72F)	470.00	17.56
PANI coated polyester fibers	454.67	16.12
Silver coated polyester fibers	505.38	21.79
PANI-Ag coated polyester fibers	483.75	20.03

3.3.5 Corrosion Resistance

After soaking in 5% NaCl solution for a period of time, the surface resistivity of different coated fibers was measured to evaluate the corrosion resistance of the fibers, as shown in Figures 3-8.

The resistivity of the two types of fibers increases with the soaking time, but the resistivity of the silver-coated fibers increases more than that of the PANI-Ag coated fibers, indicating that the corrosion resistance of the PANI-Ag coated fibers is better than that of the silver coated fibers. Maybe the PANI pre-formed layer can improve the bonding force between the fiber and the coating layer, so that the silver layer obtained by subsequent electroless silver plating was continuous, uniform, and had no obvious defects. Therefore, during the corrosion process of the PANI-Ag coated conductive fibers, the chloride ions are not easily entered the dense silver layer, improving the corrosion resistance of PANI-Ag coated fibers. By comparison, the silver layer on the surface of directly silver coated fibers is not tightly bonded with the substrate, and the structure is loose. During the corrosion process, the corrosion solution can easily enter the interior of the silver layer through some pores and cracks existing on the surface, and corroded more corrosion holes, which increase the contact area between the silver layer and the corrosion solution and produces more serious corrosion [30].

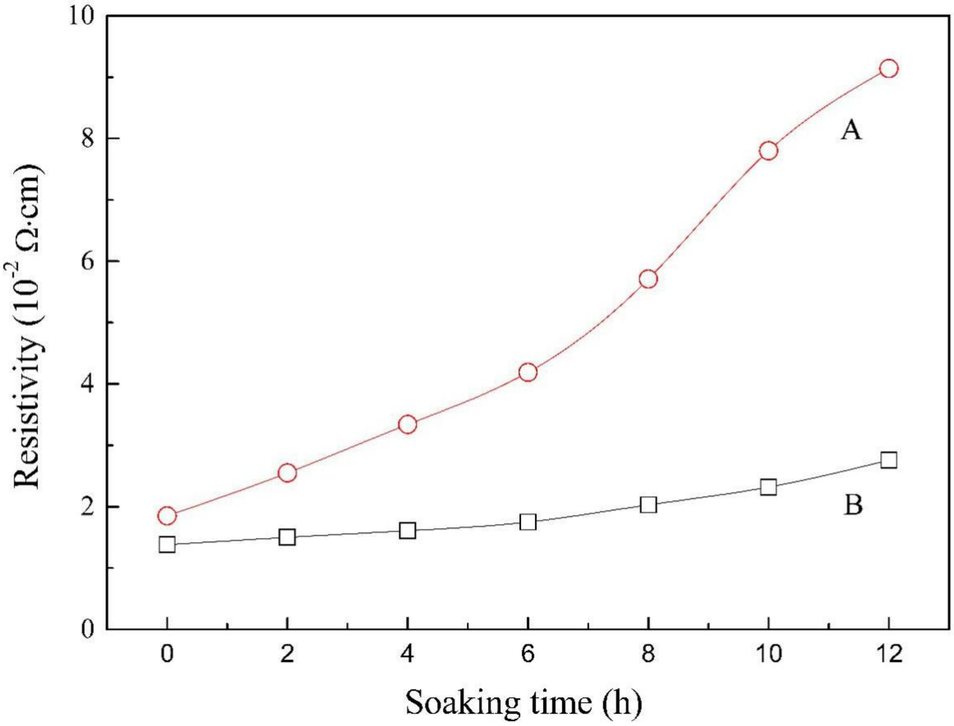

Figure 3-8. Comparison of the corrosion resistance of different fibers: (A) Silver-coated fibers;(B) polyaniline (PANI)-Ag coated polyester fibers.

3.3.6 Washability

The silver layers on the polyester or on the PANI-coated polyester fibers have great potential to be removed off by the act of washing. Therefore, it is necessary to examine the washability. The resistivity changes and the SEM images of silver and PANI coated polyester fibers are shown in Figure 3-9.

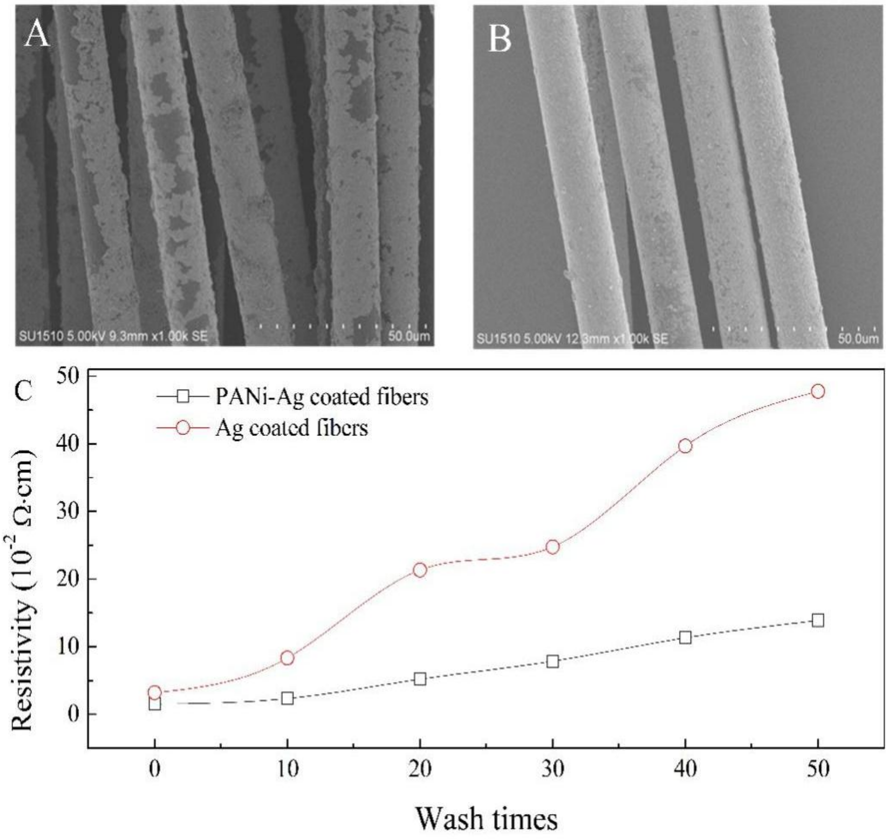

Figure 3-9. Scanning electron microscopy (SEM) images (×1000) of conductive polyester fibers after being washed for 50 times: (A) Ag coated fibers; (B) polyaniline (PANI)-Ag composite coated conductive fibers. (C) Influence of washing times on the conductivity of different fibers.

With the increase in washing times, the resistivity of silver-coated and PANI-Ag coated polyester fibers increased (Figure 3-5C). However, the resistivity of PANI-Ag coated polyester fibers only increased from 0.0154 Ω·cm to 0.139 Ω·cm after washing 50 times. In the case of the silver coated polyester fibers, the resistivity increased from 0.032 Ω·cm to 0.48 Ω·cm. It is noted that both the silver and PANI-Ag coated fibers had the similar initial resistivity. This result demonstrated that the PANI plays a positive effect on protecting the conductivity of the fibers. We believe that the pre-coated PANI on the polyester fibers increased the overall roughness, and also increased the surface area. Therefore, in the subsequent silver plating, the silver particles will firstly deposit in the grooves of PANI. The mechanical occlusion effect between the PANI layer and the silver layer increased the binding strength of the silver particles.

Figure 3-9A and 3-9B show the surface condition of silver coated and PANI-Ag composite coated polyester fibers after washing 50 times. The silver layer on the surface of the Ag-coated fiber is peeled off more than that on the surface of the PANI-Ag coated fiber. This might be caused by the friction between the silver particles (as shown in Figure 3-9C) on the surface of conductive fibers during the washing processes. By contrast, the silver layer was very smooth on the PANI-Ag composite coated polyester fibers. The smooth surface greatly decreased the friction force and resulted in better conductivity.

3.3.7 Silver Composition Analysis

Figure 3-10A demonstrates that there are three amorphous peaks of the polyester fibers before silver plating at 18°, 22° and 26°, respectively. After electroless silver plating on the polyester fibers, four new peaks at 2θ values of 38°, 44°, 64°, 77° and 82° corresponding to (111), (200), (220), (311) and (222) planes of the face-centered cubic silver were observed and compared with the standard powder diffraction card of JCPDS, silver file No. 04-0783 (Figure 3-10B) [31-37]. The sharp peak shape and narrow peak width indicate that the polyester fiber surface was coated with metallic silver with good crystallinity [38]. There was no obvious second phase, indicating that the surface of the fibers was covered with a silver layer of high purity [14].

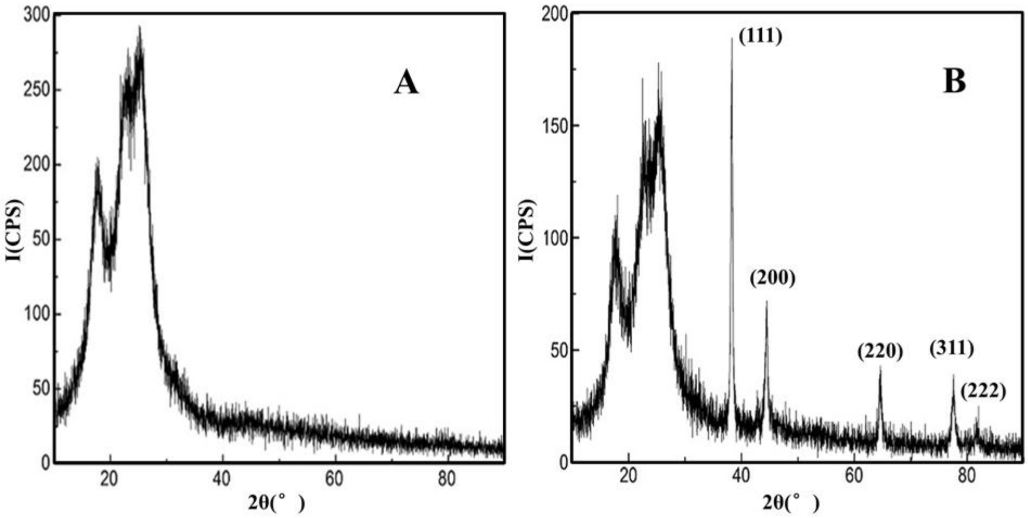

Figure 3-10. X-ray diffraction (XRD) patterns of (A) polyester fiber; (B) Ag-coated conductive fiber

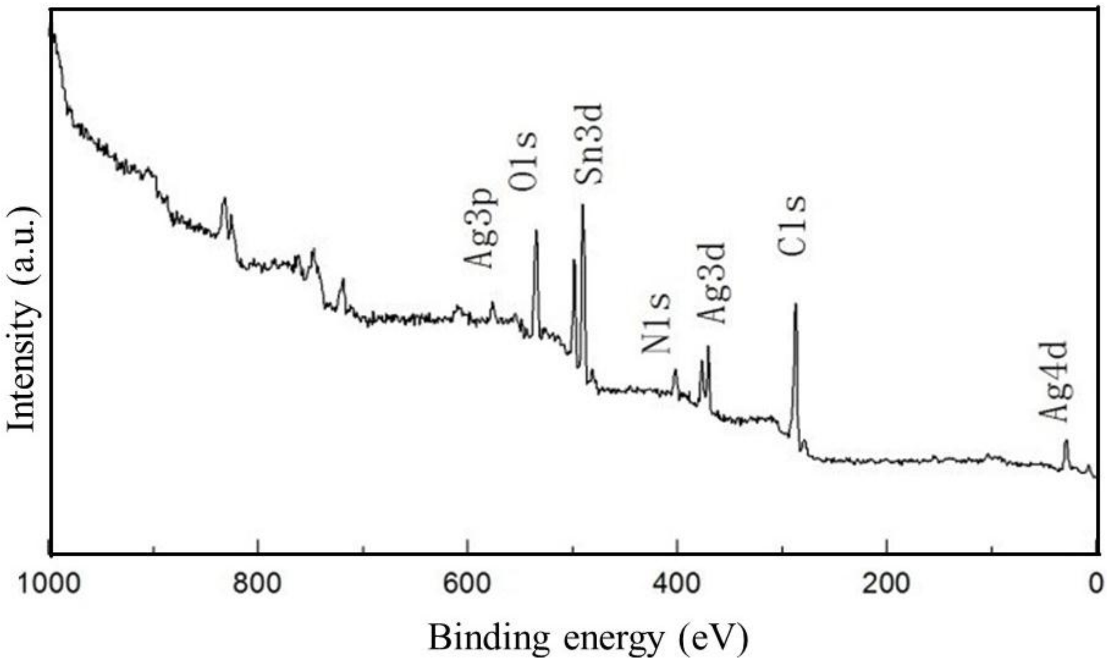

Figure 3-11. X-ray photoelectron (XPS) spectra of PANI-Ag composite conductive fiber

Figure 3-11 shows the X-ray photoelectron spectrogram (XPS) of PANI-Ag coated polyester fibers. As shown in Figure 3-11, three energy peaks appearing at 285.9 eV, 403.4 eV, and 533.5 eV are the binding energy peaks of C1s, N1s, and O1s, respectively, which indicate that the fiber surface contained elements such as C, N, and O. Since the standard Ag3d binding peak of silver is located at 368.1 eV [39], Figure 3-11 shows that the binding energy of Ag3d is 369.2 eV, which is consistent with that of silver, indicating that the surface of the PANI-Ag composite coated conductive fibers contains the silver element.

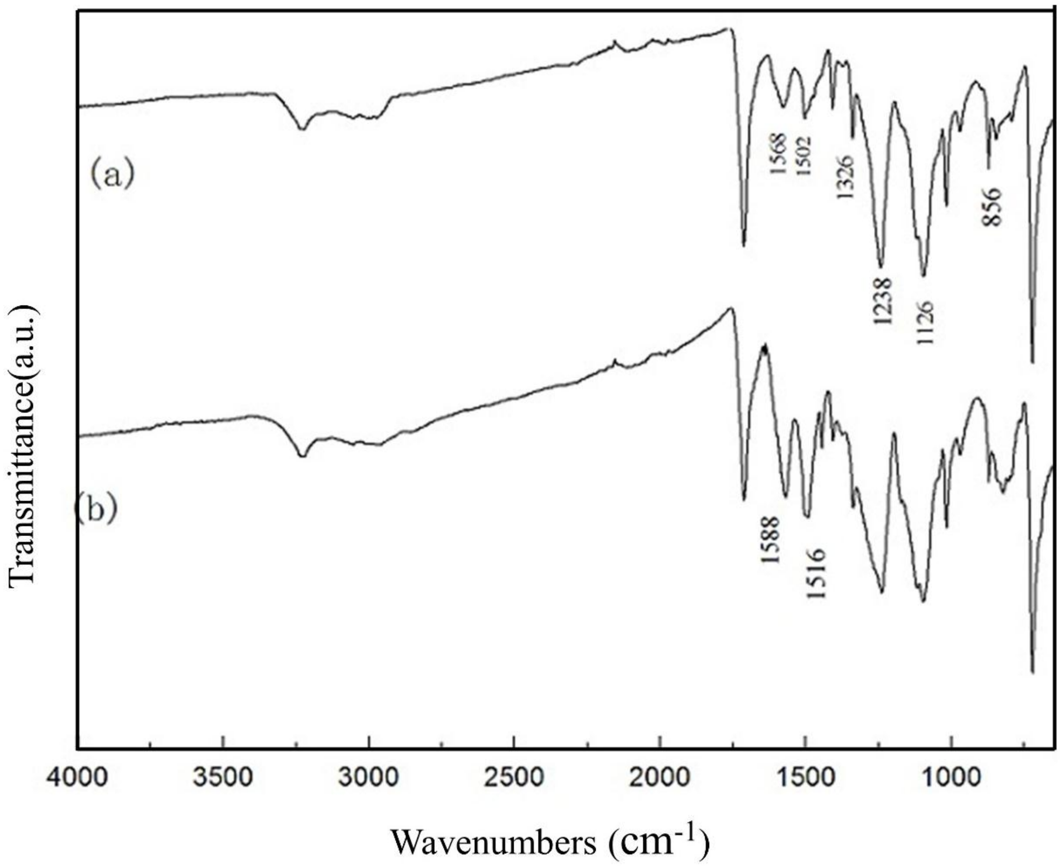

Figure 3-12. Fourier transform infrared (FTIR) spectra of different fibers: (**a**) polyaniline (PANI) coated polyester fibers; (**b**) PANI-Ag coated polyester fibers.

Figure 3-12 shows the infrared spectrogram of silver coated and PANI-Ag coated polyester fibers. The band observed at 1568 cm^{-1} and 1502 cm^{-1}corresponded to quinoid and benzenoid structures, respectively, in PANI. The degree of oxidation of PANI is reflected by the two adsorption peaks. The band at 1326 cm^{-1} was attributed to C-N stretching, and the band at 1568 cm^{-1} was characterized as 1,4-substituted phenyl stretching, which were identical to the emeraldine salt from PANI. The FTIR spectra of PANI-Ag coated polyester fibers were very similar to those of PANI coated polyester fibers. However, there were also some differences between the spectra. The specific peak of quinoid structure moved from 1568 cm^{-1} to 1588 cm^{-1}. This result demonstrated that there were some chemical interactions between silver and PANI when they were deposited on polyester fibers. Furthermore, the chemical interactions between silver and PANI improve the conductivity and washability of PANI-Ag composite coated polyester fibers.

3.4 Conclusions

In this study, conductive polyester fibers were prepared using two-step deposition of PANI and silver on the surface of the fibers. The influence of the treating time was discussed, and the influence of aniline concentration, APS concentration and nitric acid on the resistivity of PANI-Ag coated polyester fibers were studied. The optimal reaction conditions for preparing conductive polyester fibers should be: the concentration of aniline was 0.3 mol/L, concentration of APS 0.2 mol/L, concentration of nitric acid 1 mol/L and the treating time 3 min. The PANI-Ag coated polyester fibers were characterized by FTIR, SEM, AFM, XRD, XPS and TGA. Furthermore, the washability was compared with Ag-coated polyester fibers. The results demonstrated that the PANI-Ag coated polyester fibers by the two-step depositing have much better washability than Ag coated fibers.

References

1. Tong, H; Zhu, L; Li, M. Electroless silver deposition on Si(100) substrate based on the seed layer of silver itself. *Electrochim. Acta* ***2013***, *17*, 2473–2477, doi: 10.1016/S0013-4686(03)00273-1.
2. Cha, S.H.; Koo, H.C.; Kim, J.J. The inhibition of silver agglomeration by gold activation in silver electroless plating. *J. Electrochem. Soc.* **2015**, *6*, 388–391, doi: 10.1149/1.1905984.
3. Schaefers, S.; Rast, L.; Stanishevsky, A. Electroless silver plating on spin-coated silver nanoparticle seed layers. *Mater. Lett.* **2016**, *60*,706–709, doi: 10.1016/j.matlet.2005.05.085.
4. Sen, T.; Mishraa, S.; Shimpi, N.G. Synthesis and sensing applications of polyaniline nanocomposites: a review. *RSC Adv.* **2016**, *6*, 42196–42222, doi:10.1039/C6RA03049A.
5. Lu, J.T.; Li, Z.H.; Cao, D. Preparation Study of Silver-Coated Glass Fiber by Electroless Plating with Pd-Free Activation. *Rare Metal Mat. Eng.* **2010**, *39*,27–30.
6. Krulik, G.A. US Patent, US5318621A; June 7,1994.
7. Zhang, H.; Zou, X.; Liang, J; Ma, X.; Tang, Z.; Sun, J. Development of electroless silver plating on Para-aramid fibers and growth morphology of silver deposits. *J. Appl. Polym. Sci.* **2012**, *4*, 3363–3371, doi: 10.1002/app.35332.
8. Macdiarmid, A.G.; Epstein, A.J. Polyanilines: a novel class of conducting polymers. *Faraday Discuss. Chem. Soc.* **1989**, *30*, 147–152, doi: 10.1039/DC9898800317.
9. Chen, Y.; Kang, E.T.; Neoh, K.Q. Intrinsic redox states of polyaniline studied by high-resolution X-ray photoelectron spectroscopy. *Colloid Polym. Sci.* **2011**, *1*, 73–76, doi: 10.1007/s003960000.
10. Park, N.; Kim, W.; Kim, J. Copper metallization of poly (ethylene terephthalate) fabrics via intermediate polyaniline layers. *Fibers and Polymers* **2018**, *3*, 310–314, doi: 10.1007/s12221-009-0310-7.
11. Patrycja, B.; Jaroslav, S.; Miroslava, T.; Jan, P. Polyaniline–silver composites prepared by the oxidation of aniline with mixed oxidants, silver nitrate and ammonium peroxydisulfate: The control of silver content. *Polymer* **2011**, *26*, 5947–5952, doi: 10.1016/j.polymer.2011.10.025.

12. Chang, G.; Luo, Y.; Lu, W.; Qin, X.; Asiri, A.M.; Al-Youbibc, A.O.; Sun, X. Ag nanoparticles decorated polyaniline nanofibers: synthesis, characterization, and applications toward catalytic reduction of 4-nitrophenol and electrochemical detection of H_2O_2 and glucose. *Catal. Sci. Technol.* **2012**, *2*, 800–806, doi: 10.1039/C2CY00454B.
13. Liang, T.X.; Guo, W.L.; Yan, Y.H.; Tang, C.H. Development of complex agent for antifouling, decoking and maximized liquid yield. *J. Adhes.* **2017**, *28*, 55–58.
14. Jiang, S.X.; Guo, R.H.; Zheng, G.H. Studies on electrochemical polishing of stainless steel. *Electroplating and Finishing* **2009**, *7*, 22–24.
15. Cui, J.; Yuan, H.; Li, J.P.; Xu, X.B.; Shen, Y.; Lin, H.; Wang, M.K. Recent progress in efficient hybrid lead halide perovskite solar cells. *Sci. Technol. Adv. Mater.* **2015**, *16*, 036004, doi: 10.1088/1468-6996/16/3/036004.
16. KANG, E.T.; Ting, Y.P.; Neoh, K.G.; Tan, K.L. Electroless recovery of precious metals from acid solutions by N-containing electroactive polymers. *Synthetic Metals* **1995**, *69*, 477–478. doi: 10.1016/0379-6779(94)02533-5.
17. Gordana, M.; Budimir, M.; Patrycja, B.; Zuzana, R.; Jaroslav, S.; Miroslava, T.; Jan, P. The oxidative polymerization of p-phenylenediamine with silver nitrate: Toward highly conducting micro/nanostructured silver/conjugated polymer composites. *J. Polym. Sci pol. Chem.* **2011**, *49*, 3387–3403, doi: 10.1002/pola.24775.
18. Wakeford, C.A.; Blackburn, R.; Lickiss, P.D. Effect of ionic strength on the acoustic generation of nitrite, nitrate and hydrogen peroxide. *Ultrasonics Sonochemistry* **1999**, *6*,141–148, doi: 10.1016/S1350-4177(98)00039-X.
19. Dominis, A.J.; Spinks, G.M.; Kane-Maguire, L.A.P. A de-doping/re-doping study of organic soluble polyaniline. *Synthetic Metals* **2012**, *129*, 165–172, doi: 10.1016/S0379-6779(02)00048-6.
20. Zhang, Y.H.; Choi, J.R.; Park, S.J. Enhancing the heat and load transfer efficiency by optimizing the interface of hexagonal boron nitride/elastomer nanocomposites for thermal management applications. *Polymer* **2018**, *143*, 1–9, doi: 10.1016/j.polymer.2018.03.067.
21. Ahmed, F.; Kumar, S.; Arshi, N.; Anwar, M.S.; Lee S.Y.; Kil, G.S.; Park, W.; Koo, B.H.; Lee,

C.G. Preparation and characterizations of polyaniline (PANI)/ZnO nanocomposites film using solution casting method. *Thin Solid Films* **2011**, *519*, 8375–8378, doi: 10.1016/j.tsf.2011.03.090.

22. Chen, Y.F.; Li, X.G.; Xiao, Y.; Wang, S.R. Solution Processed Large-Scale Small Molecular Organic Field-Effect Transistors. *Progress in Chemistry* **2017**, *29*, 359–372, doi: 10.7536/PC161026.
23. Li, M.Y.; Guo, Y.; Alan, Y.W.; MacDiarmid, G.; Lelkes, P.I. Electrospinning polyaniline-contained gelatin nanofibers for tissue engineering applications. *Biomaterials* **2006**, *27*, 2705–2715, doi.org/10.1016/j.biomaterials.2005.11.037.
24. Lee, Y.J.; Kim, E.; Kim, K.; Lee, B.H.; Choe, S. Polyaniline effect on the conductivity of the PMMA/Ag hybrid composite. *Colloid Surface A* **2012**, *396*, 195–202, doi: 10.1016/j.colsurfa.2011.12.071.
25. Lyutov, V.; Tsakova, V. Silver particles-modified polysulfonic acid-doped polyaniline layers: electroless deposition of silver in slightly acidic and neutral solutions. *J. Solid State Electrochem*. **2011**, *15*, 2553–2561, doi: 10.1007/s10008-011-1451-3.
26. Wang, H.B.; Wang, J.Y.; Hong, J.H.; Wei, Q.F.; Gao, W.D.; Zhu, Z.F. Preparation and characterization of silver nanocomposite textile*, J. Coat. Technol. Res.* **2007**, *4*, 101–106, doi: 10.1007/s11998-007-9001-8.
27. Corte, D.A.D.; Torres, C.; Correa, P.S.; Rieder, E.S.; Malfatti, C.F. The hydrogen evolution reaction on nickel-polyaniline composite electrodes. *Int. J. Hydrogen Energ.* **2012**, *37*, 3025–3032, doi: 10.1016/j.ijhydene.2011.11.037.
28. Attout, A.; Yunus, S.; Bertrand, P. Electroless deposition of polyaniline: synthesis and characterization. *Surf. Interface Anal.***2008**, *40*, 657–660, doi: 10.1002/sia.2702.
29. Paulo, H.S.P.; Medeiros, E.S.; Pan, Z.L.; Wood, D.F.; Orts, W.J.; Mattoso, L.H.C.; Soares, B.G. Structural, Electrical, Mechanical, and Thermal Properties of Electrospun Poly(lactic

acid)/Polyaniline Blend Fibers. *Macromol. Mater. Eng.* **2010**, *295*, 618–627, doi: 10.1002/mame.201000019.

30. Kumar, S.A.; Meenakshi, K.S.; Sankaranarayanan, T.S.N.; Srikanth, S. Corrosion resistant behaviour of PANI–metal bilayer coatings. *Prog. Org. Coat.* **2008**, *62*, 285–292, doi: 10.1016/j.porgcoat.2008.01.005.
31. Bykkam, S.; Ahmadipou, M.; Narisngam, S.; Kalagadda, V.R.; Chidurala, S.C. Extensive Studies on X-Ray Diffraction of Green Synthesized Silver Nanoparticles. *Advances in Nanoparticles* 2**015**, *4*, 1–10, doi:10.4236/anp.2015.41001.
32. Thosar,N.; Basak, S.; Bahadure, R.N.; Rajurkar, M. Antimicrobial efficacy of five essential oils against oral pathogens: An in vitro study. *Eur. J. Dent*. **2013**, *7*, S71–S77, doi: 10.4103/1305-7456.119078.
33. Thapa, R.; Bhagat, C.; Shrestha, P.; Awal, S.; Dudhagara, P. Enzyme-mediated formulation of stable elliptical silver nanoparticles tested against clinical pathogens and MDR bacteria and development of antimicrobial surgical thread. *Ann. Clin. Microbiol. Antimicrob.* **2017**, *16*, 39, doi: 10.1186/s12941-017-0216-y.
34. Yang, X.; Du, Y.; Li, D.; Lv, Z.Z.; Wang, E.K. One-Step Synthesized Silver Micro-Dendrites Used as Novel Separation Medium and Its Applications in Multi-DNA Analysis. *Chem. Commun.* **2011**, *47*, 10581–10583, doi: 10.1039/c1cc11374g.
35. Corro, G.; Vidal, E.; Cebada, S.; Pal, U.; Bañuelos, F.; Vargas, D.; Guilleminot, E. Electronic state of silver in Ag/SiO_2 and Ag/ZnO catalysts and its effect on diesel particulate matter oxidation: An XPS study. *Appl. Catal. B-Environ.* **2017**, *216*, 1–10, doi: 10.1016/j.apcatb.2017.05.059.
36. Siddiqui, M.N.; Redhwi, H.H.; Achilias, D.S.; Kosmidou, E.; Vakalopoulou, E.; DIoannidou, M. Green Synthesis of Silver Nanoparticles and Study of Their Antimicrobial Properties. *J. Polym. Environ.* **2018**, *26*, 423–433, doi: 10.1007/s10924-017-0962-0.
37. Basavegowda, N.; Idhayadhulla, A.; Lee, Y. R. Phyto-synthesis of gold nanoparticles using fruit extract of Hovenia dulcis and their biological activities. *Ind. Crops Products* **2014**, *52*, 745–751, doi: 10.1016/j.indcrop.2013.12.006.

38. Bafandeh, M.R.; Abbasi, M.H.; Saidi, A.; Lee, J. Effects of $SrTiO_3$ on dielectric and piezoelectric properties of $K_{0.48}Na_{0.48}Li_{0.04}Nb_{0.96}Ta0_{.04}O_3$-based piezoceramics. *Mat. Sci. Eng. B* **2013**, *178* ,277–281, doi: 10.1016/j.mseb.2012.11.022.

39. Roza, D.; Paul, S.M.; Stephen, F.R.; Gordon, G.W. Electroless recovery of silver by inherently conducting polymer powders, membranes and composite materials. *Polymer*, 2016, 47, 4520–4530, doi: 10.1016/j.polymer.2006.03.112.

Chapter 4 Laser-Induced Silver Seeding on Fabric Surface for Selective Electroless Copper Plating

4.1 Introduction

The development of high-resolution metal patterns has allowed for significant progress in applications of the microelectronics industry such as surface-mount devices and integrated circuits [1], radio frequency identification and smart cards [2], wireless sensors and temperature sensors (T-sensor) [2–4], super hydrophobic surfaces [5], and flexible electronics [6]. In particular, in the wearable electronics industry, the flexible circuit board is a key element for boarding microelectronic devices. To our best knowledge, the technique based on photolithography processes is one of the most used methods to produce metal patterns on hard substrates. However, the photolithography processes have some disadvantages, such as needing expensive equipment, being time-consuming, and difficulties in adapting for patterning non-planar substrates. Furthermore, pattern fabrication on soft substrates using this method is hard to process.

In recent years, a new technology based on laser irradiation has been developed to form metal patterns on both hard and soft substrates. There are many related technologies such as laser-foaming technology [7], laser-induced periodic surface structure technology (LIPSS) [8], and other laser ablation-based technologies, like laser-induced forward transfer (LIFT) [9], laser interference lithography (LIL) [10], matrix-assisted pulsed laser evaporation (MAPLE) [11], and pulsed laser deposition (PLD) [12]. In addition, laser-induced machining can be tuned to both material properties and desired surface patterns by controlling certain parameters of the laser such as wavelength, fluency, intensity, pulse width, total photon count, and other illumination conditions [13].

Relatively speaking, paper has become one promising substrate material for electronics fabrication [14–16] because of its ubiquity, simple preparation, low cost, process-facilitating structure, and green attribute. Because of making from raw plant (such as rags, grasses or wood) cellulose fibers, paper is renewable and recyclable [17]. In addition, paper can be used as a substrate for humanized wearable electronic products due to its good mechanical deformability, biocompatibility, and the least adverse effect on human skin. Most importantly, the porous structure of the paper enhances its superiority over the counterpart in the application of electronic equipment. The porous structure is a masterpiece of interwoven cellulose fibers in paper, which facilitates the coating process that is a standard method of enhancing the electrical properties of paper by increasing the contact field, which further promotes the deposition of conductive additives in intrinsically electrically insulating cellulose fibers. In this chapter, filter paper (FP) was utilized as a substrate to produce copper patterns.

Conventional electroless plating methods include pretreatment, seeding or activation, and electroless plating [18]. Pretreatment can improve the interfacial adhesion between the substrate and the deposited metal [19]. Seeding or activation of the dielectric substrate is critical to subsequent successful electroless metal deposition. Herein, we demonstrate a novel method for implanting a composite film for selective electroless copper deposition using laser-induced irradiation on Ag^+ doped flexible filter paper/polyacrylonitrile (FP/PANI).

4.2 Experimental

4.2.1 Materials

Polyacrylonitrile (PANI, average Mw = 50,000) and sodium potassium tartrate were purchased from Sigma-Aldrich (Shanghai, China). Dimethylsulfoxide (DMSO) and other chemicals were commercially obtained from Sinopharm Chemical Reagent

Co., Ltd. (Shanghai, China) and used without any further purification. Commercially available filter papers with a thickness of 0.5 mm (measured using micrometer calipers) were soaked in a PANI/ SnO_2/DMSO solution, followed by drying under a vacuum to prepare the FP/PANI films (with a thickness of 0.8–1.2 mm).

4.2.2 Laser-Induced Setup

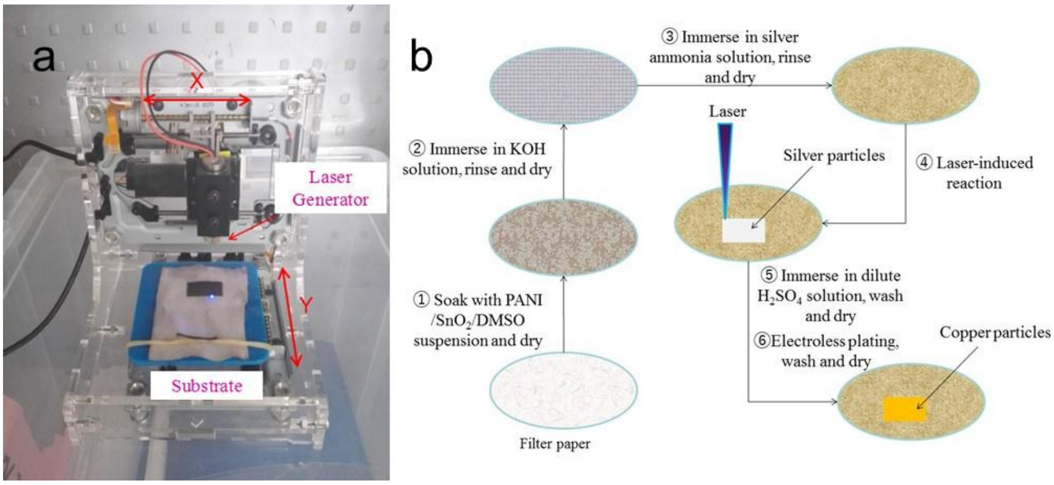

Figure 4-1. (**a**) Laser-induced set-up; and (**b**) diagram of the laser-induced and electroless plating processes.

Self-made equipment was modified from a CD/DVD optical device ($\lambda = 405$ nm) and used to provide the laser source, as shown in Figure 4-1a. The laser beam could be adjusted by a lens, and the focus spot size on the substrate was estimated to be 100 μm in diameter. The laser beam could be mounted by a computer-controlled x–y moving stage, which provided the relative motion of the laser beam for patterning on the composite films. In our experiments, we developed a real-time controlling microcomputer system. The system can control the laser head according to a certain trajectory by controlling the parameters of stepper motor by single chip microprocessor, and can control the laser output system, such as the laser output power, pulse frequency, scanning speed, scanning distance and other experimental parameters, which is conducive to finding the optimal range of working parameters for laser processing. The operation interface of the system is shown in Figure 4-2. The laser-induced process was operated in air at room temperature.

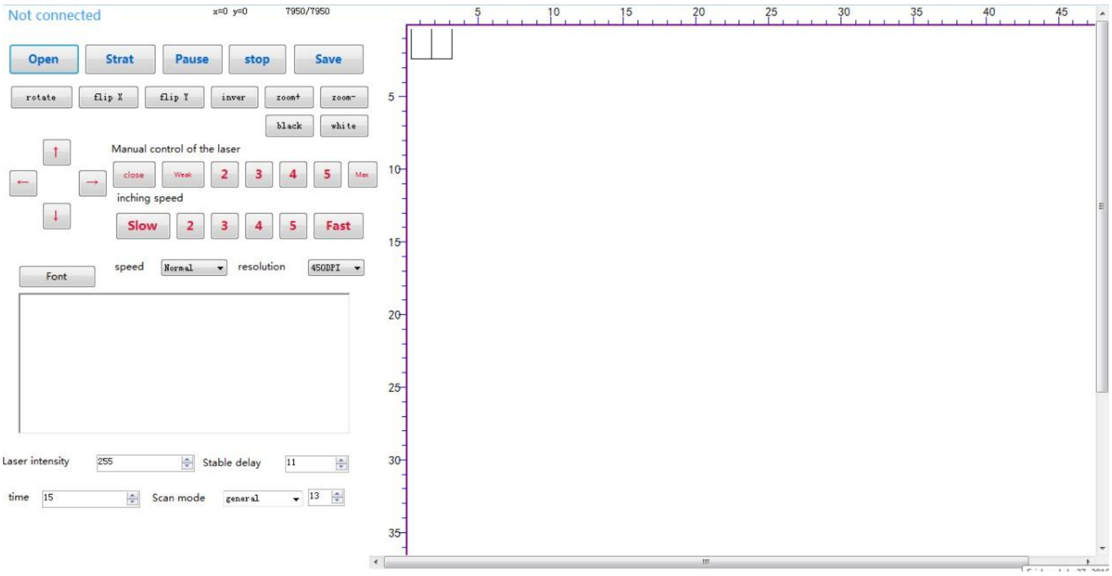

Not connected

x=0 y=0

7950/7950

speed Normal

resolution 450DPI

Laser intensity 255

Stable delay 11

time 15

Scan mode general 13

Figure 4-2. The operation interface of the real-time control system

4.2.3 Laser-Induced and Electroless Plating

The entire process of forming copper patterns on filter paper is similar with Chen's report [20], as schematically shown in Figure 4-1b. First, the filter paper was immersed in a suspension with SnO_2 (10 wt %) and PANI/DMSO solution with the PANI concentration of 0.03 g/mL for 5 min. The filter paper with the PANI solution adsorbent was then taken out and dried under a vacuum at 60 °C for 1 h to remove the Dimethyl sulfoxide. Thereafter, the film was immersed in KOH solution (0.5 mol/L) at 50 °C for 25 min. After rinsing with distilled water and drying, the composite film of SnO_2/FP/PANI was immersed in silver ammonia solution at 40 °C for 60min, then rinsed again with distilled water. After drying, the Ag^+-doped film was then placed on the laser-induced stage and fixed with a rubber band, as shown in Figure 4-1a. The silver ions on the desirable pattern area were irradiated by laser and reduced to metallic silver, whose reaction equations are as shown in Reaction (4-1) and (4-2), whereas the other Ag^+ remained in an ionic state. The film was immersed in a 1 wt % H_2SO_4 solution for about 15 min to exchange Ag^+ ions with H^+ ions. Then, the film was rinsed with distilled water and dried. Finally, the film was immersed in an electroless plating bath at room temperature for 40 min to deposit the copper patterns. The electroless plating bath consisted of NaOH (14 g/L), sodium potassium tartrate ($NaKC_4H_4O_6$, 24 g/L), $CuSO_4$ (8 g/L), and 12 mL/L of formaldehyde aqueous solution (37 wt %). $CuSO_4$ is the main salt in this electroless copper-plating solution, and sodium potassium tartrate is a complexing agent for forming a complex with copper ions (Reaction 4-3, Reaction 4-4) to prevent the precipitation of $Cu(OH)_2$. At the same time, potassium sodium tartrate is a buffer that maintains the optimum pH value required for the reaction. Formaldehyde is a strong reducing agent, and its reducing ability increases with the increase of pH value and the concentration of formaldehyde. NaOH is used to adjust the pH of the plating solution, to maintain the stability of the solution and to provide an alkaline environment with a strong reducing ability of formaldehyde.

$$2SnO_2 \rightarrow 2SnO + O_2 \uparrow \tag{4-1}$$

$$SnO + 2[Ag(NH_3)_2]OH \rightarrow SnO_2 + 2Ag\downarrow + 4NH_3 + H_2O \tag{4-2}$$

$$CuSO_4 + 2NaOH \rightarrow Cu(OH)_2 + Na_2SO_4 \tag{4-3}$$

$$Cu(OH)_2 + 3C_4H_4O_6^{2-} \rightarrow [Cu(C_4H_4O_6)_3]^{4-} + 2OH^- \tag{4-4}$$

The redox reaction equation of electroless copper-plating is as shown in Reaction (4-5). The deposition steps were terminated by removing the film from the bath and washing with distilled water.

$$Cu^{2+} + 2HCHO + 4OH^- \rightarrow Cu^0 \downarrow + 2HCOO^- + H_2 \uparrow + 2H_2O \tag{4-5}$$

4.2.4 Characterizations

The AFM images of the filter paper films before and after laser treatment were investigated using atomic force microscopy (AFM) (Being Nano-Instruments CSPM-4000, Ben Yuan Ltd., Beijing, China) operated in tapping mode. Size distribution of silver particles on the FP/PANI film after laser irradiation was analyzed by post-processing software from the CSPM4000 Atomic Force Microscope. Scanning electron microscopy (SEM, Hitachi 3400N, Hitachi, Japan) was applied to investigate the surface morphology of the deposited copper after coating the samples with gold. The current-voltage (I–V) characteristics of the deposited copper were measured using a direct-current voltage and a current source/monitor (Keithley, 4200-SCS, Cleveland, USA).

4.3 Results and Discussions

4.3.1 Formation of Ag Particles on Filter Paper/PANI Films

The scanning speed of the laser has a great influence on the surface properties of Ag-deposited FP/PANI films. In Chen's report [20], they developed a simple equation to analyze the relationship between the scanning speed of the pulsed laser and the laser-active area on the substrate:

$$s = \frac{v}{f}, \tag{4-6}$$

where s, f, and v represent the distance of two adjacent spots created by the laser pulse (mm), repetition rate of pulsed laser (Hz), and the scanning speed (mm/s), respectively. For the deposited silver to be connected and effective for the subsequent deposition of copper, s is generally smaller than the diameter of any laser spot. However, a very small value of v would lead to the laser pulse irradiating on the contiguous area, repeatedly, and the laser would heat this area to a very high temperature to carbonize the composite film. This equation has great potential for helping us choose a suitable scanning speed.

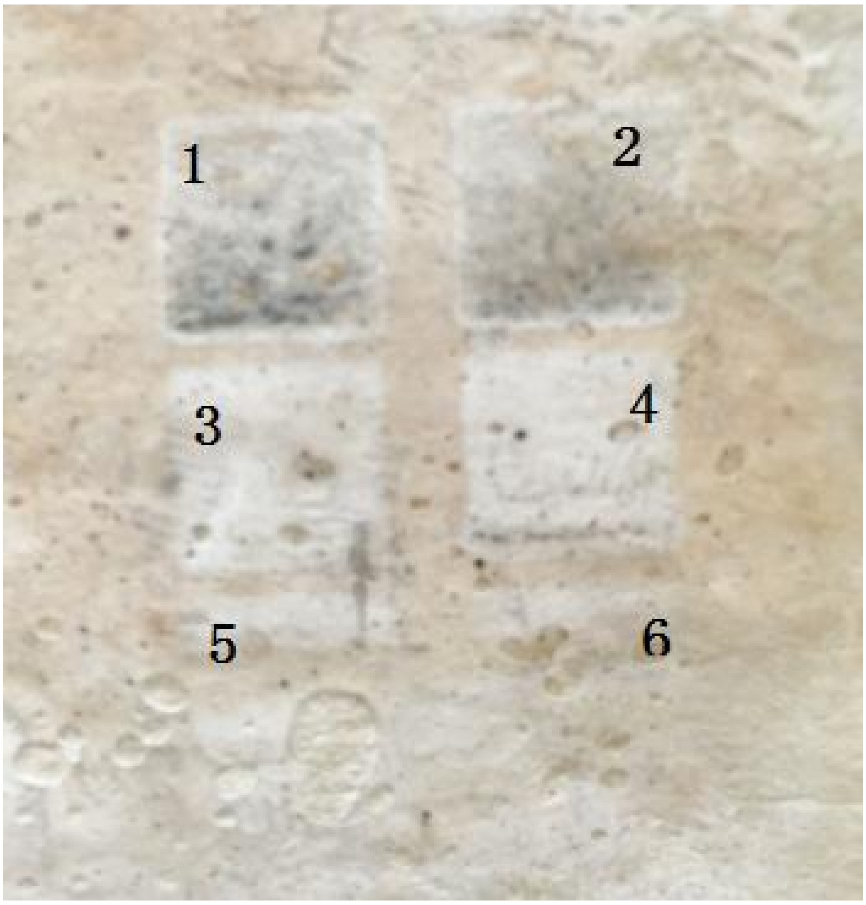

Figure 4-3. Effect of laser scanning speed on the Ag-deposited composite films of FP/PANI. Sample (**1**) 1 mm/s; (**2**) 2 mm/s; (**3**) 4 mm/s; (**4**) 6 mm/s; (**5**) 8 mm/s; (**6**) 10 mm/s.

Six different scanning speeds were tried, and it was showed that the irradiation intensity increased with decreasing scanning speed. Figure 4-3 shows the topography of the FP/PANI films after being irradiated by a laser with various scanning speeds. It is demonstrated that a very high speed of laser scanning produced only a small amount of Ag particles on the composite film, as shown in Figure 4-3 (samples 5 and 6, with a scanning speed of 8 mm/s and 10 mm/s, respectively). On the other hand, if the scanning speed decreased below 2 mm/s, the Ag particle pattern became less uniform and some parts of the irradiated area turned charcoal gray, as shown in Figure 4-3 (samples 1 and 2). This may have been caused by the formation of Ag_2O under the high temperature of the laser. Therefore, the most suitable scanning speed was 4–6 mm/s (samples 3 and 4 in Figure 4-3).

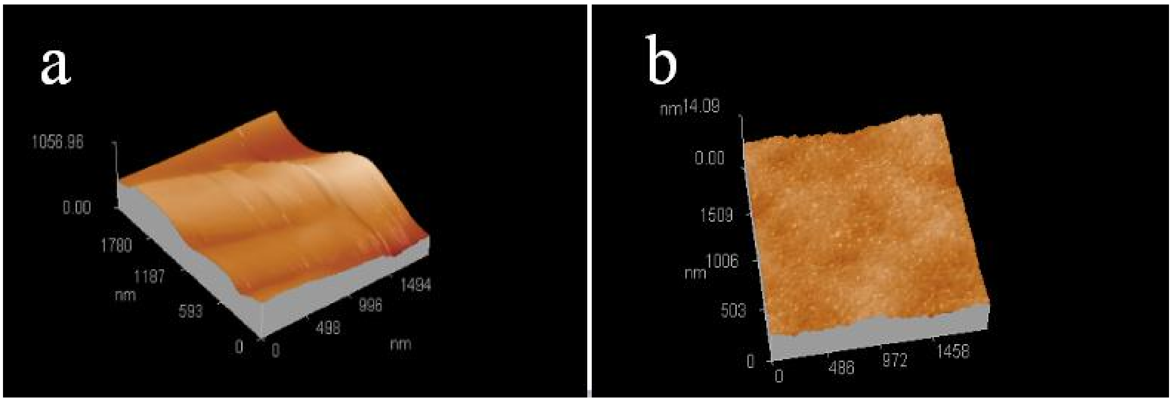

Figure 4-4. AFM images of filter-paper/PANI composite films (**a**) before and (**b**) after laser irradiation.

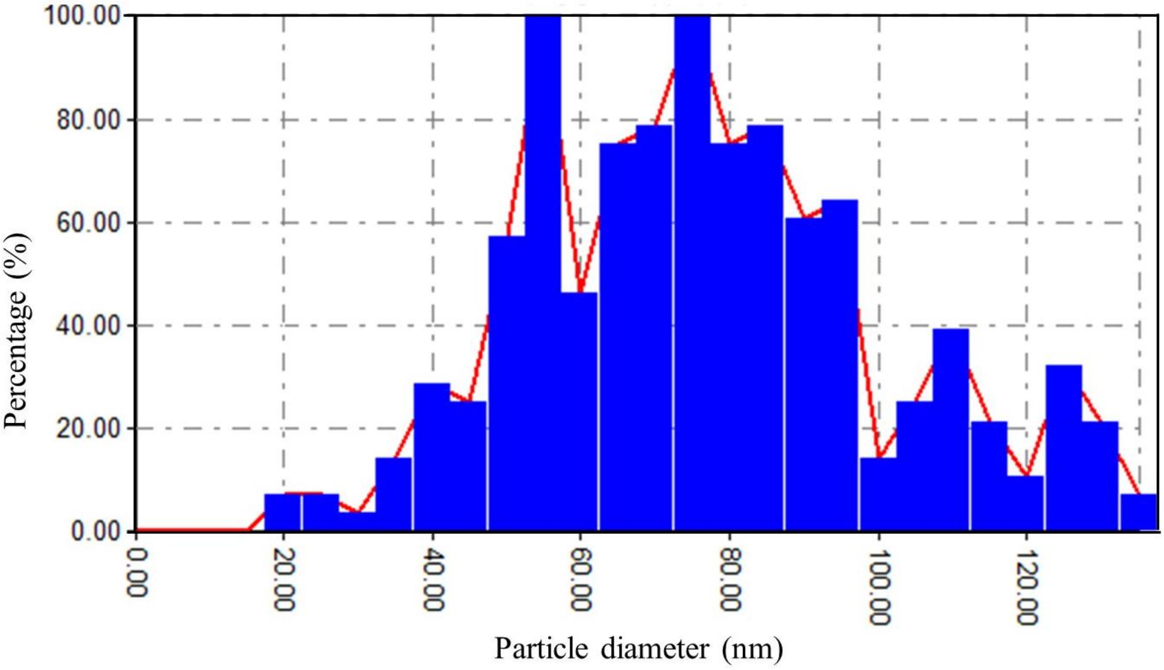

Figure 4-5. Size distribution of silver particles on the FP/PANI film after laser irradiation.

Figure 4-4 presents the AFM micrographs of FP/PANI composite film before and after laser irradiation. The scanning speed and fluency of laser were controlled at 5.0 mm/s and 1.0 mJ/cm^2, respectively. It was easy to detect that the surface of the film was relatively smooth, whereas it became much rougher after irradiation by a laser due to the presence of silver particles. The silver particles agglomerated through the surface tension and resulted in a size of 40 to 100 nm, as shown in Figure 4-5.

4.3.2 Electroless Plating of Cu

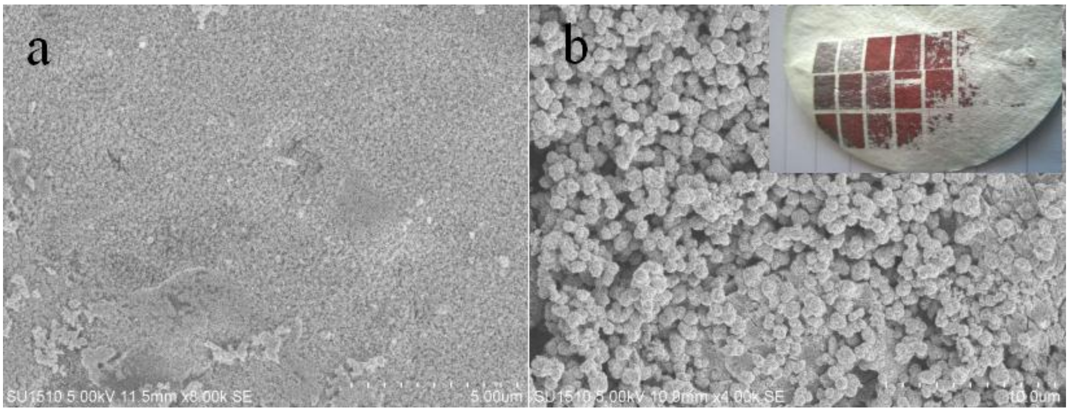

Figure 4-6. SEM images of silver particle (**a**) and copper particle (**b**) deposition on the composite films of FP/PANI. The inset photograph indicates the electroless deposited copper pattern on the composite film of FP/PANI.

The processes of forming silver particles on the surface of FP/PANI film can be described as follows [19,20]: when the laser beam is focused on the film surface, the $AgNO_3$ and PANI substrate absorbs the energy of the laser pulse, and a radial temperature area is formed that leads to the decomposition of PANI. The Ag^+ is reduced by the C element from the decomposed PANI, then the reduced silver melts and agglomerates into particles at high temperature. Subsequently, the silver particles are fully covered by the copper coating during the electroless plating process. It should be noted that copper can hardly be deposited on the area without laser irradiation.

Therefore, it was considered that the silver particles were the active seeds for the copper plating reaction, and it was possible to produce designed copper patterns on the FP/PANI composite films. Figure 4-6 shows the copper patterns obtained by electroless copper plating. This demonstrated that this method yielded good selectivity to prepare metal patterns on the composite films of FP/PANI. As shown in Figure 4-7, the AFM image of the FP/PANI film after copper plating presented a rather rough surface.

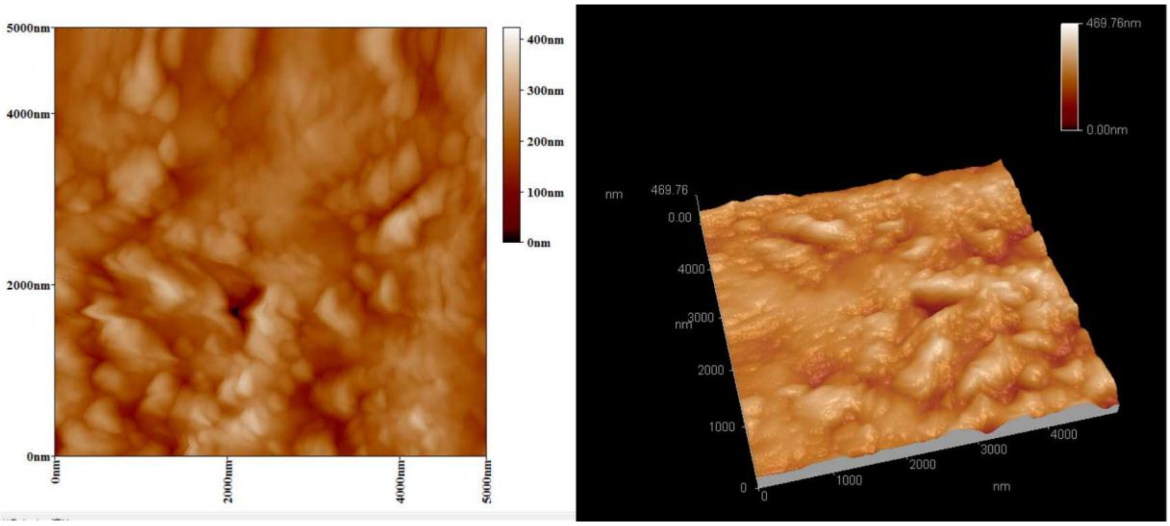

Figure 4-7. AFM images of the FP/PANI composite film after the electroless plating of copper.

4.3.3 Conductivity of Deposition Copper

With a scanning velocity of 5 mm/s, laser irradiation produced a rectangular copper film with a width of 5 mm and the length of 20 mm. Next, we coated some conductive silver paste at the margins of the rectangular copper film. After drying the silver paste under a vacuum, the electrode was clamped on the silver paste for testing the performance of I–V. Figure 4-8 shows the linear I–V curve, which indicated the good conductivity of electroless deposited copper patterns on the composite films of FP/PANI.

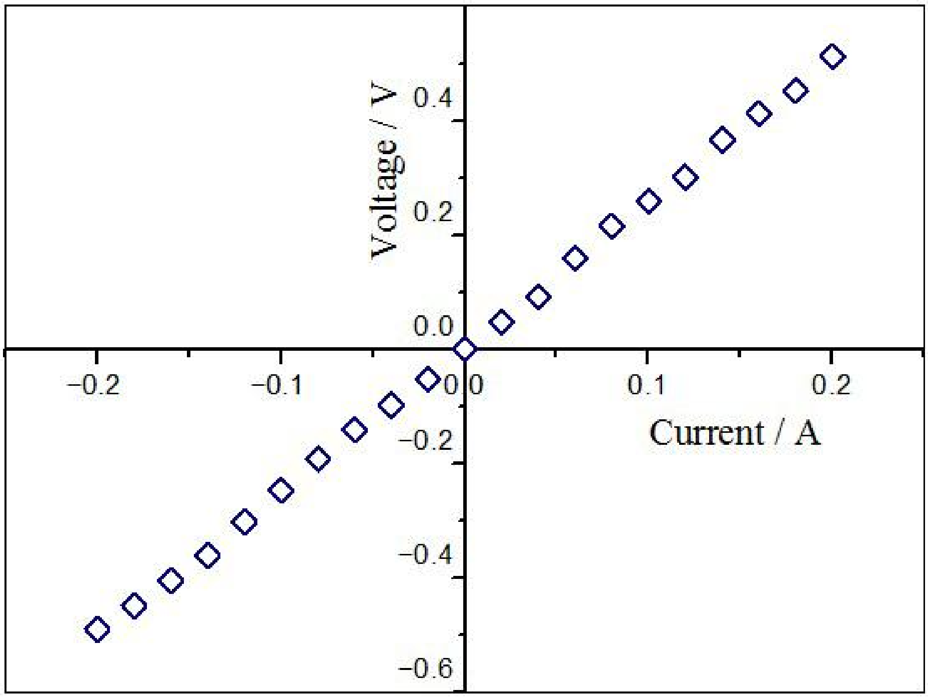

Figure 4-8. I–V curves of electroless deposited copper patterns on the composite films of FP/PANI.

4.4 Conclusions

This charpter reported a method using laser-induced deposition silver on FP/PANI composite films for selective electroless plating copper. The Ag+ iron was doped into a composite film and selectively reduced to silver particles using a pulsed laser source. Then, copper was deposited by means of electroless plating with silver particles as the seeds. The experimental results demonstrated that the scanning speed of the laser pulse greatly affected the redox reaction. The I–V curve indicated that the copper patterns on the FP/PANI composite films had good conductivity. This method provides new insight into preparing a flexible circuit board.

References

1. Scott, M.; Nicholas, A.C.; Kristin, M.; Alberto, P. Manufacturing Microelectronics Using ‘Lase-and-Place’. *Photonics Spectra* **2007**, *10*, 70–74.
2. Jayna, S.; David, B.; Julien, N.; Gary, N.T. Printing technology for ubiquitous electronics. *Circ. World* **2010**, *32*, 40–47, doi:10.1108/03056121011041690.
3. Zanatta, A.R.; Scoca, D.; Alvarez, F. A suitable (wide-range + linear) temperature sensor based on Tm^{3+} ions. *Sci. Rep.* **2017**, *7*, 14113, doi:10.1038/s41598-017-14535-1.
4. Fujii, Y.; Henares, T.G.; Kawamura, K.; Endo, T.; Hisamoto, H. Bulk- and surface-modified combinable PDMS capillary sensor array as an easy-to-use sensing device with enhanced sensitivity to elevated concentrations of multiple serum sample components. *Lab Chip* **2012**, *12*, 1522–1526, doi:10.1039/c2lc21242k.
5. Guo, F.; Su, X.J.; Hou, G.L.; Li, P. Superhydrophobic silver surface with dendrites structure on steel substrate by a facile electroless galvanic deposition process. *Appl. Surf. Sci.* **2012**, *11*, 4906–4910, doi: 10.1016/j.apsusc.2012.01.112.
6. Yang, C.; Lin, W.; Li, Z.Y.; Zhang, R.W.; Wen, H.R.; Gao, B.; Chen, G.H.; Gao, P.; Yuen, M.M.F.; Wong, C.P. Water-based isotropically conductive adhesives: Towards green and low-cost flexible electronics. *Adv. Funct. Mater.* **2011**, *21*, 4582–4588, doi:10.1002/adfm.201101433.
7. Lazare, S.; Tokarev, V.; Sionkowska, A.; Wis´niewski, M. Surface foaming of collagen, chitosan and other biopolymer films by KrF excimer laser ablation in the photomechanical regime. *Appl. Phys. A* **2005**, *81*, 465–470, doi:10.1007/s00339-005-3260-y.
8. Bolle, M.; Lazare, S.; Blanc, M.L.; Wilmes, A. Submicron periodic structures produced on polymer surfaces with polarized excimer laser ultraviolet radiation. *Appl. Phys. Lett.* **1992**, *60*, 674–676, doi:10.1063/1.106588.
9. Thomas, B.; Alloncle, A.P.; Delaporte, P.; Sentis, M.; Sanaur, S.; Barret, M.; Collot, P. Experimental investigations of laser-induced forward transfer process of organic thin films. *Appl. Surf. Sci.* **2007**, *254*, 1206–1210, doi: 10.1016/j.apsusc.2007.09.042.

10. Yu, F.Y.; Li, P.; Shen, H.; Mathur, S.; Lehr, C.M.; Bakowsky, U.; Mücklich, F. Laser interference lithography as a new and efficient technique for micropatterning of biopolymer surface. *Biomaterials* **2005**, *26*, 2307–2312, doi: 10.1016/j.biomaterials.2004.07.021.

11. Piqué, A.; McGill, R.C.R.A.; Chrisey, D.B.; Callahan, J.; Mlsna, T.E. Matrix assisted pulsed laser evaporation (MAPLE) of polymeric materials: Methodology and mechanistic studies. *MRS Proc.* **1998**, *526*, 375–383, doi:10.1557/PROC-526-375.

12. Sirajuddin, M.; Reddy, P.J. Pyroelectric behaviour of laser-evaporated poly(vinyl fluoride) films. *Thin Solid Films* **1985**, *124*, 149–154, doi:10.1016/0040-6090(85)90257-3.

13. Bäuerle, D.W. *Laser Processing and Chemistry*, 4th ed.; Springer: Berlin, Germany, 2011; pp. 81–97, ISBN 978-3-642-17613-5.

14. Liao, X.Q.; Liao, Q.L.; Yan, X.Q.; Liang, Q. J.; Si, H.N.; Li, M.H.; Wu, H.L.; Cao, S.Y.; Zhang,Y. Flexible and Highly Sensitive Strain Sensors Fabricated by Pencil Drawn for Wearable Monitor. *Adv. Funct. Mater.* **2015**, *25*, 2395–2401, doi: 10.1002/adfm.201500094.

15. Lin, C.W.; Zhao, Z.B.; Kim, J.Y.; Huang, J.X. Pencil Drawn Strain Gauges and Chemiresistors on Paper. *Sci. Rep. 4* **2014**, 3812, doi: 10.1038/srep03812.

16. Lessing, J.; Glavan,A.C.; Walker,S.B.; Keplinger, C.; Lewis, J.A.; Whitesides,G.M. Inkjet Printing of Conductive Inks with High Lateral Resolution on Omniphobic “RF Paper” for Paper-Based Electronics and MEMS. *Adv. Mater.* **2014**, *26*, 4677–4682, doi: 10.1002/adma.201401053.

17. Liu, J.P.; Yang, C.; Wu, H.Y.; Lin, Z.Y.; Zhang, Z.X.; Wang, R.H.; Li, B.H.; Kang, F.Y.; Shi, L.; Wong,C.P. Future paper based printed circuit boards for green electronics: fabrication and life cycle assessment. *Energy Environ. Sci.* **2014**, *7*, 3674–3682, doi: 10.1039/C4EE01995D.

18. Mallory, G.O.; Hajdu, J.B. Electroless copper in printed circuit fabrication. In *Electroless Plating: Fundamentals and Applications*; American Electroplaters and Surface Finishers Society: Orlando, FL, USA, 1990; pp. 331–376, ISBN 978-0936569079.

19. Siau, S.; Vervaet, A.; Schacht, E.; Calster, A.V. Influence of chemical pretreatment of epoxy polymers on the adhesion strength of electrochemically deposited Cu for use in electronic interconnections. *J. Electrochem. Soc.* **2004**, *151*, C133–C141, doi:10.1149/1.1639159.

20. Chen, D.S.; Lu, Q.H.; Zhao, Y. Laser-induced site-selective silver seeding on polyimide for electroless copper plating. *Appl. Surf. Sci.* **2006**, *3*, 1573–1580, doi: 10.1016/j.apsusc.2006.02.039.

21. Chen, D.S.; Li, Y.; Lu, Q.H.; Yin, J.; Zhu, Z.K. Selective silver seeding on laser modified polyimide for electroless copper plating. *Appl. Surf. Sci.* **2005**, *246*, 167–173, doi: 10.1016/j.apsusc.2004.11.005.

Chapter 5. Summary

As mentioned in Chapter 1, flexible electrically-conductive fabrics have attracted more and more attention for their wide variety of applications in industries such as clothing, medical, sports, and military. Polyester fiber is widely used as flexible substrate in various fields because of its low price, easy availability, excellent physical and mechanical properties and chemical stability, while its easily generating static electricity and poor conductivity limit its applications in wearable smart devices, static dissipation, electromagnetic shielding, microelectronics industry. Plating silver on the surface of the polyester enables the fabrics to have both the original properties of the polyester fiber and the excellent electrical conductivity, antibacterial property, metallic luster and other excellent characteristics of the metallic silver. Electroless plating is a simple and cost-effective method to coat a Nano silver layer on fibers in order to obtain conductive textiles. However, the electroless silver-plated fibers often haven’t enough bonding strength between the surface silver layer and substrate. So this study chose two methods to improve the silver plating effect. One is to perform cyanide-free electroplating of silver after electroless silver plating, another is to coat a polyaniline intermediate layer with good conductive durability and environmental stability between the fibers and electroless plated silver layer. Besides, due to its better performance, the filter paper was utilized to replace polyester fabrics as the substrate to deposit patterned copper by means of electroless plating through laser-induced deposited silver particles as the seeds.

In Chapter 2, the silver-coated polyester fibers were prepared by a continuous two-step method, which combined the operations of continuous electroless plating without an activation step and subsequent cyanide-free electroplating step. Furthermore, a specialized equipment for the continuous plating of silver on the polyester fibers was designed. According to the machine conditions, the pretreatments, electroless silver-plating, and electroplating silver-plating process were improved accordingly, and the silver-plated conductive fibers were successfully prepared. The influence of the power supply method, control voltage, and electroplating time on electroplating silver was studied. The optimal conditions for electroplating silver conductive polyester fibers should include the power supply method having a constant voltage power, the best control voltage range of 1.5–2.0 V, and an electroplating time of 4 min. The silver-composition and morphology of Ag-coated polyester fibers were characterized by SEM, FTIR, and XRD. Moreover, the mechanical properties and washability of the electroplating silver-plating fibers were compared with the electroless silver-plating fibers. The results demonstrated that after the continuous two-step silver plating, the surface coating of the fiber was obviously thickened, and the surface silver particles were denser and continuous, with better mechanical properties and washability. The electrical resistivity reached 2.3×10^{-4} Ω·cm, and the conductivity was obviously improved. The light bulb experiment also showed that the conductive fiber prepared by the continuous two-step silver plating method had good electrical conductivity.

In Chapter 3, the composite conductive fibers were prepared by the two-step deposition of PANI and Ag layers on the surface of polyester fibers through oxidative polymerization and redox reaction, respectively. Batch experimental results showed that the concentration of reagents and the reaction time could affect the resistance of polyaniline-silver coated conductive fibers. The optimal reaction condition of preparing conductive polyester fibers should be: the concentration of aniline was 0.3 mol/L, APS 0.2 mol/L, nitric acid 1 mol/L and the treating time was 3 min. The morphology, thermostability, mechanical properties, washing resistance and corrosion resistance of resultant fibers obtained from different synthesis condition were analyzed. The results demonstrated that the PANI-Ag-coated polyester fibers by the two-step depositing have much better properties than Ag-coated fibers.

In Chapter 4, a uniform copper pattern with good conductivity properties was obtained on a soft substrate of filter paper/polyacrylonitrile (FP/PANI) film, where the filter paper was commercially available. The pattern of Ag nanoparticles was first produced on an Ag^+-doped FP/PANI composite film using a pulsed laser source, followed by selective electroless plating of copper using the metal silver nanoparticles as activated seeds. The *in-situ* reductions of silver particles and the formation of the silver agglomeration patterns were induced by laser irradiation technology on the FP/PANI/$AgNO_3$ composite film. The morphology of metal particles on the fabric surface and the conductivity of copper deposited patterns were tested. The experimental results demonstrated that the scanning speed of the laser pulse greatly affected the redox reaction, and the most suitable scanning speed was 4–6 mm/s. The I–V curve indicated that the copper patterns on the FP/PANI composite films had good conductivity. This method provides new insight into preparing a flexible circuit board.